LOCAL TRANSLATION DURING AXON GUIDANCE IN THE ZEBRAFISH RETINOTECTAL SYSTEM

by

John Anthony Gaynes

A dissertation submitted to the faculty of
The University of Utah
in partial fulfillment of the requirements for the degree of

Doctor of Philosophy

Interdepartmental Program in Neuroscience

The University of Utah

December 2014

The University of Utah Graduate School

STATEMENT OF DISSERTATION APPROVAL

The dissertation of **John Anthony Gaynes**

has been approved by the following supervisory committee members:

Edward M. Levine	, Chair	**5/08/14** Date Approved
Sheryl A. Scott	, Member	**5/08/14** Date Approved
Monica L. Vetter	, Member	**5/08/14** Date Approved
Jody Rosenblatt	, Member	**5/12/14** Date Approved
Brenda L. Bass	, Member	**5/08/14** Date Approved

and by **Kristen A. Keefe** , Chair/Dean of the Department/College/School of **Interdepartmental Program in Neuroscience**

and by David B. Kieda, Dean of The Graduate School.

ABSTRACT

Development of the nervous system involves establishment of precise long distance connections between distinct single cells called neurons. During development, long axons extend from the cell body and grow, following a very specific pathway through a complex environment to their target. The growth cone is a dynamic structure with finger-like filopodia that sense guidance cues in the surrounding environment through receptors. External guidance cues can be attractive or repulsive, and growth cone turning in response to a guidance cue is driven by actin dynamics, with increased polymerization during attractive turning and increased disassembly during repulsive turning. Therefore, regulators of actin dynamics such as actin-binding proteins are the targets of signaling in the growth cone initiated by external guidance cues. The growth cone changes its behavior very rapidly in response to guidance cues, even as it becomes further and further from the cell body. Growth cones have the ability to act autonomously to guidance cues, in order to continue to react quickly without delay. Local mRNA translation in growth cones has an important role in growth cone behavior, giving the ability to respond to external guidance cues without communication with the cell body. Local translation is regulated by RNA-binding proteins and directly influences actin dynamics that are important for growth cone behavior. While *in vitro* studies have revealed a wealth of knowledge about the mechanisms involved with local translation

during axon guidance, the requirement for the function of RNA-binding proteins *in vivo* has not been tested extensively. In this dissertation, an *in vivo* local translation timelapse assay, performed in the zebrafish retinotectal system, demonstrates that the zebrafish β-actin3'UTR is sufficient to target Kaede expression to RGC growth cones. Also, Igf2bp1 is shown to be the zebrafish ZBP1 ortholog, and a bipartite "zipcode element," required for interaction with ZBP1, is identified in the β-actin3'UTR. I also present the first evidence to date that Igf2bp1/ZBP1 function is required for axon guidance, and furthermore provide data that suggest that Igf2bp1 function may be required for axon specification or elongation, contrary to the common belief that ZBP1 function is required only for axon branching and arbor formation, and that local β-actin translation is only required for growth cone turning during axon guidance.

TABLE OF CONTENTS

LIST OF FIGURES

CHAPTER 1

OVERVIEW

Introduction

The human nervous system is an extremely elaborate cellular network, which coordinates sensory input from external stimuli with complex behavior output. The complexity of human behavior coincides with communication through trillions of connections between billions of cells called neurons (Tessier-Lavigne and Goodman 1996).

Santiago Ramon y Cajal introduced the "Neuron Doctrine" over 100 years ago. This model proposed that the nervous system is composed of distinct cells called neurons. At that time, in the late 1800s and early 1900s, the nervous system was believed to be a reticular network of fibers that transmitted impulses throughout the body. Cajal established that neurons are distinct and autonomous cells that transmit information between one another through connections called synapses. A neuron receives input on its post-synaptic dendrites and transmits an impulse called an action potential down the axon and to other neurons through presynaptic terminals. The Neuron Doctine remains a fundamental principle of neuroscience (Seranno-Castro et al. 2012).

The complexity of nervous system structure is amplified by the dynamic nature of synaptogenesis (Hua and Smith 2004). Synaptogenesis begins before birth and continues to adulthood playing an essential role in learning and memory, with activity-dependent changes to synapses taking place through adulthood (Lagercrantz 2001). The function of neural circuits is highly dependent on correct formation of axon tracts and connections during development. Although synaptic activity establishes the functional wiring of the nervous system, the formation of the initial contact between cells and their targets is established through the development of axons. Axons grow to their targets in a process

known as axon guidance or pathfinding (Tessier-Lavigne 1996). Axon guidance is a genetically controlled process through which the architecture for trillions of synapses is established. However, the human genome has a comparatively small number of approximately 30,000 genes. The spatial and temporal activities of genes are regulated with extreme precision during axon guidance. There are several known human diseases that are caused by mutations in genes that function in axon guidance, including corpus callosum agenesis, L1 syndrome, Joubert syndrome, horizontal gaze palsy with progressive scoliosis, Kallmann syndrome, and potine tegmental cap dysplasia (Nugent et al. 2012). Therefore correct regulation of axon guidance is very important.

The growth cone is a dynamic motile structure at the tip of a growing axon discovered by Cajal (Serrano-Castro et al. 2012). The growth cone directs the rate and direction of growth by sensing the mechanical and chemical properties of its surrounding environment. Growth cone behavior is controlled by cytoskeletal changes through intracellular signaling activated by external stimuli. These signaling mechanisms control gene function during axon guidance. Recent studies have shown that local translation of mRNA in the growth cone is a fundamental mechanism that allows precise genetic control over growth cone behavior during axon guidance (Jung et al. 2012). Chapter 1 of this dissertation gives an overview of nervous system development and the importance of local mRNA translation during axon guidance. A specific emphasis is given to the importance of local β-actin translation and its dependence on ZBP1 function in the context of axon guidance, which is the rationale for the research described in Chapter 3.

Nervous system development

The structure of the vertebrate nervous system is formed during embryonic development when homogeneous tissue is organized into separate organs. Multipotent neural progenitor cells leave the cell cycle and differentiate into neurons. After differentiation the neuron becomes polarized and outgrowth of dendrites and the axon is initiated. Polarization and axon specification require cytoskeletal dynamics that involve actin (Flynn et al. 2009, Stiess and Bradke 2010). An axon begins as a process called a neurite. After a neurite is specified as an axon, it extends from the cell body and navigates to its target, where it terminates and forms synapses (Stiles 2010). Axon formation is essential for the ability of a neuron to transmit impulses. Therefore correct axon guidance is critical for neuron function. Since the growth cone directs axon growth, it is a large focus of research.

The growth cone is a "fan-like extension" at the tip of a growing axon. The morphology of a growth cone is characterized by several long thin protrusions called filopodia and broad extensions between filopodia, called lamellipodia. Filopodia and lamellipodia explore the surrounding extracellular environment by constantly extending and retracting (Dent and Gerler 2003, Lowery and Van Vactor 2009, Dent et al. 2011). These changes in growth cone structure are caused by polymerization and disassembly of filamentous actin (F-actin), which is the major component of the peripheral growth cone cytoskeleton. Filopodia are made from dense parallel bundles of F-actin pushing against the growth cone membrane, while the rest of the growth cone contains cross-linked networks of F-actin (Lewis and Bridgman 1992). The extension and retraction of filopodia is the result of changes in the balance of actin polymerization with actin

disassembly and retrograde flow of F-actin towards the central growth cone (Okabe and Hirokawa 1991, Mallavarapu and Mitchison 1999).

Guidance cues in the extracellular environment bind to growth cone receptors and trigger growth cone turning. Attractive guidance cues cause turning towards the extracellular source and repulsive cues cause turning away from the source. The growth cone is extremely sensitive to concentration gradients of guidance cues, able to detect changes as little as 0.1% (Rosoff et al. 2004). This sensitivity results in asymmetric changes in actin dynamics within the growth cone. Actin polymerization increases on the side of the growth cone closest to the source of an attractive cue, while actin disassembly increases on the side of the growth cone closest to the source of a repulsive cue. In either case asymmetric extension of filopodia on one side of the growth cone leads to turning (Gundersen and Barrett 1980, Isbister and O'Connor 2000). F-actin can also flow towards the central growth cone. This is caused by activity of the motor protein myosin II, which is required for growth cone turning. Myosin II interacts with F-actin inside the peripheral region of the growth cone, which is anchored to extracellular adhesion molecules through the membrane, pulling the growth cone forward in the direction of turning. Axon elongation still occurs without actin polymerization and myosin II, however, it is slower (Marsh and Letourneau 1984, Turney and Bridgman 2005)

Axon guidance

Growth cones follow very specific paths over long distances through the complex environment of the developing embryonic nervous system. An axon can grow to targets that are several centimeters away, thousands of times greater than the cell body diameter. However, axons follow very predictable trajectories. Cajal originally postulated that

growing axons were attracted to concentration gradients of chemicals secreted by their targets (Tessier-Lavigne and Goodman 1996). This idea was confirmed in 1963 when Roger Sperry reported observations of axons extending "advance filaments" that sensed the surrounding environment to determine the direction of axon growth. Sperry proposed that the path of axon growth is determined by its reaction to chemical gradients, known as "the chemoaffinity hypothesis" (Sperry 1963).

Growth cone behavior can be influenced by long-range diffusible guidance cues or non-diffusible short-range cues in the extracellular matrix (ECM) or on the surface of neighboring cells (Tessier-Lavigne and Goodman 1996). The most well-understood axon guidance cue families are netrins, slits, semaphorins and ephrins. However, there are other guidance cues with well-studied functions that are not in these families, such as the attractive cue brain-derived neurotrophic factor (BDNF). The chemical structures of different guidance cues are very similar to each other and some guidance cues can be both attractive and repulsive at different points in an axon tract. Therefore, the effect a guidance cue exerts on pathfinding depends on regulation of receptors expressed in the growth cone (Tessier-Lavigne and Goodman 1996)

Netrins are best known from their role in attracting commissural axons to the ventral midline (Kennedy et al. 1994, Serafini et al.1994, Culotti and Merz 1998), however, they can be either attractive or repulsive (Hedgecock et al. 1990) and can act long-range up to several millimeters (Yee et al. 1999) or short range (Winberg et al. 1998). A well-studied netrin receptor is Deleted in Colorectal Cancer (DCC) that mediates attractive turning towards netrin (Tanaka and Sabry 1995, Schaefer et al. 2002, O'Connor et al. 1990, Culotti and Merz 1998, Keleman and Dickson 2001).

Slits are secreted proteins that signal through robo receptors and act as repulsive cues to axons after midline crossing (Seeger et al 1993, Kidd et al. 1998, Battye et al. 1999, Kidd et al. 1999, Piper et al. 2000, Li et al. 1999), but can also promote elongation and branching of sensory axons (Wang et al. 1999). The function of slit-robo signaling in axon guidance is also highly conserved across species (Seeger et al. 1993, Zallen et al. 1998, Fricke et al. 2001). Retinal ganglion cell (RGC) axons in *astray*/robo2$^{-/-}$ mutants make severe errors at all points throughout the retinotectal projection and also have defects in error correction (Fricke et al. 2001, Hutson and Chien 2002).

Semaphorins include both secreted proteins as well as transmembrane receptors (Kolodkin et al. 1992, Luo et al. 1993) and act as repulsive guidance cues. Semaphorin receptors are large plexin-containing complexes of transmembrane proteins (Tamagnone et al. 1999), ncamL1 (Castellani et al. 2000), and the receptor tyrosine kinase Met (Giordano et al. 2002). Semaphorins are short-range repulsive cues that function to keep axons from growing into incorrect regions along their pathway (Raper 2000, Cheng et al. 2001).

Ephrins are transmembrane proteins that signal through receptor tyrosine kinases (Cheng et al. 1995, Drescher et al. 1995). Ephrins are known for the role they play in establishment of topographic mapping of retinal gangion cell axons. The position of RGCs in the retina along both the anterior-posterior (A-P) axis (Feldheim et al. 2000) and the dorsal-ventral (D-V) axis (Hindges et al. 2002, Mann et al. 2002) determines the termination location along both axes on the optic tectum. Ephrins can be both attractive and repulsive (Wilkinson 2001).

Regulation of growth cone response to guidance cues

In order to navigate to a distant target, an axon grows past several intermediate targets. A growth cone can respond differently to guidance cues, which allows it to grow past an intermediate target (Dickson 2002). A classic example is seen in pathfinding commissural axons that form axon tracts that connect the right and left sides of the central nervous system (CNS) (Dickson 2006). The attractive cue netrin and the repulsive cue slit are both expressed at the midline (Charron et al. 2003, Kennedy et al. 1994, Serafini et al. 1994). Commissural axons are initially attracted to netrin but insensitive to slit-mediated repulsion. At the midline, growth cones lose sensitivity to netrin and become sensitive to slit-mediated repulsion. This change occurs through regulation of guidance receptor expression and activity in the growth cone. The Slit receptors Robo, Robo2, and Robo3 are differentially regulated during commissural axon guidance. Before reaching the midline, commissural growth cones have very low Robo and Robo2 expression but high Robo3 expression. However, after midline crossing Robo and Robo2 become strongly expressed and Robo3 expression is dramatically decreased (Rajagopalan et al. 2000, Simpson et al. 2000, Long et al. 2004). The changes in receptor levels and activity are regulated through direct interactions with other transmembrane proteins. In vertebrates, Robo3 inhibits Robo activity prior to midline crossing (Jen et al. 2004, Sabatier et al. 2004). However, after midline crossing the dramatic increase in Robo and Robo2 makes the growth cone gain sensitivity to slit. Comm is a protein in drosophila melanogaster that regulates Robo levels in commissural growth cones (Keleman et al. 2002, Keleman et al. 2005, McGovern and Seeger 2003). Vertebrate commissural axons in the hindbrain lose attraction to netrin-1 after crossing the midline

(Shirasaki et al. 1998, Stein and Tessier-Lavigne 2001). This is likely due to inhibition of DCC by Slit-Robo signaling. When Slit binds to Robo, the CC1 domain interacts with the P3 domain of DCC, which blocks attraction to netrin (Stein and Tessier-Lavigne 2001, Stein et al. 2001). This example illustrates the importance of receptor regulation during axon guidance.

The response of a growth cone to a guidance cue can also be influenced by changes in cyclic nucleotide activity (Ming et al. 1997, Song et al. 1997, Song et al. 1998). A decrease in cyclic adenosine monophosphate (cAMP) levels and protein kinase A (PKA) activity within a growth cone can change from attractive to repulsive turning response to netrin-1. In *Xenopus laevis*, RGC axons are attracted to netrin-1 expressed at the optic nerve head where they exit the eye, but then become insensitivite to netrin-1 as they grow through the brain and eventually become repelled by netrin-1 when they reach the tectum. This change in response to netrin reflects a gradual decrease in cAMP in the growth cone throughout pathfinding (Shewan et al. 2002). Increased cyclic nucleotide levels may also switch the growth cone response to Sema3A from repulsive to attractive (Polleux et al. 2000).

Cytoskeletal dynamics in the growth cone

The behavior of a growth cone is the direct result of actin dynamics. Molecules that regulate polymerization or disassembly of actin within the growth cone are the targets of intracellular signaling that occurs in response to guidance cues. Enhanced F-actin disassembly is known to cause axon guidance errors *in vitro* and *in vivo* (Marsh and Letourneau 1984, Lafont et al. 1993). F-actin is a polymer of globular actin (G-actin) monomers that have a (+) barbed end and a (–) pointed end. The bond between G-actin

monomers is formed between the (+) and (–) ends, with fastest polymerization at the barbed end. In the growth cone, the barbed ends of F-actin are facing the tips of filopodia, where G-actin monomers polymerize most efficiently (Carlier and Pantaloni 2007, Pollard and Borisy 2003, Yarmola and Bubb 2009).

Actin binding proteins play an important role during axon guidance

Actin-binding proteins (ABPs) control all aspects of actin dynamics (Revenu 2004, Korn 1982, Pollard et al. 2000) (Figure 1.1). Actin polymerization requires free barbed ends of F-actin and available G-actin monomers, and ABPs regulate the availability of both. During retraction of filopodia, ABPs cap barbed ends and block polymerization (Dent et al. 2011). Other ABPs can inhibit barbed end capping to promote polymerization (Bear et al. 2002, Breitsprecher et al. 2008, Dent et al. 2011). ABPs also control the availability of actin monomers. When non-polymerizable adenosine diphosphate (ADP)-G-actin detaches from the (–) end, profilin converts it to adenosine triphosphate (ATP)-G-actin and localizes to the leading edge of filopodia. Another ABP, β-thymosin binds to ATP-G-actin and prevents it from polymerizing until it releases it in response to a drop in G-actin concentration (Kiuchi et al. 2011, Lee et al. 2013). ABPs also control the availability of barbed ends, such as the actin related proteins 2 and 3 (Arp2/3) complex, which promotes F-actin branching by catalyzing nucleation along existing filaments (Rotty et al. 2013). Arp2/3 also binds to profilin, which increases ATP-G-actin availability required for nucleation and polymerization (Gomez and Letourneau 2014). Actin depolymerizing factor (ADF) and cofilin create barbed ends by severing F-actin, which can promote polymerization at the leading edge of the growth cone where they are localized. However, high levels of ADF/cofolin

Figure 1.1 Regulation of actin dynamics determines growth cone behavior. The schematic represents polymerization of G-actin into F-actin (left side), with faster polymerization taking place at the (+) end that faces the tip of filopodia and drives extension. Polymerization is promoted by nucleation by Arp2/2, ADP exchange for ATP by profilin, and availability of free G-actin by β-thymosin. Filopodia retraction (right side) is promoted by barbed end capping of F-actin, severing by ADF/cofilin, and F-actin flow towards the central growth cone.

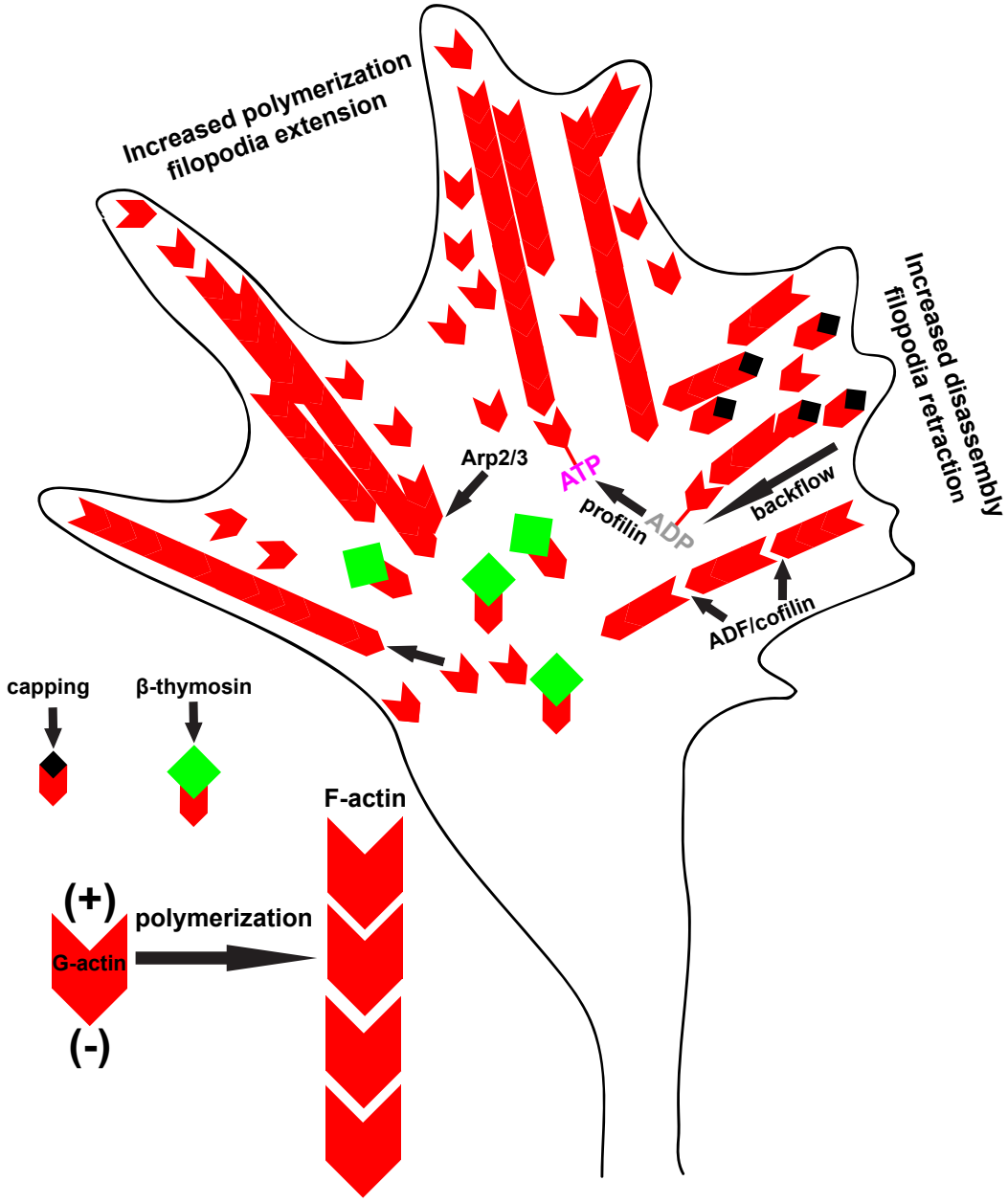
Increased polymerization
filopodia extension
Increased disassembly
filopodia retraction
Arp2/3
ATP
profilin
ADP
backflow
ADF/cofilin
capping
β-thymosin
F-actin
(+)
polymerization
G-actin
(-)

activity result in actin degradation that can lead to filopodia retraction (Dent et al. 2011, Marsick et al. 2012, Sarmiere and Bamburg 2004). ABPs can also connect F-actin to the growth cone membrane (Marsick et al. 2012b, Mintz et al. 2003, Sakurai et al. 2008) or guidance receptors that bind to cell adhesion molecules, such as laminin in the extracellular matrix (Bard et al. 2008, Myers et al. 2011, Vicente-Manzanares et al. 2009).

Growth cone signaling regulates actin dynamics

A growth cones response to attractive guidance cues involves increased extension and adhesion of filopodia in the direction of the guidance cue source, which reflects increased actin polymerization and decreased retrograde movement of F-actin (Vitriol and Zheng 2012). Repulsive guidance cues have an opposite effect on growth cones, causing decreased filopodial extension and adhesion on the side of the growth cone closest to the source. Repulsive turning may also be enhanced by increased F-actin flow towards the central growth cone and decreased adhesion in response to repulsive cues (Gomez and Letourneau 2013).

Given the importance of ABP function in growth cone turning in response to guidance cues, it is important to understand the signaling mechanisms that regulate ABP function and actin dynamics (Quinn and Wadsworth 2008). Rho family GTPases are involved in signaling initiated by many guidance cues (Hall and Lalli 2010). Rho GTPases hydrolyze guanosine triphosphate (GTP) to guanosine diphosphate (GDP) and require the exchange of GDP for GTP by guanosine exchange factors (GEFs) for re-activation (Etienne-Manneville and Hall 2002). Some guidance receptors can have GTPase activity while others stimulate GTPases through GEFs and GTPase activating

proteins (GAPs) (Lowery and Van Vactor 2009). Rho GTPases can either be activated or deactivated by guidance cues (Li et al. 2002, Yuan et al. 2002). The GTPases RhoA, Rac1, and Cdc42 regulate ABPs involved in actin polymerization, depolymerization and adhesion. RhoA acts in repulsive growth cone turning while Rac1 and Cdc42 act in attractive turning (Luo et al. 2000). RhoA can activate RhoA kinase (ROCK), increasing myosin II activity and retrograde F-actin movement in response to repulsive guidance cues (Shamah et al. 2001, Niederost et al. 2002, Swiercz et al. 2002). ROCK also activates LIM kinase, which promotes actin stability by inhibiting ADF/cofilin from severing F-actin (Sarmiere and Bamburg 2004). Growth cone turning in response to the repulsive cues slit3, ephrin-A2 and semaphorin 3A involves a reduction in barbed ends due to decreased cofilin activity (Marsick 2012a). RhoA and ROCK function can also be important for growth cone turning in response to attractive cues such as nerve growth factor (NGF) or BDNF. Attractive turning in response to BDNF has been observed to occur on the side of the growth cone with decreased cofilin activity (Wen et al. 2007, Loudon et al. 2006).

Rac1 and Cdc42 signaling in response to netrin or BDNF can activate ABPs that promote actin polymerization and adhesion. An example is WASP family verprolin-homologous protein (WAVE) which promotes nucleation and polymerization through Arp2/3, and therefore increases filopodial extension and adhesion that lead to growth cone turning towards the source (Briancon-Marjollet et al. 2008, Myers et al. 2012, Shekarabi et al. 2005). Rac1 promotes polymerization through ADF/cofilin activation in response to netrin and NGF, increasing free barbed ends (Marsick et al. 2010). Rac1 signaling is also involved in growth retraction in response to Sema3A and ephrin-A2 by

promoting membrane endocytosis, which also requires increased actin polymerization (Jurney et al. 2002, Marston et al. 2003, Vastrik et al. 1999).

Growth cone signaling can target Src family kinases in response to both attractive and repulsive cues (Knoll and Drescher 2004, Li et al. 2004, Robles and Gomez 2006, Yam et al. 2009). Src can mediate localization and activity of ABPs that promote actin polymerization through Rho GTPase signaling (Renkema et al. 2002, Torres and Rosen 2003).

Both attractive and repulsive guidance cues can activate Ca^{2+} channels. The resulting Ca^{2+} influx can trigger signaling mechanisms that regulate actin dynamics. (Kerstein et al. 2013, Li et al. 2009, Li et al. 2005, Shim et al. 2005, Wang and Poo 2005, Wen et al. 2007, Robles et al. 2003, Kaczmarek et al. 2012). Netrin and BDNF promote activation of Ca^{2+}-dependent calmodulin kinase II, which promotes growth cone turning by increasing Rac1 activity and decreasing RhoA activity (Jin et al. 2005).

Genetic control over growth cone behavior involves local translation

The reaction of a growth cone to guidance cues involves diverse intracellular signaling mechanisms. However, all signaling pathways ultimately act to regulate actin dynamics within the growth cone. It is well established that growth cones respond rapidly and autonomously to guidance cues. This is intriguing since growth cones grow further and further away from the cell body during pathfinding. One *in vivo* study in *Xenopus laevis* showed that RGC axons could navigate correctly to the tectum and form arbors after the eye was removed (Harris et al. 1987), illustrating growth autonomy from the cell body. The genes inside the nucleus that regulate axon guidance become increasingly distant from the growth cone. How can genetic control be achieved over

such rapid changes occurring in the distant growth cone in response to external cues that are also far away? Genes function through transcription of mRNA, which is translated into functional proteins. While active anterograde transport of proteins to the growth cone does occur, it has been established in recent years that local translation of mRNA in growth cones is a common mechanism that is required for correct growth cone response to attractive and repulsive guidance cues. The following sections will provide background about local mRNA translation during axon guidance, which is the focus of the research presented in Chapter 3.

Advantages of local translation

Local translation in the growth cone provides efficient and precise spatial and temporal genetic control over turning responses to external cues (Jung et al. 2014). One mRNA molecule can yield many protein molecules, therefore less mRNA is needed in the growth cone and the expense of energy and materials required for transport is far less than transporting all protein from the cell body to the growth cone. Also, the activity of newly translated proteins may function differently than older proteins that have more post-translational modifications (PTMs). Certain growth cone responses may require the functions of unmodified proteins. Local translation in the growth cone can generate unmodified proteins, which can participate in signaling without vulnerability to modifications. An example is β-actin, which forms the actin cytoskeleton in growth cones. β-actin can be exposed to glutathionylation (Wang et al. 2001) or argininylation (Karakozova et al. 2006). These modifications decrease the activity of β-actin monomers in nucleation and polymerization, compared to unmodified β-actin monomers. Local translation in the growth cone delivers a rapid increase in concentration of unmodified β-

actin monomers that are readily available for polymerization in response to attractive cues (Holt and Bullock 2009). Therefore, local translation of β-actin in growth cones preserves time and resources.

Rapid response to guidance cues requires the function of many different proteins at specific times and locations within the growth cone. This can be accomplished through regulation of mRNA localization and translation. The mRNA can be localized to a specific subcellular compartment, localizing protein activity to that location before it is translated. A small amount of protein can cause a rapid local increase in concentration and activity in the area it is translated. An example would be a filopodia that senses netrin1 or BDNF and activates translation of proteins that promote actin polymerization, such as β-actin at the tip, causing asymmetric filopodia extension and attractive turning (Leung et al. 2006, Yao et al. 2006). Alternatively, local translation of ADF/cofilin (Piper et al. 2006) or RhoA (Wu et al. 2005) can promote repulsive growth cone turning through asymmetric decrease in filopodia extension. This illustrates that local translation can minimize the amount of protein synthesis required for growth cone turning and maximize efficiency and precision of control over actin dynamics.

Evidence for local mRNA translation in axons

The Central Dogma of Biology, established by Francis Crick in 1958, states that genetic information encoded by DNA in the nucleus is transcribed into mRNA, which is then translated into protein (Crick 1970). While increased understanding has revealed that regulation over gene expression is vastly complex, the Central Dogma remains a fundamental principle of molecular biology. Translation occurs through the protein synthesis activity of ribosomes as it "reads" mRNA in the 5' to 3' direction. A classic

example of mRNA localization occurs in the *Drosophila melanogaster* embryo, which begins development as large "multi-nucleate syncytium" with well-defined patterns of mRNA distribution (Johnstone and Lasko 2001).

The high degree of polarity seen in neurons makes them likely candidates for local translation (Taylor et al. 2009, Zivraj et al. 2010). The first evidence for protein synthesis in axons came from mammalian studies in the 1960s (Giuditta et al. 1968). In the 1980s mRNA (Giuditta et al. 1986), ribosomal RNA, and actively translating polysomes were found in the squid giant axon. Ribosomes have also been detected in axons of mammalian neurons *in vitro* and *in vivo* (Bassell et al. 1998, Bunge 1973, Tennyson 1970, Tcherkezian et al. 2010). Ribosomes have also been shown to bind to growth cone receptors (Tcherkezian et al. 2010). Recent studies that analyzed the transcriptome of axons and growth cones *in vitro* identified thousands of mRNAs, some of which were specifically enriched in either axons or growth cones (Andreassi et al. 2010, Zivraj et al. 2010, Gumy 2010, Taylor et al. 2009). A recent study in zebrafish showed several mRNAs to be localized to axons *in vivo* (Baraban et al. 2013). Guidance receptor mRNAs have been observed in axons, such as ephrin type-A receptor (EPHA2) (Brittis et al. 2002). This is intriguing since localization and function of transmembrane proteins requires post-translational processing by rough endoplasmic reticulum (RER) and golgi apparatus. One study demonstrated that receptor proteins synthesized in the axon are inserted into the plasma membrane (Zheng et al. 2001). Also, while the typical structures of RER and Golgi have not been seen with electron microscopy (EM) (Bassell et al. 1998, Bunge 1973, Tennyson 1970), protein components of RER and Golgi have been detected in axons (Merianda et al. 2009, Willis et al. 2005, Lyles et al. 2006),

suggesting the existence of "functional equivalents" that lack detectable organelle structure. Therefore, the components necessary for local translation of both cytoplasmic proteins and transmembrane proteins are present in axons. There is also direct evidence from metabolic labeling studies that protein synthesis does occur in axons. (Giuditta et al. 1968, Eng et al. 1999, Koenig 1991, Tobias and Koenig 1975). Evidence also exists that local translation in axons is required for growth cone turning. *In vitro* studies have also demonstrated that growth cones can respond correctly to guidance cues applied after severing the cell body from the axon, but not when protein synthesis inhibitors are applied (Cambell and Holt 2001, Ming et al. 2002).

Local translation is important for growth cone turning

The requirement of local translation for growth cone turning has been demonstrated *in vitro* in response to both attractive and repulsive guidance cues including netrin1 (Campbell and Holt 2001, Hengst et al. 2009, Leung et al. 2006, Yao et al. 2007), semaphorin3A (SEMA 3A) (Campbell and Holt 2001, Wu et al. 2005), slit2 (Piper et al. 2006), engrailed1 (EN1) and engrailed2 (EN2) (Alvarez-Fischer 20011, Brunet et al. 2005, Wizenmann et al. 2009), pituitary adenylate cyclase-activating peptide (ADCYAP1) (Guirland et al. 2003), nerve growth factor (NGF) (Hengst et al 2009, Cox et al. 2008), brain-derived neurotrophic factor (BDNF) (Yao et al. 2006), and neurotrophin 3 (NT3) (Je et al. 2011, Zhang et al. 1999). Local translation-dependent growth cone turning was first shown to be required for turning in response to netrin1 and sema3A. Metabolic labeling was used to view protein synthesis in growth cones, and repulsive turning in response to sema3A was blocked by the protein synthesis inhibitors cyclohexamide and anisomycin. It was also shown that both guidance cues activated

translation through the mammalian target of rapamycin (mTOR). Inhibition of mTOR activity with rapamycin blocked protein synthesis and growth cone turning in response to sema3A (Campbell and Holt 2001).

Growth cone turning in response to other guidance cues does not require local translation. EphrinB (Mann et al. 2003), Lyso-phosphatidic acid (Campbell and Holt 2001) and sphingosine1-phosphate (Strochlic et al. 2008), do not stimulate local translation when applied to growth cones. Most guidance cues that elicit local translation-dependent growth cone turning activate translation in the growth cone through mTOR (Campbell and Holt 2001, Piper et al. 2006, Brunet et al. 2005). It is interesting that both attractive and repulsive cues activate translation through a common mechanism.

The differential translation model

The decision between attractive and repulsive growth cone turning in response to a certain guidance cue is determined by the specific mRNAs that are translated. The differential translation model predicts that attractive turning occurs through local translation of proteins that promote actin polymerization and repulsive turning occurs through local translation of proteins that promote actin disassembly (Figure 1.2) (Lin and Holt 2007). This makes sense given the determinant role that actin dynamics play in growth cone behavior and is supported by detection of mRNAs for regulators of actin dynamics in axons (Andreassi et al. 2010, Zivraj et al. 2010, Gumy et al. 2011, Taylor et al. 2009). Turning in response to netrin1 and BDNF occurs through asymmetric local translation of β-actin mRNA, on the side of the growth cone closest to the source (Leung et al. 2006, Yao et al. 2006). The local increase in β-actin monomer concentration

Figure 1.2: The differential translation model. Microtubules (green) are the major cytoskeletal component of the axon, while F-actin (red) is the major cytoskeletal component of the growth cone. The central growth cone is a network of cross-linked F-actin and filopodia in the peripheral growth cone are formed from parallel bundles of F-actin pushing against the membrane. When an attractive cue binds to growth cone receptors, asymmetric local translation of proteins that promote actin polymerization occurs on the side of the growth cone closest to the source. When a repulsive cue binds to growth cone receptors, asymmetric local translation of proteins that promote actin disassembly occurs on the side of the growth cone closest to the source. In both cases, the growth cone turns in the direction of more actin polymerization.

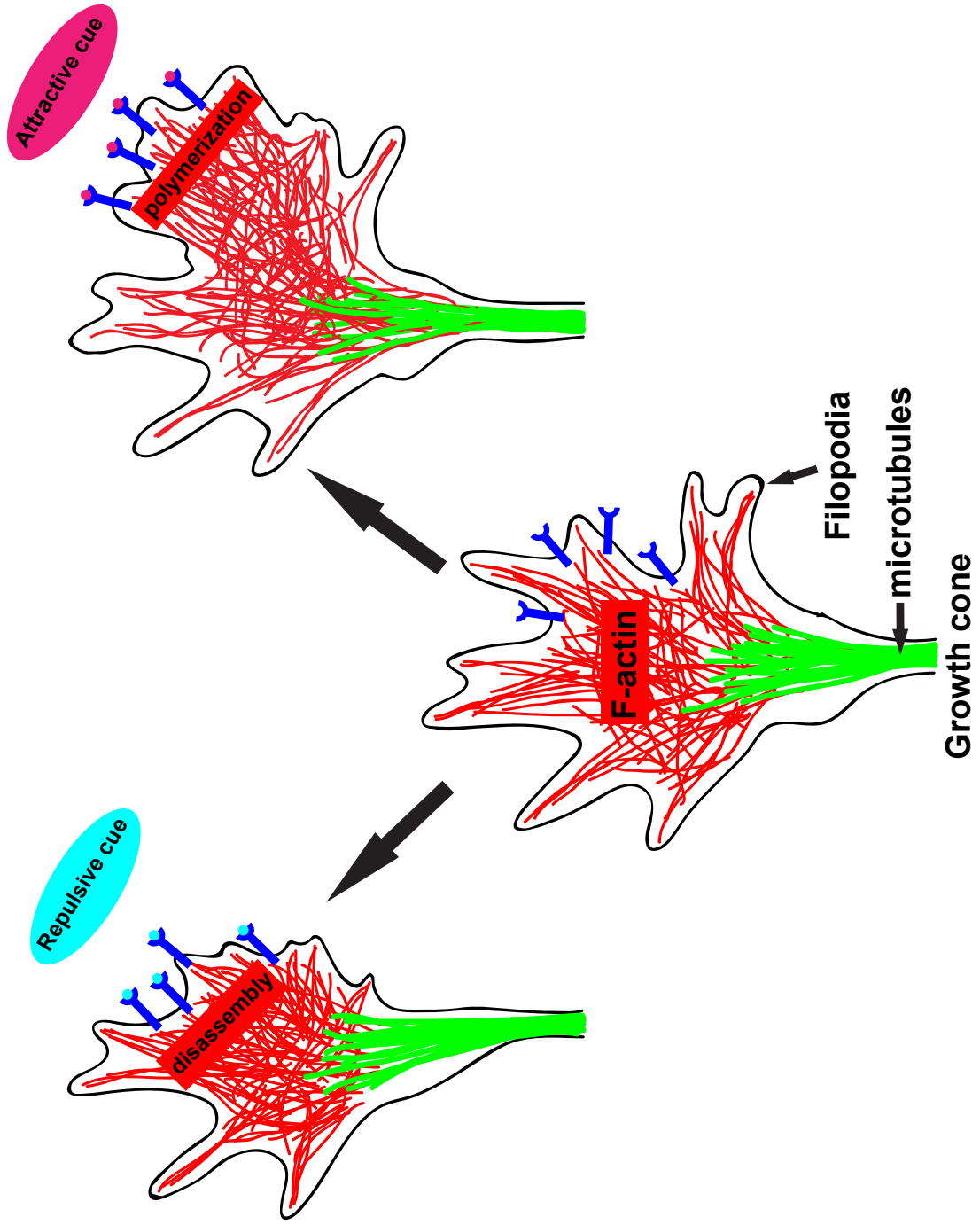
Attractive cue
polymerization
Filopodia
microtubules
Growth cone
F-actin
Repulsive cue
disassembly

promotes polymerization and drives turning. Slit2 and sema3A do not activate local β-actin translation. Instead, proteins involved in actin depolymerization such as cofilin (Piper et al. 2006) and RHOA (Wu et al. 2005) are translated locally in growth cones as they turn in response to these repulsive cues.

Local translation is important for survival, axon maintenance and elongation

Axon elongation is considered to be separate from growth cone turning. There is evidence that short-term growth of axons does not require local translation (Eng et al. 1999). In culture, axons can elongate for 2-5 hours after cell body removal, even when protein synthesis inhibitors are applied (Campbell and Holt 2001, Leung et al. 2006). However, there is also evidence that guidance cues can promote axon elongation. Application of netrin1 or NGF to axons *in vitro* can promote axon elongation through local translation of proteinase-activated receptor 3 (PAR3), which is part of a complex that controls cytoskeletal dynamics (Hengst et al. 2009). Application of brain lysate to axons in culture activates local translation of β-thymosin in neurites, which can inhibit actin polymerization. However, inhibition of β-thymosin translation increases neurite length (Van Kesteren et al. 2006). Therefore, local translation may play a role in regulating axon guidance. Interestingly, local translation of β-thymosin shows that elongation may require actin dynamics.

Continued axon elongation and maintenance require growth cone signaling in response to growth factors during pathfinding. Cultured peripheral sensory neurons and sympathetic neurons require local translation of inositol monophosphatase 1 (IMPA1) in response to nerve-derived growth factor (NGF) for survival (Andreassi et al. 2010).

Cyclic AMP responsive element (CREB) is a transcription factor that promotes cell survival. CREB is translated locally in axons in response to NGF in cultured neurons. After translation, CREB is transported to the nucleus where it acts to promote cell survival. Interestingly, cell survival in response to NGF specifically requires CREB that is translated in axons; expression of CREB in the cell body cannot promote a similar survival response. These findings support the idea that unique properties of newly translated proteins are required in some cases (Cox et al. 2008). Local translation of CREB may be required for survival and axon maintenance in certain cell types (Gumy et al. 2011, Cox et al. 2008).

Another way that local translation can promote survival and maintenance of neurons is by synthesizing proteins that support local mitochondria function. Axons contain mRNAs for mitochondrial proteins (Aschrafi et al. 2010) as well as proteins that regulate mitochondrial function (Andreassi et al. 2010, Zivraj et al. 2010, Gumy et al. 2011, Taylor et al. 2009). Survival of cultured mouse midbrain dopaminergic neurons is promoted by local translation of mitochondrial proteins in response in engrailed2 (Alvarez-Fischer et al. 2011). There is also evidence that local translation supports mitochondrial function *in vivo* (Yoon et al. 2012). The nuclear protein laminB2 is translated and localized to mitochondria in *Xenopus laevis* RGC axons in response to engrailed1. It has been shown that continuous local translation of laminB2 is required for mitochondria function *in vitro*, and axon maintenance *in vivo* (Yoon et al. 2012).

It is not surprising that growth cone turning is dependent on the mutual activity of local translation and actin dynamics. However, axon elongation and survival are both critical during axon guidance. While there is some evidence that these two processes

require local translation, this requirement is not as obvious as it is for turning *in vitro*. It is possible that elongation and survival have a more pronounced requirement for local translation during axon guidance *in vivo*, in the complex environment of the developing embryonic nervous system. New strategies are needed to test the requirement for local translation during elongation and survival *in vivo*.

Regulation over mRNA translation

Different guidance cues activate local translation of different sets of mRNAs through a common mechanism within the growth cone. This is achieved through careful regulation over which mRNAs are translated. In addition, local translation is likely to play a role to regulate the switching of the growth cone response to a guidance cue during axon guidance, as is the case with slit and netrin. Therefore, it is important to understand how this regulation is accomplished.

One study has shown that a guidance receptor can regulate local translation through a direct interaction with ribosomes. The netrin receptor DCC binds to the L5 protein, which is part of the 60s ribosomal subunit (Koenig et al. 2000), which stalls translation of mRNA that is in complex with the ribosome. When netrin1 binds DCC, the ribosome-mRNA complex dissociates from DCC and begins translation. This mechanism controls when and where protein is present very precisely by restricting translation within the growth cone to the location and time that netrin binds to DCC (Tcherkezian 2010) and this is essential for axon guidance.

RNA binding proteins regulate mRNA transport to the growth cone

RNA-binding proteins (RBPs) are critical for regulation of mRNA localization and translation. RBPs interact with mRNA during transcription in the nucleus, during translation in the growth cone and every step in between. A specific RBP binds to specific mRNAs and assembles with RNA granules, which are ribonucleoprotein particles (mRNPs) found in neurons (Kiebler and Bassell 2006). RNA granules are large complexes that contain mRNAs, regulatory RNAs, translation regulators, and molecular motors (Liu-Yesucevitz et al. 2011). However, the exact composition of a RNA granule varies and likely reflects the specific mRNAs that are part of the complex. There is some evidence to suggest that mRNPs carry only one type of mRNA (Kato et al. 2012). There is also evidence that RNA granules carry several mRNAs for proteins that have related functions (Gao et al. 2008). Therefore, RBPs may selectively assemble one or a few functionally related mRNAs for transport to the growth cone for local translation. RNA granules are actively transported along microtubules in the axon to the growth cone by molecular motors. RBPs repress mRNA translation during transport and within the growth cone (Kim-Ha et al. 1995, Nakamura et al. 2004, Paquin et al. 2007). An example is fragile X mental retardation protein (FMRP), which may block translation elongation by recruiting the eukaryotic initiation factor 4E (eIF4E) binding protein CYFIP1 (Napoli et al. 2008).

An RBP binds to its target mRNA at a specific recognition element in the mRNA molecule. These can be either primary sequences or secondary structures such as hairpins (Macdonald and Struhl 1988, Chartrand et al. 1998). Most recognition elements are located in the 3' untranslated region (3'UTR), as seen in β-actin, RhoA, EphA2,

CoxIV, and Impa1 (Andreassi et al. 2010, Aschrafi et al. 2010, Bassel et al. 1998, Brittis et al. 2002, Zhang et al. 2001). However, recognition elements can be located in the 5'UTR (Tsai et al. 2007) or coding mRNA as seen in FMRP (Ascano et al. 2012, Darnell et al. 2011) and Robo3 mRNA (Kuwako et al. 2010).

Mechanisms that regulate mRNA local translation

Another mechanism through which RBPs can regulate translation is by controlling the length of the poly (A) tail. Cytoplasmic polyadenylation element binding protein (CPEB) controls translation by polyadenylation. It binds directly to CPE sequence in the 3'UTR of mRNAs (Richter 2007). *Xenopus laevis* RGC growth cone collapse in response to Sema3A is reduced when polyadenlylation is blocked (Lin et al. 2009). When CPEB function is blocked in hippocampal neurons, NT-3 induced β-actin translation in the growth cone is reduced, possibly through Ca^{2+} mediated activation of inositol triphosphate (IP3) and Ca^{2+}/calmodulin dependent protein kinase II (CamKII) activation (Kundel et al. 2009).

Local translation can be regulated through phosphorylation of RBPs in response to guidance cues. An example is FMRP phosphorylation ((Narayanan et al. 2008, Muddashetty et al. 2011, Coffee et al. 2012). Phosphorylation of an RBP can be targeted to the time and location of a guidance cue binding to a growth cone receptor.

Small noncoding RNAs can also regulate local translation in the growth cone. Micro RNAs (miRNAs) can interact with RBPs (Schratt et al. 2006, Edbauer et al. 2010). miRNA molecules and RNA-induced silencing complex (RISC) components have been shown to associate with FMRP (Caudy et al. 2002, Jin et al. 2004, Muddashetty et al. 2011). FMRP may require miRNAs to repress translation of some of its target mRNAs

(Muddashetty et al. 2011). Furthermore, miRNAs have been detected in axons (Natera-Naranjo et al. 2010, Dajas-Bailador et al. 2012) and appear to play a role in response to guidance cues. Dicer knockdown causes axon guidance defects in the mouse visual system (Pinter and Hindges 2010) and loss of miRNA-124 causes guidance defects in RGC axons by blocking the growth cone response to Sema3A (Baudet et al. 2012).

Diseases caused by mutations in RBPs

Neurodegenerative and neurodevelopmental diseases are caused by mutations in mRNA binding proteins with well-known functions in mRNA localization and translation in axons. These diseases include fragile X syndrome (FXS), spinal muscular atrophy (SMA), and amyotrophic lateral sclerosis (ALS). Therefore, the importance of local translation in neurons is apparent during development and in adulthood (Liu-Yesucevitz et al. 2011).

The neurodevelopmental disorder fragile X syndrome (FXS) is the most common genetic cause for autism and intellectual disabilities. This is caused by mutations in the FMR1 gene, which codes for the RBP fragile X mental retardation protein (FMRP) (Garber et al. 2008). Loss of FMRP function causes defects in the development and activity of synapses. FXS pathology is known to involve post-synaptic dendrites, where FMRP is known to repress local mRNA translation (Bear et al. 2008). However, FMRP has been seen in the presynaptic region of axons as well (Hanson and Madison 2007).

CYFIP2 may be involved in regulating local translation during axon guidance

FMRP interacts directly with cytoplasmic FMRP interacting proteins 1 and 2 (CYFIP1 and CYFIP2) (Schenk et al. 2001). FMRP can repress activity-dependent translation in dendrites through CYFIP1 (Napolo et al. 2008). CYFIP2 is a member of the WAVE/SCAR complex, which activates Arp2/3-dependent actin nucleation. This occurs in response to the small GTPase Rac, which binds directly to CYFIP2 (Eden et al, 2002, Miki et al. 1998, Machesky et al. 1999). It is intriguing that CYFIP2 functions both as a regulator of actin dynamics through the WAVE/SCAR complex, and as a potential mediator of local translation through interaction with FMRP. Guidance receptors signal through Rac to regulate actin dynamics, so the presence of FMRP in axons and its known ability to interact with CYFIP2 suggests that FMRP could possibly play a role in axon guidance. Evidence for this comes from the demonstration that CYFIP2 function is required cell-autonomously for correct axon sorting in zebrafish embryos (Pittman et al. 2010), which is Chapter 2 of this dissertation.

Another interesting characteristic of FMRP is that it forms RNA granules with SMN (Piazzon et al. 2008). SMN is also an RBP, which regulates translation of candidate plasticity gene 14 (cpg15 or NRN1) (Akten et al. 2011). SMN regulates pre-mRNA splicing in the nucleus (Pellizzoni et al. 1998) and is also known to localize to axons and growth cones (Sharma et al. 2005, Rossoll et al. 2003). SMN is well known for its involvement in SMA pathology, which is a neurodegenerative motor neuron disease caused by deletions in SMN1 (Lefevbre et al. 1995). A recent study has shown that SMN is actively transported in motor axons by RNA granules that contain ZBP1

(Fallini et al. 2013), which regulates local β-actin mRNA translation in growth cones and has been implicated in the pathology of certain types of cancer (Vainer et al. 2008). Chapter 3 of this dissertation is used to investigate the requirement of ZBP1 function *in vivo* during axon guidance.

ZBP1 is required for β-actin local translation

ZBP1 is an RBP that is required for localization of β-actin mRNA. The mechanism through which ZBP1 targets β-actin mRNA for local translation is highly conserved across species and different cell types. ZBP1 was first defined by its ability to interact directly with β-actin mRNA (Ross et al. 1997). β-actin was observed to be localized to the leading edge of chick embryonic fibroblasts. The β-actin 3'UTR was found to target expression of β-galactosidase reporter mRNA similar to β-actin expression at the leading edge of migrating fibroblasts. The first 54 nucleotides of the 3'UTR after the stop codon, named the zipcode, were found to contain the necessary information for targeting an mRNA for local translation. Antisense oligonucleotides targeted to bind the β-actin zipcode blocked mRNA localization and translation (Kislauskis et al. 1994). ZBP1, or zipcode binding protein 1, was discovered by its ability to directly bind to the zipcode (Ross et al. 1997). The interaction between ZBP1and the β-actin zipcode was found to be necessary for β-actin mRNA localization and translation at the leading edge of fibroblasts. In addition to blocking local translation, the morphology and migration of the fibroblasts were disrupted (Kislauskis et al. 1994, Shestakova et al. 2001, Katz et al 2012). These studies demonstrated that migration of fibroblasts requires ZBP1-dependent local translation of β-actin mRNA.

Fibroblast migration is dependent on actin dynamics at the leading edge, and they resemble the shape and behavior of growth cones. ZBP1 functions similarly to localize β-actin mRNA to growth cones. ZBP1 and β-actin mRNA co-localization in axons and growth cones is well documented (Zhang et al. 2001, Yao et al. 2006, Leung et al. 2006, Welshans and Bassel 2011). Also, asymmetric synthesis of β-actin protein in growth cones has been demonstrated, in response to certain guidance cues (Leung et al. 2006).

Local translation of β-actin in growth cones

A timelapse assay was used to demonstrate that the β-actin 3'UTR is sufficient to target local translation of the photoconvertible fluorescent protein Kaede in *Xenopus laevis* RGC growth cones *in vitro* (Leung et al. 2006, Leung and Holt 2008). Native Kaede has green fluorescence, however, exposure to UV or 405nm wavelengths causes an irreversible photocleavage that switches the fluorescence to red. In cultured retinal explants, the growth cones of RGCs expressing Kaede with the β-actin 3'UTR were exposed to netrin1, photoconverted from green to red with a UV laser, and then timelapse was performed. The rapid return of newly synthesized green fluorescence in the growth cone demonstrated that the β-actin 3'UTR is sufficient to target mRNA for local translation in growth cones, similar to chick fibroblasts (Leung and Holt 2008, Leung et al. 2006). A similar assay was performed in cultured neurons from ZBP1$^{-/-}$ mice with similar results. This assay also demonstrated that ZBP1 function is required for β-actin 3'UTR-dependent local Kaede translation in the growth cone (Welshans and Bassell 2011).

In *Xenopus laevis*, attractive turning of RGC growth cones in response to netrin1 (Leung 2006) and BDNF (Yao 2006) requires the ZBP1 ortholog Vg1RBP *in vitro*. Ca^{2+}

dependent turning towards BDNF was blocked when interaction between ZBP1 and β-actin mRNA was prevented (Yao 2006). ZBP1 function is also required for mammalian growth cones to respond to netrin1 and BDNF (Welshans and Bassell 2011). Defective β-actin translation also causes morphological defects in neurons (Zhang 2001, Huttelmaier 2005, Leung 2006, Yao 2006, Welshans and Bassell 2011). ZBP1 also has a similar function in dendrites (Buxbaum 2014, Perycz 2011).

Mechanism for ZBP1 control over local translation of β-actin

ZBP1 is highly conserved across several species. ZBP1 protein has six conserved RNA binding domains; two RNA recognition motifs (RRM) and four KH domains (Chao et al. 2010). ZBP1 is present in cytoplasm in the cell body, axon, and growth cone. ZBP1 protein also has nuclear import and export signals and is thought to first bind β-actin mRNA in the nucleus (Ross et al. 1997).

The binding mechanism of ZBP1 to the β-actin zipcode was determined from crystal structure. A sequence of 21 nucleotides in the zipcode loops around ZBP1, interacting directly with the third and fourth K homology (KH) domains (KH34). The binding region of the zipcode is a bipartite element with two motifs, GGACT and ACA, separated by 13 nucleotides, (GGACT)-n_{13}-(ACA) (Chao 2010). Zipcode binding protein 2 (ZBP2) assists the export of the complex of ZBP1 and β-actin mRNA from the nucleus (Pan et al. 2007). The complex of ZBP1 and β-actin mRNA assembles into RNA granules, which are actively transported along microtubules in the axon. Transport of granules that contain β-actin mRNA and ZBP1 along axons has been visualized (Zhang et al. 2001, Eom et al. 2003). There is also evidence that ZBP1 may be transported by myosinVa to axons (Nalavadi et al. 2012). ZBP1 remains bound to β-actin mRNA after

it reaches the growth cone and it represses translation by blocking recruitment of the 60s ribosomal subunit (Huttelmaier et al 2005). The critical signaling event that activates β-actin translation is phosphorylation of the ZBP1 at the Y396 residue by Src tyrosine kinase. When the attractive guidance cue BDNF binds to a growth cone receptor, Src phosphorylation causes ZBP1 to dissociate from β-actin mRNA, which initiates translation. Src is activated asymmetrically on the side of the growth closest to the BDNF source *in vitro* (Huttelmaier 2005, Sasaki 2010, Yao 2006).

ZBP1 is required for growth cone turning *in vitro*

ZBP1 has a well-understood role in regulating local β-actin translation during axon guidance *in vitro* (Figure 1.3). ZBP1 function is essential for transport of β-actin mRNA to the growth cone, and for regulating β-actin translation. ZBP1-dependent local translation of β-actin in response to attractive guidance cues is required for growth cone turning. Intriguingly, while ZBP1 is not an ABP, it is similar in the sense that it regulates β-actin mRNA by sequestering it in a translationally inactive state by preventing ribosomal assembly on the mRNA. It is also a target of Src activity, which is known to regulate actin dynamics in the growth cone in response to guidance cues. ZBP1 is the target of BDNF induced signaling which activates translation. Therefore, ZBP1 is a regulator of actin dynamics that promote growth cone turning in response to attractive guidance cues from mRNA translation, and β-actin protein is translated on the side of te growth cone closest to the source. Assymetric activation of polymerization drives attractive turning.

It is not clear whether or noth ZBP1 function is required for axon guidance *in vivo*. ZBP1 has been genetically deleted in mice. Homozygous $ZBP1^{-/-}$ mutation causes

Figure 1.3: ZBP1-dependent local β-actin translation in response to an attractive guidance cue. The β-actin zipcode in the mRNA 3'UTR binds directly to the KH34 domains of ZBP1, which represses translation. When an attractive guidance cue binds to growth cone receptors, Src phosphorylates Y396 and ZBP1 dissociates from the β-actin zipcode to allow local translation of β-actin.

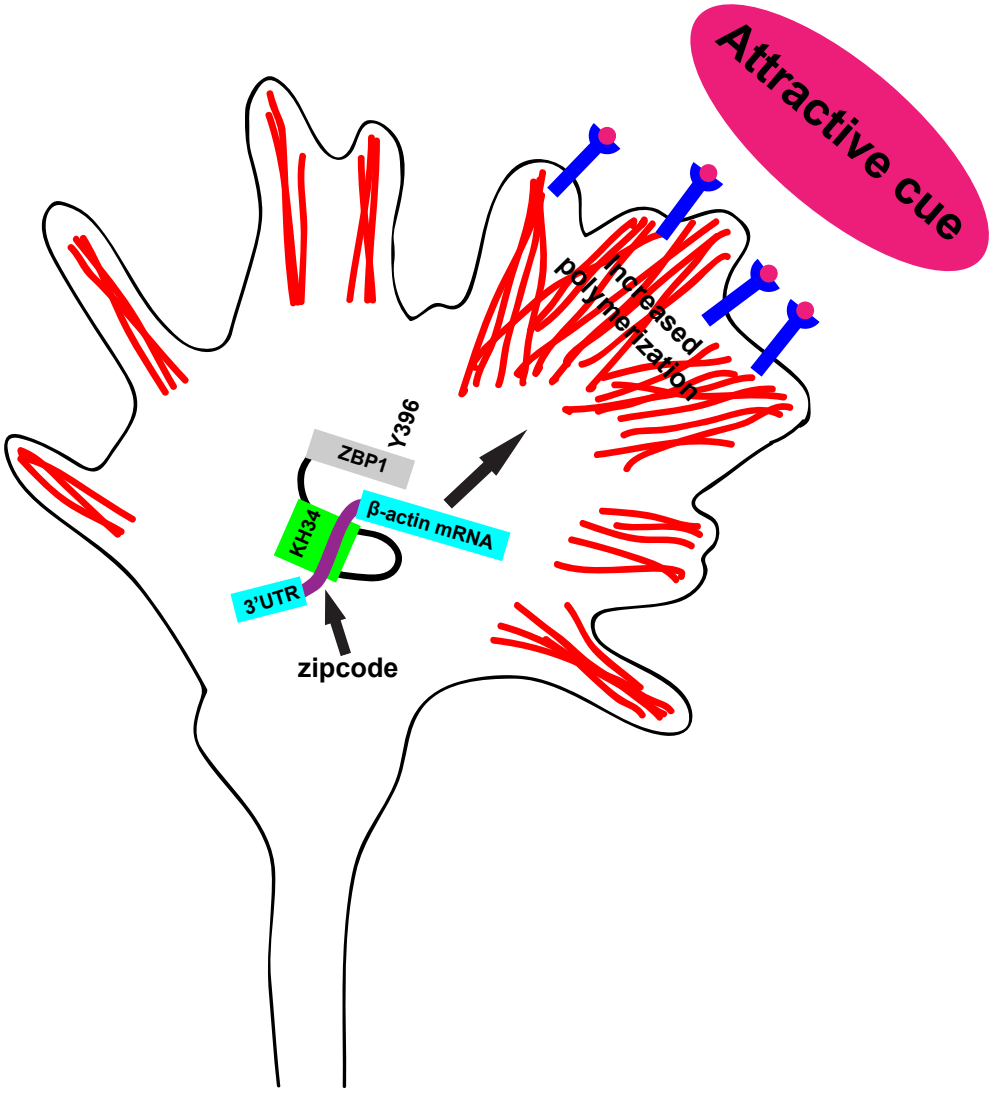
Attractive cue
Increased polymerization
Y396
ZBP1
KH34
β-actin mRNA
3'UTR
zipcode

embryonic lethality. Heterozygous ZBP1$^{+/-}$ carriers survive, but do not have obvious axon guidance defects. However, axon regeneration after crush injury is slower and branching during this process is deficient (Donnelly et al. 2011). A recent study in *Xenopus laevis* was aimed at determining whether Vg1RBP is required for RGC axon guidance *in vivo* (Kalous et al. 2014). Vg1RBP translation was blocked with a morpholino oligonucleotide (MO). Endogenous Vg1RBP function was also perturbed by expression of a dominant negative form of Vg1RBP in RGCs. It was concluded that long-range RGC axon growth and guidance do not require VgRBP1function. However, axon branching and arbor formation on the optic tectum was defective. To date there is no direct evidence that ZBP1 function is required for axon specification, elongation, maintenance, or growth cone turning *in vivo*.

Zebrafish retinotectal system as an *in vivo* model for axon guidance

Zebrafish or *Danio rerio* are small tropical fish found in freshwater rivers in India, Pakistan, and South-East Asia. Adult zebrafish develop to reproductive maturity in 2-3 months and can produce embryos for over 2 years. Spawning can be controlled using a predictable light dark cycle. One adult pair can consistently produce hundreds of embryos in a day, up to once every 7 days (Glass and Dahm 2004). Zebrafish embryos have translucent skin and pigment formation can be inhibited with phenylthiourea (PTU) treatment, making a powerful model for *in vivo* imaging. High-resolution imaging can be performed with a confocal microscope. Figure 1.4A-C show images taken from live 3dpf zebrafish, including whole embryo (Figure 1.4A), a lateral view of RGC axons in the optic tract (Figure 1.4B), and a single RGC axon in the optic tract (Figure 1.4C). These examples illustrate the diversity and strength of imaging live zebrafish embryos.

Figure 1.4: Images of live and fixed 3dpf zebrafish embryos. A whole embryo in A taken under a dissecting microscope, RGCs growing though the optic tract with a 40x water lens with a confocal microscope (B), and a single RGC axon growing through the optic tract (C). D shows a coronal view made from a 3D reconstruction in Fluorender (Wan et al. 2013) from a confocal dataset from a 3 dpf Tg(isl2b:mCherryCAAX)^{ZC23} embryo, showing that all RGC axons project contralaterally to the opposite tectum relative to the eye.

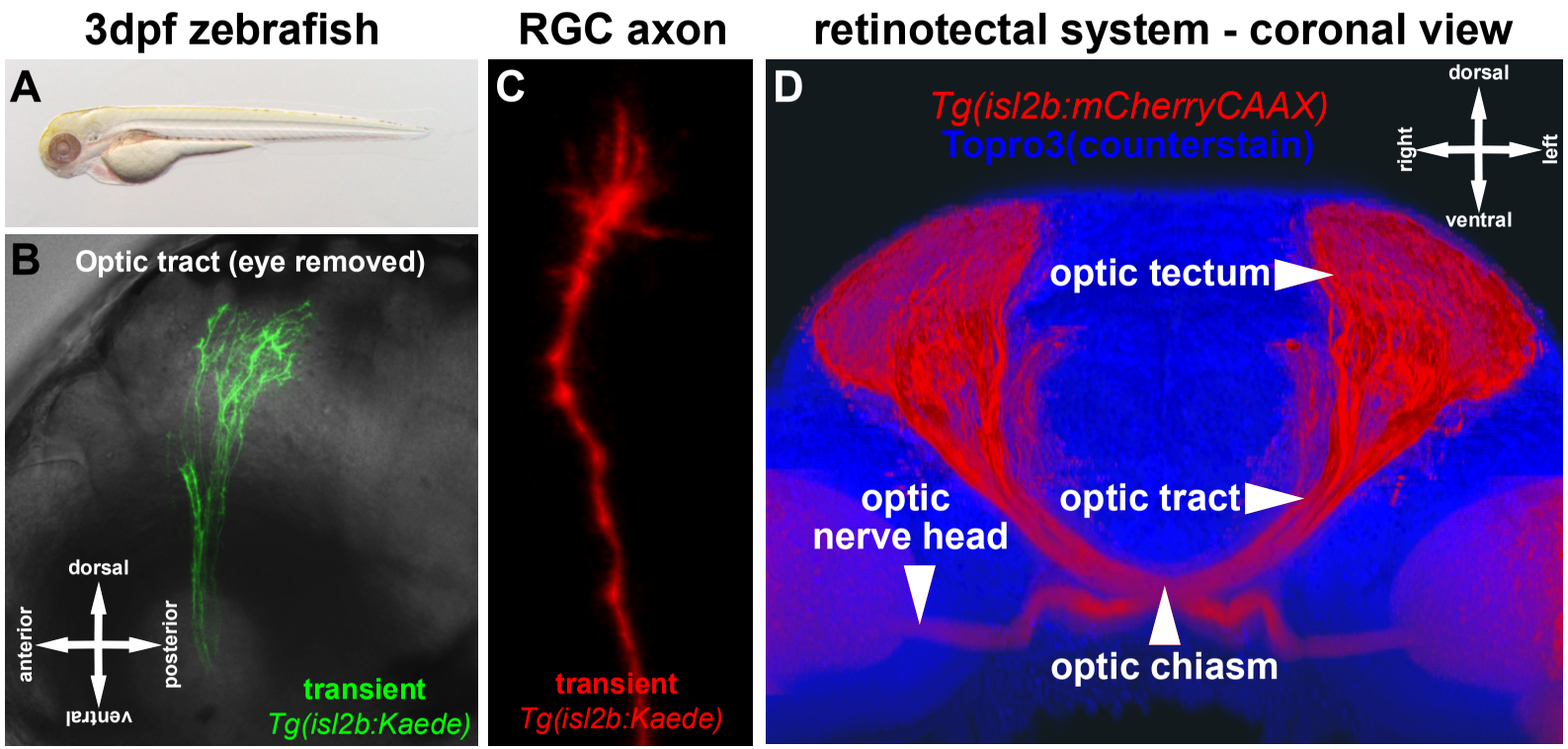
3dpf zebrafish
RGC axon
retinotectal system - coronal view
A
B
Optic tract (eye removed)
dorsal
anterior
posterior
ventral
transient
Tg(isl2b:Kaede)
C
transient
Tg(isl2b:Kaede)
D
Tg(isl2b:mCherryCAAX)
Topro3(counterstain)
dorsal
right
left
ventral
optic tectum
optic
nerve head
optic tract
optic chiasm

The zebrafish retinotectal projection is formed by retinal ganglion cell (RGC) axons, which transmit visual information from the eye to the contralateral optic tectum in the midbrain. RGC cell bodies form the inner most layer in the retina adjacent to the lens. RGC development begins at 28 hours postfertilization (hpf) when the first RGCs are born. The first RGC axons exit the eye (Figure 1.5-1) through the optic disc at 30-32 hpf, cross the midline ventrally at the optic chiasm (Figure 1.5-2) at 34-36 hpf, and project dorsally through the optic tract (Figure 1.5-3) to the tectum (Figure 1.5-4), where they terminate at 48 hpf. All RGC axons project to the contralateral tectum (Figure 1.4D) due to lack of binocular vision. RGC axons are arranged topographically along the anterior posterior axis and the dorsal ventral axis on the tectum according to their position in the retina (Stuermer 1988) (Figure 1.5).

Transient or stable transgenic lines that express fluorescent proteins in RGCs can be generated with ease and provide a method to take high-resolution timelapse datasets of pathfinding RGC axons (Kwan et al. 2007, Pittman et al. 2008). Also, forward genetic screens have identified many mutants with retinotectal defects with mutations in genes with important function in RGC axon guidance (Baier et al. 1996, Karlstrom et al. 1996, Trowe et al. 1996). Recently, reverse genetics have become possible with the development of gene targetting strategies. Morpholino oligonucleotides are a simple and effective tool that can be used to target to knockdown expression of a specific gene. The zebrafish retinotectal projection is a powerful model to study axon guidance *in vivo*. The technical strength of this system comes from the imaging capabilities as well as the available molecular tools that can be used to test gene functions during axon guidance.

Figure 1.5: Dorsal view of a 3dpf zebrafish head. Imaged with a confocal microscope (20x lens), showing the retinotectal projection (3D reconstruction rendered with Fluorender software (Wan et al. 2013). RGC cell bodies are in the retina (green) and axons (red) exit the eye (1), project across the midlne through the optic chiasm (2), project through the optic tract (3) to the tectum (4) where they terminate and form arbors.

Zebrafish retinotectal system - dorsal view

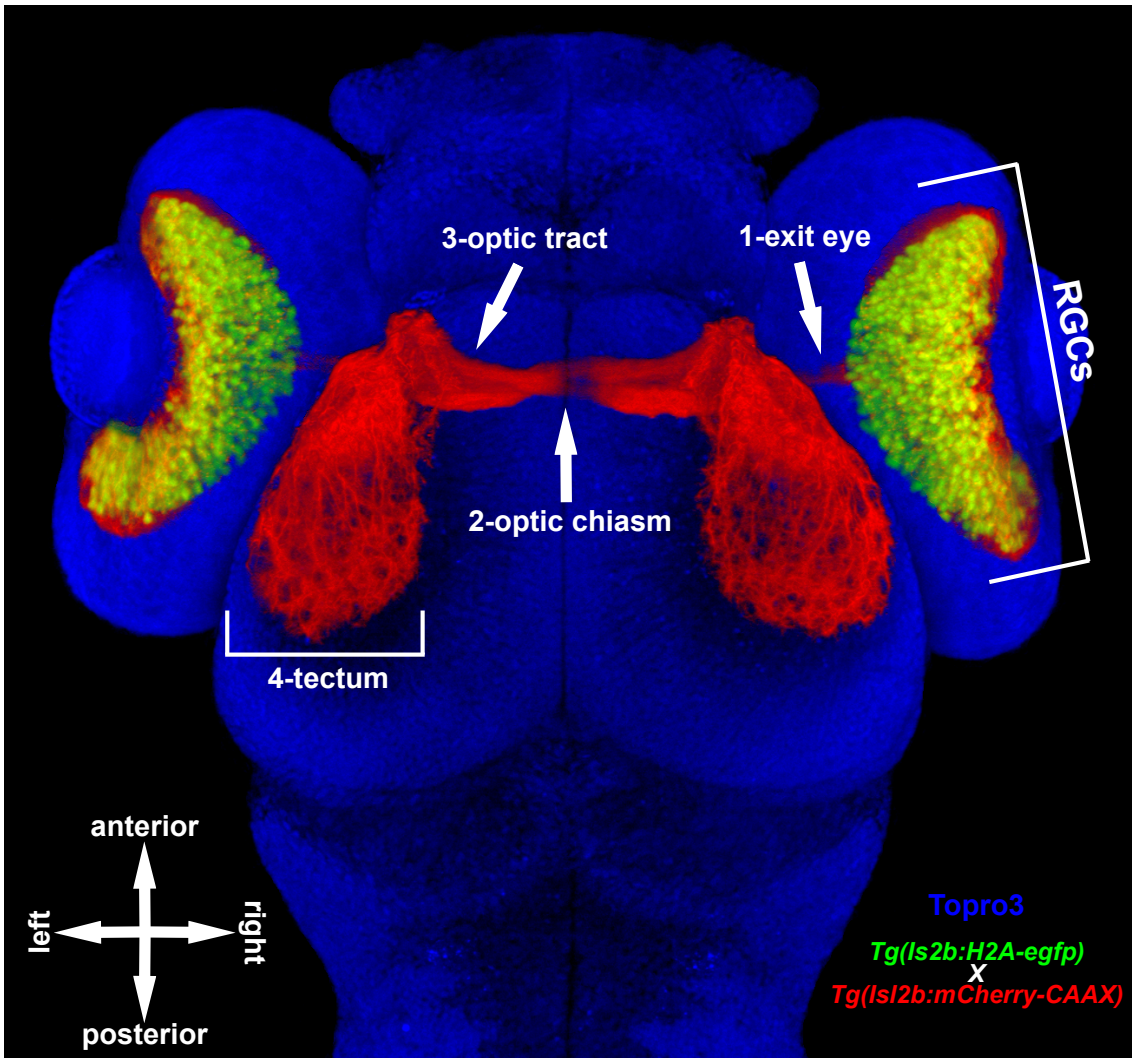

Research summary

For Chapter 2, I tested whether Cyfip2 functions cell autonomously during RGC axon guidance. First, I adapted a technique for *in vivo* single cell focal electroporation to zebrafish RGCs and used it to express cDNA constructs during pathfinding. I targeted dorsonasal RGCs and coexpressed enhanced green fluorescenct protein (EGFP) and wild-type Cyfip2 to visualize RGC axons and to rescue the missorting phenotype in homozygous nevermind/Cyfip2 mutants.

For Chapter 3, I investigated local translation and the function of ZBP1 function during RGC axon pathfinding *in vivo*. I adapted a local translation assay that exploits the irreversible photoconversion of the fluorescent protein Kaede to demonstrate the ability of the β-actin 3'UTR to target local Kaede translation in RGC growth cones *in vivo*. I used phylogenic analysis to identify Igf2bp1 as the ZBP1 ortholog in zebrafish and showed that it is expressed in RGCs during axon guidance. I also describe defects caused by Igf2bp1 splice-blocking MO (sbMO) injection, including increased cell death, undeveloped retina, and underdeveloped retinotectal projection. I also used a dominant negative to show that loss of Igf2bp1 function in RGCs prevents axons from growing to the tectum.

In summary, I adapted a technically challenging technique to target cDNA expression to single RGCs cells and used it to demonstrate that cell autonomous function of Cyfip2 is required during dorsonasal RGC pathfinding. I adapted a local translation assay using *in vivo* timelapse imaging to demonstrate that the β-actin 3'UTR is sufficient to target Kaede for local translation in RGC growth cones. Finally, I characterized the

expression of the zebrafish ZBP1 ortholog, Igf2bp1, and provided the first evidence that Igf2bp1 function is required for axon guidance *in vivo*.

References

Akten, B., Kye, M. J., Hao, L. T., Wertz, M. H., Singh, S., Nie, D., Sahin, M. (2011). Interaction of survival of motor neuron (SMN) and HuD proteins with mRNA cpg15 rescues motor neuron axonal deficits. Proceedings of the National Academy of Sciences of the United States of America, 108(25), 10337–10342.

Alvarez-Fischer, D., Fuchs, J., Castagner, F., Stettler, O., Massiani-Beaudoin, O., Moya, K. L., Prochiantz, A. (2011). Engrailed protects mouse midbrain dopaminergic neurons against mitochondrial complex I insults. Nature Neuroscience, 14(10), 1260-1266.

Andreassi, C., Zimmermann, C., Mitter, R., Fusco, S., De Vita, S., Devita, S. Riccio, A. (2010). An NGF-responsive element targets myo-inositol monophosphatase-1 mRNA to sympathetic neuron axons. Nature Neuroscience, 13(3), 291–301.

Ascano, M., Mukherjee, N., Bandaru, P., Miller, J. B., Nusbaum, J. D., Corcoran, D. L., Tuschl, T. (2012). FMRP targets distinct mRNA sequence elements to regulate protein expression. Nature, 492(7429), 382–386.

Aschrafi, A., Natera-Naranjo, O., Gioio, A. E., Kaplan, B. B. (2010). Regulation of axonal trafficking of cytochrome c oxidase IV mRNA. Molecular and Cellular Neurosciences, 43(4), 422–430.

Baier, H., Klostermann, S., Trowe, T., Karlstrom, R. O., Nüsslein-Volhard, C., Bonhoeffer, F. (1996). Genetic dissection of the retinotectal projection. Development, 123, 415–425.

Baraban, M., Anselme, I., Schnieder-Maunuory, S., Guidicelli, F. (2013). Zebrafish embryonic neurons transport messenger RNA to axons and growth cones *in vivo.* The Journal of Neuroscience, 33(40), 15726-15724.

Bard, L., Boscher, C., Lambert, M., Mège, R.-M., Choquet, D., Thoumine, O. (2008). A molecular clutch between the actin flow and N-cadherin adhesions drives growth cone migration. The Journal of Neuroscience, 28(23), 5879–5890.

Bassell, G. J., Zhang, H., Byrd, A. L., Femino, A. M., Singer, R. H., Taneja, K. L., Kosik, K. S. (1998). Sorting of beta-actin mRNA and protein to neurites and growth cones in culture. The Journal of Neuroscience*,* 18(1), 251–265.

Battye, R., Stevens, A., Jacobs, J. R. (1999). Axon repulsion from the midline of the Drosophila CNS requires slit function. Development, 126(11), 2475–2481.

Baudet, M.-L., Zivraj, K. H., Abreu-Goodger, C., Muldal, A., Armisen, J., Blenkiron, C., Holt, C. E. (2012). miR-124 acts through CoREST to control onset of Sema3A sensitivity in navigating retinal growth cones. Nature Neuroscience, 15(1), 29–38.

Bear, J. E., Svitkina, T. M., Krause, M., Schafer, D. A, Loureiro, J. J., Strasser, G. A., Gertler, F. B. (2002). Antagonism between Ena/VASP proteins and actin filament capping regulates fibroblast motility. Cell, 109(4), 509–521.

Bear, M. F., Dölen, G., Osterweil, E., Nagarajan, N. (2008). Fragile X: translation in action. Neuropsychopharmacology, 33(1), 84–87.

Bianco, I. H., Carl, M., Russell, C., Clarke, J. D. W., Wilson, S. W. (2008). Brain asymmetry is encoded at the level of axon terminal morphology. Neural Development, 3, 9.

Breitsprecher, D., Kiesewetter, A. K., Linkner, J., Urbanke, C., Resch, G. P., Small, J. V., Faix, J. (2008). Clustering of VASP actively drives processive, WH2 domain-mediated actin filament elongation. The EMBO Journal, 27(22), 2943–2954.

Briançon-Marjollet, A., Ghogha, A., Nawabi, H., Triki, I., Auziol, C., Fromont, S., Lamarche-Vane, N. (2008). Trio mediates netrin-1-induced Rac1 activation in axon outgrowth and guidance. Molecular and Cellular Biology, 28(7), 2314–2323.

Brittis, P. A, Lu, Q., Flanagan, J. G. (2002). Axonal protein synthesis provides a mechanism for localized regulation at an intermediate target. Cell, 110(2), 223–235.

Brunet, I., Weinl, C., Piper, M., Trembleau, A., Volovitch, M., Harris, W., Holt, C. (2005). The transcription factor Engrailed-2 guides retinal axons. Nature, 438(7064), 94–98.

Bunge, M. B. (1973). Fine structure of nerve fibers and growth cones of isolated sympathetic neurons in culture. The Journal of Cell Biology, 56, 713-735.

Buxbaum, A. R., Wu, B., Singer, R. H. (2014). Single β-actin mRNA detection in neurons reveals a mechanism for regulating its translatability. Science, 343(6169), 419–422.

Campbell, D. S., Holt, C. E. (2001). Chemotropic responses of retinal growth cones mediated by rapid local protein synthesis and degradation. Neuron, 32(6), 1013–1026.

Carlier, M.-F., Pantaloni, D. (2007). Control of actin assembly dynamics in cell motility. The Journal of Biological Chemistry, 282(32), 23005–23009.

Castellani, V., Chédotal, A., Schachner, M., Faivre-Sarrailh, C., Rougon, G. (2000). Analysis of the L1-deficient mouse phenotype reveals cross-talk between Sema3A and L1 signaling pathways in axonal guidance. Neuron, 27(2), 237–249.

Caudy, A. A., Myers, M., Hannon, G. J., Hammond, S. M. (2002). Fragile X-related protein and VIG associate with the RNA interference machinery. Genes and Development, 16(19), 2491–2496.

Chao, J. A., Patskovsky, Y., Patel, V., Levy, M., Almo, S. C., Singer, R. H. (2010). ZBP1 recognition of beta-actin zipcode induces RNA looping. Genes and Development, 24(2), 148–158.

Charron, F., Stein, E., Jeong, J., McMahon, A. P., Tessier-Lavigne, M. (2003). The morphogen sonic hedgehog is an axonal chemoattractant that collaborates with netrin-1 in midline axon guidance. Cell, 113(1), 11–23.

Chartrand, P., Meng, X. H., Singer, R. H., Long, R. M. (1999). Structural elements required for the localization of ASH1 mRNA and of a green fluorescent protein reporter particle *in vivo*. Current Biology, 9(6), 333–336.

Cheng, H. J., Nakamoto M., Bergemann, A. D., Flanagan, J. G. (1995). Complementary gradients and binding of ELF-1 and Mek4 in development of the topographic retinotectal projection map. Cell, 82(1), 371-381.

Cheng, H. J., Bagri, A, Yaron, A., Stein, E., Pleasure, S. J., Tessier-Lavigne, M. (2001). Plexin-A3 mediates semaphorin signaling and regulates the development of hippocampal axonal projections. Neuron, 32(2), 249–263.

Coffee, R. L., Williamson, A. J., Adkins, C. M., Gray, M. C., Page, T. L., Broadie, K. (2012). *In vivo* neuronal function of the fragile X mental retardation protein is regulated by phosphorylation. Human Molecular Genetics, 21(4), 900–915.

Cox, L. J., Hengst, U., Gurskaya, N. G., Lukyanov, K. A., Jaffrey, S. R. (2008). Intra-axonal translation and retrograde trafficking of CREB promotes neuronal survival. Nature Cell Biology, 10(2), 149–159.

Crick, F. (1970). Central dogma of molecular biology. Nature, 227, 561-563.

Culotti, J. G., Merzt, D. C. (1998). DCC and netrins. Current Opinion in Cell Biology, 10, 609–613.

Dajas-Bailador, F., Bonev, B., Garcez, P., Stanley, P., Guillemot, F., Papalopulu, N. (2012). microRNA-9 regulates axon extension and branching by targeting Map1b in mouse cortical neurons, Nature Neuroscience, 15(5), 697-699.

Darnell, J. C., Van Driesche, S. J., Zhang, C., Hung, K. Y. S., Mele, A., Fraser, C. E., Darnell, R. B. (2011). FMRP stalls ribosomal translocation on mRNAs linked to synaptic function and autism. Cell, 146, 247-261.

Dent, E. W., Gertler, F. B. (2003). Cytoskeletal dynamics and transport in growth cone motility and axon guidance. Neuron, 40(2), 209–227.

Dent, E. W., Gupton, S. L., Gertler, F. B. (2011). The growth cone cytoskeleton in axon outgrowth and guidance. Cold Spring Harbor Perspectives in Biology, 3(3).

Dickson, B. J. (2002). Molecular mechanisms of axon guidance. Science, 298, 1959-1964.

Dickson, B. J., Giorgio, F. G. (2006). Regulation of commissural axon pathfinding by slit and its robo receptors. Annual Review of Cell and Developmental Biology, 22, 651-675.

Drescher, U., Kremoser, C., Handwerker, C., Löschinger, J., Noda, M., Bonhoeffer, F. (1995). *In vitro* guidance of retinal ganglion cell axons by RAGS, a 25 kDa tectal protein related to ligands for Eph receptor tyrosine kinases. Cell, 82(3), 359–370.

Edbauer, D., Neilson, J. R., Foster, K. A., Wang, C.-F., Seeburg, D. P., Batterton, M. N., Sheng, M. (2010). Regulation of synaptic structure and function by FMRP-associated microRNAs miR-125b and miR-132. Neuron, 68(1), 161–161.

Eden, S., Rohatgi, R., Podtelejnikov, A. V., Mann, M., Kirschner, M. W. (2002). Mechanism of regulation of WAVE1-induced actin nucleation by Rac1 and Nck. Nature, 418(6899), 790–793.

Eng, H., Lund, K., Campenot, R. B. (1999). Synthesis of beta-tubulin, actin, and other proteins in axons of sympathetic neurons in compartmented cultures. The Journal of Neuroscience, 19(1), 1–9.

Eom, T., Antar, L. N., Singer, R. H., Bassell, G. J. (2003). Localization of a beta-actin messenger ribonucleoprotein complex with zipcode-binding protein modulates the density of dendritic filopodia and filopodial synapses. The Journal of Neuroscience, 23(32), 10433–10444.

Etienne-Manneville, S., Hall, A. (2002). Rho GTPases in cell biology. Nature, 420(6916), 629–635.

Fallini, C., Rouanet, J. P., Donlin-Asp, P. G., Guo, P., Zhang, H., Singer, R. H., Bassell, G. J. (2014). Dynamics of survival of motor neuron (SMN) protein interaction with the mRNA-binding protein IMP1 facilitates its trafficking into motor neuron axons. Developmental Neurobiology, 74(3), 319–332.

Feldheim, D. A., Kim, Y. I., Bergemann, A. D., Frisén, J., Barbacid, M., Flanagan, J. G. (2000). Genetic analysis of ephrin-A2 and ephrin-A5 shows their requirement in multiple aspects of retinocollicular mapping. Neuron, 25(3), 563–574.

Flynn, K. C., Pak, C. W., Shaw, A. E., Bradke, F., Bamburg, J. R. (2009). Growth cone-like waves transport actin and promote axonogenesis and neurite branching. Developmental Neurobiology, 69(12), 761–779.

Fricke, C., Lee, J. S., Geiger-Rudolph, S., Bonhoeffer, F., Chien, C. B. (2001). Astray, a zebrafish roundabout homolog required for retinal axon guidance. Science, 292(5516), 507–510.

Gao, Y., Tatavarty, V., Korza, G., Levin, M. K., Carson, J. H. (2008). Multiplexed dendritic targeting of calcium calmodulin-dependent protein kinase I, neurogranin, and activity-regulated cytoskeleton-associated protein RNAs by the A2 pathway, Molecular Biology of the Cell 19, 2311–2327.

Garber, K. B., Visootsak, J., Warren, S. T. (2008). Fragile X syndrome. European Journal of Human Genetics, 16(6), 666–672.

Giordano, S., Corso, S., Conrotto, P., Artigiani, S., Gilestro, G., Barberis, D., Comoglio, P. M. (2002). The semaphorin 4D receptor controls invasive growth by coupling with Met. Nature Cell Biology, 4(9), 720–724.

Giuditta, A., Dettbarn, W.-D., Brzin, M. (1968) Protein synthesis in the isolated giant axon of the squid. Woods Hole, 59, 1284-1287.

Giuditta, A., Hunt, T., Santella, L. (1986). Rapid important paper, Neurochemistry International, 8(3), 435–442.

Gomez, T. M., Letourneau, P. C. (2013). Actin dynamics in growth cone motility and navigation. Journal of Neurochemistry, 129, 229-234.

Guirland, C., Buck, K. B., Gibney, J. A., DiCicco-Bloom, E., Zheng, J. Q. (2003). Direct cAMP signaling through G-protein-coupled receptors mediates growth cone attraction induced by pituitary adenylate cyclase-activating polypeptide. The Journal of Neuroscience, 23(6), 2274–2283.

Gumy, L. F., Yeo, G. S. H., Tung, Y.-C. L., Zivraj, K. H., Willis, D., Coppola, G., Fawcett, J. W. (2011). Transcriptome analysis of embryonic and adult sensory axons reveals changes in mRNA repertoire localization. RNA, 17(1), 85–98.

Gundersen, R. W., Barrett, J. N. (1980). Characterization of the turning response of dorsal root neurites toward nerve growth factor establishing the drug gradient, The Journal of Cell Biology, 87, 546-554.

Hall, A., Lalli, G. (2010). Rho and Ras GTPases in axon growth, guidance, and branching. Cold Spring Harbor Perspectives in Biology, 2(2), 1-18.

Hanson, J. E., Madison, D. V. (2007). Presynaptic FMR1 genotype influences the degree of synaptic connectivity in a mosaic mouse model of fragile X syndrome. The Journal of Neuroscience, 27(15), 4014–4018.

Harris, W. A., Holt, C. E., Bonhoeffer, F. (1987). Retinal axons with and without their somata, growing to and arborizing in the tectum of *Xenopus* embryos: a time-lapse video study of single fibres *in vivo*. Development, 101(1), 123–33.

Hedgcock, E. M., Culotti, J. G., Hall, D. H. (1990). The unc-5 and unc-40 genes guide circumferential migration of pioneer axons and mesodermal cells on the epidermis in *c. elegans*. Neuron, 2, 61-85.

Hengst, U., Deglincerti, A., Kim, H. J., Jeon, N. L., Jaffrey, S. R. (2009). Axonal elongation triggered by stimulus-induced local translation of a polarity complex protein. Nature Cell Biology, 11(8), 1024–1030.

Hindges, R., McLaughlin, T., Genoud, N., Henkemeyer, M., O'Leary, D. D. M. (2002). EphB forward signaling controls directional branch extension and arborization required for dorsal-ventral retinotopic mapping. Neuron, 35(3), 475–487.

Holt, C. E., Bullock, S. L. (2009). Subcellular mRNA localization in animal cells and why it matters. Science, 326(5957), 1212–1216.

Hu, M., Easter, S. S. (1999). Retinal neurogenesis: the formation of the initial central patch of postmitotic cells. Developmental Biology, 207(2), 309–321.

Hua, J. Y., Smith, S. J. (2004). Neural activity and the dynamics of central nervous system development. Nature Neuroscience, 7(4), 327–332.

Hutson, L. D., Chien, C. Bin. (2002). Pathfinding and error correction by retinal axons: the role of astray/robo2. Neuron, 33(2), 205–217.

Hüttelmaier, S., Zenklusen, D., Lederer, M., Dictenberg, J., Lorenz, M., Meng, X., Singer, R. H. (2005). Spatial regulation of beta-actin translation by Src-dependent phosphorylation of ZBP1. Nature, 438(7067), 512–515.

Isbister, C. M., Connor, T. P. O. (2000). Mechanisms of Growth Cone Guidance and Motility in the Developing Grasshopper Embryo, Neurobiology, 44, 271–280.

Je, H. S., Ji, Y., Wang, Y., Yang, F., Wu, W., Lu, B. (2011). Presynaptic protein synthesis required for NT-3-induced long-term synaptic modulation. Molecular Brain, 4(1), 1-8.

Jen, J. C., Chan, W.-M., Bosley, T. M., Wan, J., Carr, J. R., Rüb, U., Engle, E. C. (2004). Mutations in a human ROBO gene disrupt hindbrain axon pathway crossing and morphogenesis. Science, 304(5676), 1509–1513.

Jin, M., Guan, C., Jiang, Y., Chen, G., Zhao, C., Cui, K., Yuan, X. (2005). Ca2+-dependent regulation of rho GTPases triggers turning of nerve growth cones. The Journal of Neuroscience, 25(9), 2338–2347.

Jin, P., Zarnescu, D. C., Ceman, S., Nakamoto, M., Mowrey, J., Jongens, T. A, Warren, S. T. (2004). Biochemical and genetic interaction between the fragile X mental retardation protein and the microRNA pathway. Nature Neuroscience, 7(2), 113–117.

Johnstone, O., Lasko, P. (2001). Translational regulation and RNA localization in drosophila oocytes and embryos. Annual Reviews Genetics, 35, 365–406.

Jung, H., Yoon, B. C., Holt, C. E. (2012). Axonal mRNA localization and local protein synthesis in nervous system assembly, maintenance and repair. Nature Reviews Neuroscience, 13(5), 308–324.

Jung, H., Gkogkas, C. G., Sonenberg, N., Holt, C. E. (2014). Remote control of gene function by local translation. Cell, 157, 26-40.

Jurney, W. M., Gallo, G., Letourneau, P. C., McLoon, S. C. (2002). Rac1-mediated endocytosis during ephrin-A2- and semaphorin 3A-induced growth cone collapse. The Journal of Neuroscience. 22(14), 6019–6028.

Kaczmarek, J. S., Riccio, A., Clapham, D. E. (2012). Calpain cleaves and activates the TRPC5 channel to participate in semaphorin 3A-induced neuronal growth cone collapse. Proceedings of the National Academy of Sciences, 109(20), 7888–7892.

Kalous, A., Stake, J. I., Yisraeli, J. K., Holt, C. E. (2014). RNA-binding protein Vg1RBP regulates terminal arbor formation but not long-range axon navigation in the developing visual system. Developmental Neurobiology, 74(3), 303–318.

Karakozova, M., Kozak, M., Wong, C. C. L., Bailey, A. O., Yates, J. R., Mogilner, A., Kashina, A. (2006). Arginylation of beta-actin regulates actin cytoskeleton and cell motility. Science, 313(5784), 192–196.

Karlstrom, R. O., Trowe, T., Klostermann, S., Baier, H., Brand, M., Crawford, A. D., Bonhoeffer, F. (1996). Zebrafish mutations affecting retinotectal axon pathfinding. Development, 123, 427–438.

Kato, M., Han, T. W., Xie, S., Shi, K., Du, X., Wu, L. C., McKnight, S. L. (2012). Cell-free formation of RNA granules: low complexity sequence domains form dynamic fibers within hydrogels. Cell, 149(4), 753–767.

Katz, Z. B., Wells, A. L., Park, H. Y., Wu, B., Shenoy, S. M., Singer, R. H. (2012). β-Actin mRNA compartmentalization enhances focal adhesion stability and directs cell migration. Genes and Development, 26(17), 1885–1890.

Keleman, K., Dickson, B. J. (2001). Short- and long-range repulsion by the Drosophila Unc5 netrin receptor. Neuron, 32(4), 605–617.

Keleman, K., Rajagopalan, S., Cleppien, D., Teis, D., Paiha, K., Huber, L. A, Dickson, B. J. (2002). Comm sorts robo to control axon guidance at the Drosophila midline. Cell, 110(4), 415–427.

Keleman, K., Ribeiro, C., Dickson, B. J. (2005). Comm function in commissural axon guidance: cell-autonomous sorting of Robo *in vivo*. Nature Neuroscience, 8(2), 156–163.

Kennedy, T. E., Serafini, T., de la Torre, J. R., Tessier-Lavigne, M. (1994). Netrins are diffusible chemotropic factors for commissural axons in the embryonic spinal cord. Cell, 78(3), 425–435.

Kerstein, P. C., Jacques-Fricke, B. T., Rengifo, J., Mogen, B. J., Williams, J. C., Gottlieb, P. A., Gomez, T. M. (2013). Mechanosensitive TRPC1 channels promote calpain proteolysis of talin to regulate spinal axon outgrowth. The Journal of Neuroscience, 33(1), 273-285.

Kidd, T., Brose, K., Mitchell, K. J., Fetter, R. D., Tessier-lavigne, M., Goodman, C. S., Tear, G. (1998). Roundabout controls axon crossing of the CNS midline and defines a novel subfamily of evolutionarily conserved guidance receptors. Cell, 92, 205–210.

Kidd, T., Bland, K. S., Goodman, C. S. (1999). Slit is the midline repellent for the robo receptor in Drosophila. Cell, 96(6), 785–794.

Kiebler, M. A, Bassell, G. J. (2006). Neuronal RNA granules: movers and makers. Neuron, 51(6), 685–690.

Kim-Ha, J., Kerr, K., Macdonald, P. M. (1995). Translational regulation of oskar mRNA by bruno, an ovarian RNA-binding protein, is essential. Cell, 81(3), 403–412.

Kislauskis, E. H., Zhu, X., Singer, R. H. (1994). Sequences responsible for intracellular localization of beta-actin messenger RNA also affect cell phenotype. The Journal of Cell Biology, 127(2), 441–451.

Kiuchi, T., Nagai, T., Ohashi, K., Mizuno, K. (2011). Measurements of spatiotemporal changes in G-actin concentration reveal its effect on stimulus-induced actin assembly and lamellipodium extension. Journal of Cell Biology, 193(2), 365-380.

Knöll, B., Drescher, U. (2004). Src family kinases are involved in EphA receptor-mediated retinal axon guidance. The Journal of Neuroscience, 24(28), 6248–6257.

Koenig, E. (1991). Evaluation of local synthesis of axonal proteins in the goldfish Mauthner cell axon and axons of dorsal and ventral roots of the rat *in vitro*. Molecular and Cellular Neurosciences, 2(5), 384–394.

Koenig, E., Martin, R., Titmus, M., Sotelo-Silveira, J. R. (2000). Cryptic peripheral ribosomal domains distributed intermittently along mammalian myelinated axons. The Journal of Neuroscience, 20(22), 8390–8400.

Kolodkin, A. L., Matthes, D. J., O'Connor, T. P., Patel, N. H., Admon, A., Bentley, D., Goodman, C. S. (1992). Fasciclin IV: sequence, expression, and function during growth cone guidance in the grasshopper embryo. Neuron, 9(5), 831–845.

Korn, E. D. (1982). Actin polymerization and its regulation by proteins from nonmuscle cells. Physiological Reviews, 62(2), 672–737.

Kundel, M., Jones, K. J., Shin, C. Y., Wells, D. G. (2009). Cytoplasmic polyadenylation element-binding protein regulates neurotrophin-3-dependent beta-catenin mRNA translation in developing hippocampal neurons. The Journal of Neuroscience, 29(43), 13630–13639.

Kuwako, K., Kakumoto, K., Imai, T., Igarashi, M., Hamakubo, T., Sakakibara, S., Okano, H. (2010). Neural RNA-binding protein Musashi1 controls midline crossing of precerebellar neurons through posttranscriptional regulation of Robo3/Rig-1 expression. Neuron, 67(3), 407–421.

Kwan, K. M., Fujimoto, E., Grabher, C., Mangum, B. D., Hardy, M. E., Campbell, D. S., Chien, C.-B. (2007). The Tol2kit: a multisite gateway-based construction kit for Tol2 transposon transgenesis constructs. Developmental Dynamics, 236(11), 3088–3099.

Lafont, F., Rouget, M., Rousselet, A, Valenza, C., Prochiantz, A. (1993). Specific responses of axons and dendrites to cytoskeleton perturbations: an *in vitro* study. Journal of Cell Science, 104, 433–443.

Lagercrantz, H., Ringstedt, T. (2001). Organization of the neuronal circuits in the central nervous system during development. Acta Paediatrica, 90(7), 707–715.

Lee, C. W., Vitriol, E. A., Shim, S., Wise, A. L., Velayutham, R. P., Zheng, J. Q. (2013). Dynamic localization of G-actin during membrane protrusion in neuronal motility. Current Biology, 23(12), 1046–1056.

Lefebvre, S., Bürglen, L., Reboullet, S., Clermont, O., Burlet, P., Viollet, L., Zeviani, M. (1995). Identification and characterization of a spinal muscular atrophy-determining gene. Cell, 80(1), 155–165.

Leung, K.-M., van Horck, F. P. G., Lin, A. C., Allison, R., Standart, N., Holt, C. E. (2006). Asymmetrical beta-actin mRNA translation in growth cones mediates attractive turning to netrin-1. Nature Neuroscience, 9(10), 1247–1256.

Leung, K.-M., Holt, C. E. (2008). Live visualization of protein synthesis in axonal growth cones by microinjection of photoconvertible Kaede into Xenopus embryos. Nature Protocols, 3(8), 1318–1327.

Lewis, K., Bridgman, C. (1992). Nerve growth cone lamellipodia contain two populations of actin filaments that differ in organization and polarity, The Journal of Cell Biology, 119(5), 1219–1243.

Li, H., Chen, J., Wu, W., Fagaly, T., Zhou, L., Yuan, W., Louis, S. (1999). Vertebrate slit, a secreted ligand for the transmembrane protein roundabout, is a repellent for olfactory bulb axons, Cell, 96, 807–818.

Li, L., Hutchins, B. I., Kalil, K. (2009). Wnt5a induces simultaneous cortical axon outgrowth and repulsive axon guidance through distinct signaling mechanisms, The Journal of Neuroscience 29(18), 5873–5883.

Li, W., Lee, J., Vikis, H. G., Lee, S.-H., Liu, G., Aurandt, J., Guan, K.-L. (2004). Activation of FAK and Src are receptor-proximal events required for netrin signaling. Nature Neuroscience, 7(11), 1213–1221.

Li, Y., Jia, Y.-C., Cui, K., Li, N., Zheng, Z.-Y., Wang, Y.-Z., Yuan, X.-B. (2005). Essential role of TRPC channels in the guidance of nerve growth cones by brain-derived neurotrophic factor. Nature, 434(7035), 894–898.

Li, Z., Aizenman, C. D., Cline, H. T., Brook, S., York, N. (2002). Regulation of rho GTPases by crosstalk and neuronal activity *in vivo*, Cell, 33, 741–750.

Lin, A. C., Holt, C. E. (2007). Local translation and directional steering in axons. The EMBO Journal, 26(16), 3729–3736.

Lin, A. C., Tan, C. L., Lin, C.-L., Strochlic, L., Huang, Y.-S., Richter, J. D., Holt, C. E. (2009). Cytoplasmic polyadenylation and cytoplasmic polyadenylation element-dependent mRNA regulation are involved in *Xenopus* retinal axon development. Neural Development, 4, 8.

Liu-Yesucevitz, L., Bassell, G. J., Gitler, A. D., Hart, A. C., Klann, E., Richter, J. D., Wolozin, B. (2011). Local RNA translation at the synapse and in disease. The Journal of Neuroscience, 31(45), 16086–16093.

Long, H., Sabatier, C., Ma, L., Plump, A., Yuan, W., Ornitz, D. M., Tessier-Lavigne, M. (2004). Conserved roles for Slit and Robo proteins in midline commissural axon guidance. Neuron, 42(2), 213–223.

Loudon, R. P., Silver, L. D., Yee, H. F., Gallo, G. (2006). RhoA-kinase and myosin II are required for the maintenance of growth cone polarity and guidance by nerve growth factor, Wiley Periodicals, 847–867.

Lowery, L. A., Vactor, D. Van. (2009). The trip of the tip: understanding the growth cone machinery, Nature Reviews, 10, 332-343.

Luo, Y., Raible, D., Raper, J. A. (1993). Collapsin: a protein in brain that induces the collapse and paralysis of neuronal growth cones. Cell, 75(2), 217–227.

Luo, L. (2000). Rho GTPases in neuronal morphogenesis. Nature Reviews Neuroscience, 1(3), 173–180.

Machesky, L. M., Mullins, R. D., Higgs, H. N., Kaiser, D. A., Blanchoin, L., May, R. C., Pollard, T. D. (1999). Scar, a WASP-related protein, activates nucleation of actin filaments by the Arp2/3 complex. Proceedings of the National Academy of Sciences, 96(7), 3739–3744.

Mallavarapu, A., Mitchison, T. (1999). Regulated actin cytoskeleton assembly at filopodium tips controls their extension and retraction. The Journal of Cell Biology, 146(5), 1097–1106.

Mann, F., Ray, S., Harris, W., Holt, C. (2002). Topographic mapping in dorsoventral axis of the *Xenopus* retinotectal system depends on signaling through ephrin-B ligands. Neuron, 35(3), 461–473.

Mann, F., Miranda, E., Weinl, C., Harmer, E., Holt, C. E. (2003). B-type eph receptors and ephrins induce growth cone collapse through distinct intracellular pathways. Jounal of Neurobiology, 57, 323-336.

Marsh, L., Letourneau, P. C. (1984). Growth of neurites without filopodial or lamellipodial activity in the presence of cytochalasin B. The Journal of Cell Biology, 99(6), 2041–2047.

Marsick, B. M., Flynn, K. C., Santiago-Medina, M., Bamburg, J. R., Letourneau, P. C. (2010). Activation of ADF/cofilin mediates attractive growth cone turning toward nerve growth factor and netrin-1. Developmental Neurobiology, 70(8), 565–588.

Marsick, B. M., Roche, F. K., Letourneau, P. C. (2012). Repulsive axon guidance cues ephrin-A2 and slit3 stop protrusion of the growth cone leading margin concurrently with inhibition of ADF/cofilin and ERM proteins. Cytoskeleton, 69(7), 496–505.

Marsick, B. M., San Miguel-Ruiz, J. E., Letourneau, P. C. (2012). Activation of ezrin/radixin/moesin mediates attractive growth cone guidance through regulation of growth cone actin and adhesion receptors. The Journal of Neuroscience, 32(1), 282–296.

Marston, D. J., Dickinson, S., Nobes, C. D. (2003). Rac-dependent trans-endocytosis of ephrinBs regulates Eph-ephrin contact repulsion. Nature Cell Biology, 5(10), 879–888.

McGovern, V. L., Seeger, M. A. (2003). Mosaic analysis reveals a cell-autonomous, neuronal requirement for Commissureless in the Drosophila CNS. Development Genes and Evolution, 213(10), 500–504.

Merianda, T. T., Lin, A. C., Lam, J. S. Y., Vuppalanchi, D., Willis, D. E., Karin, N., Twiss, J. L. (2009). A functional equivalent of endoplasmic reticulum and Golgi in axons for secretion of locally synthesized proteins. Molecular and Cellular Neurosciences, 40(2), 128–142.

Miki, H., Suetsugu, S., Takenawa, T. (1998). WAVE, a novel WASP-family protein involved in actin reorganization induced by Rac. The EMBO Journal, 17(23), 6932–6941.

Ming, G., Wong, S. T., Henley, J., Yuan, X., Song, H., Spitzer, N. C., Poo, M. (2002). Adaptation in the chemotactic guidance of nerve growth cones. Nature, 417(6887), 411–418.

Ming, G. L., Song, H. J., Berninger, B., Holt, C. E., Tessier-Lavigne, M., Poo, M. M. (1997). cAMP-dependent growth cone guidance by netrin-1. Neuron, 19(6), 1225–1235.

Mintz, C. D., Dickson, T. C., Gripp, M. L., Salton, S. R. J., Benson, D. L. (2003). ERMs colocalize transiently with L1 during neocortical axon outgrowth. The Journal of Comparative Neurology, 464(4), 438–448.

Muddashetty, R. S., Nalavadi, V. C., Gross, C., Yao, X., Xing, L., Laur, O., Bassell, G. J. (2011). Reversible inhibition of PSD-95 mRNA translation by miR-125a, FMRP phosphorylation, and mGluR signaling. Molecular Cell, 42(5), 673–688.

Myers, J. P., Santiago-Medina, M., Gomez, T. M. (2011). Regulation of axonal outgrowth and pathfinding by integrin-ECM interactions. Developmental Neurobiology, 71(11), 901–923.

Nakamura, A., Sato, K., Hanyu-Nakamura, K. (2004). Drosophila cup is an eIF4E binding protein that associates with Bruno and regulates oskar mRNA translation in oogenesis. Developmental Cell, 6(1), 69–78.

Nalavadi, V. C., Griffin, L. E., Picard-Fraser, P., Swanson, A. M., Takumi, T., Bassell, G. J. (2012). Regulation of zipcode binding protein 1 transport dynamics in axons by myosin Va. The Journal of Neuroscience, 32(43), 15133–15141.

Napoli, I., Mercaldo, V., Boyl, P. P., Eleuteri, B., Zalfa, F., De Rubeis, S., Bagni, C. (2008). The fragile X syndrome protein represses activity-dependent translation through CYFIP1, a new 4E-BP. Cell, 134(6), 1042–1054.

Narayanan, U., Nalavadi, V., Nakamoto, M., Thomas, G., Ceman, S., Bassell, G. J., Warren, S. T. (2008). S6K1 phosphorylates and regulates fragile X mental retardation protein (FMRP) with the neuronal protein synthesis-dependent mammalian target of rapamycin (mTOR) signaling cascade. The Journal of Biological Chemistry, 283(27), 18478–18482.

Natera-Naranjo, O., Aschrafi, A., Gioio, A. E., Kaplan, B. B. (2010). Identification and quantitative analyses of microRNAs located in the distal axons of sympathetic neurons. RNA, 16(8), 1516–1529.

Niederöst, B., Oertle, T., Fritsche, J., McKinney, R. A., Bandtlow, C. E. (2002). Nogo-A and myelin-associated glycoprotein mediate neurite growth inhibition by antagonistic regulation of RhoA and Rac1. The Journal of Neuroscience, 22(23), 10368–10376.

Nugent, A. A., Kolpak, A. L., Engle, E. C. (2012). Human disorders of axon guidance. Current Opinion in Neurobiology, 22(5), 837–843.

O'Connor, T. P., Duerr, J. S., Bently, D. (1990). Pioneer growth cone steering decisions mediated by single filopodial contacts *in situ*. The Journal of Neuroscience, 10(12), 3935-3946.

Okabe, S., Hirokawa, N. (1991). Actin dynamics in growth cones. The Journal of Neuroscience, 11(7), 1918–1929.

Pan, F., Hüttelmaier, S., Singer, R. H., Gu, W. (2007). ZBP2 facilitates binding of ZBP1 to beta-actin mRNA during transcription. Molecular and Cellular Biology, 27(23), 8340–8351.

Paquin, N., Ménade, M., Poirier, G., Donato, D., Drouet, E., Chartrand, P. (2007). Local activation of yeast ASH1 mRNA translation through phosphorylation of Khd1p by the casein kinase Yck1p. Molecular Cell, 26(6), 795–809.

Pellizzoni, L., Kataoka, N., Charroux, B., Dreyfuss, G. (1998). A novel function for SMN, the spinal muscular atrophy disease gene product, in pre-mRNA splicing. Cell, 95(5), 615–624.

Perycz, M., Urbanska, A. S., Krawczyk, P. S., Parobczak, K., Jaworski, J. (2011). Zipcode binding protein 1 regulates the development of dendritic arbors in hippocampal neurons. The Journal of Neuroscience, 31(14), 5271–5285.

Piazzon, N., Rage, F., Schlotter, F., Moine, H., Branlant, C., Massenet, S. (2008). *In vitro* and *in cellulo* evidences for association of the survival of motor neuron complex with the fragile X mental retardation protein. The Journal of Biological Chemistry, 283(9), 5598-5610.

Pinter, R., Hindges, R. (2010). Perturbations of microRNA function in mouse dicer mutants produce retinal defects and lead to aberrant axon pathfinding at the optic chiasm. PloS One, 5(4), e10021.

Piper, M., Georgas, K., Yamada, T., Little, M. (2000). Expression of the vertebrate Slit gene family and their putative receptors, the Robo genes, in the developing murine kidney. Mechanisms of Development, 94(1-2), 213–217.

Piper, M., Anderson, R., Dwivedy, A., Weinl, C., van Horck, F., Leung, K. M., Holt, C. (2006). Signaling mechanisms underlying Slit2-induced collapse of Xenopus retinal growth cones. Neuron, 49(2), 215–228.

Pittman, A. J., Gaynes, J. A., Chien, C.-B. (2010). Nev (Cyfip2) is required for retinal lamination and axon guidance in the zebrafish retinotectal system. Developmental Biology, 344(2), 784–794.

Pittman, A. J., Law, M.-Y., Chien, C.-B. (2008). Pathfinding in a large vertebrate axon tract: isotypic interactions guide retinotectal axons at multiple choice points. Development, 135(17), 2865–2871.

Pollard, T. D., Blanchoin, L., Mullins, R. D. (2000). Molecular mechanisms controlling actin filament dynamics in nonmuscle cells. Annual Reviews Biomolecular Structures, 29, 545-576.

Pollard, T. D., Borisy, G. G. (2003). Cellular motility driven by assembly and disassembly of actin filaments. Cell, 112(4), 453–465.

Polleux, F., Morrow, T., Ghosh, A. (2000). Semaphorin 3A is a chemoattractant for cortical apical dendrites. Nature, 404(6778), 567–573.

Polymerization, A., Wang, J., Boja, E. S., Tan, W., Tekle, E., Fales, H. M., English, S. (2001). Reversible glutathionylation regulates actin polymerization in A431 cells. The Journal of Biological Chemistry, 276(51), 47763–47766.

Quinn, C. C., Wadsworth, W. G. (2008). Axon guidance: asymmetric signaling orients polarized outgrowth. Trends in Cell Biology, 18(12), 597–603.

Rajagopalan, S., Vivancos, V., Nicolas, E., Dickson, B. J. (2000). Selecting a longitudinal pathway: Robo receptors specify the lateral position of axons in the Drosophila CNS. Cell, 103(7), 1033–1045.

Raper, J. A. (2000). Semaphorins and their receptors in vertebrates and invertebrates. Current Opinion in Neurobiology, 10(1), 88–94.

Renkema, G. H., Pulkkinen, K., Saksela, K. (2002). Cdc42 / Rac1-mediated activation primes PAK2 for superactivation by tyrosine phosphorylation Cdc42 / Rac1-mediated activation primes PAK2 for superactivation by tyrosine phosphorylation. Molecular and Cellular Biology, 22(19), 6719-6725.

Revenu, C., Athman, R., Robine, S., Louvard, D. (2004). The co-workers of actin filaments: from cell structures to signals. Nature Reviews. Molecular Cell Biology, 5(8), 635–646.

Richter, J. D. (1999). Cytoplasmic polyadenylation in development and beyond. Molecular Biology and Molecular Biology Reviews, 63(2), 446-456.

Robles, E., Huttenlocher, A., Gomez, T. M. (2003). Filopodial calcium transients regulate growth cone motility and guidance through local activation of calpain. Neuron, 38(4), 597–609.

Robles, E., Gomez, T. M. (2006). Focal adhesion kinase signaling at sites of integrin-mediated adhesion controls axon pathfinding. Nature Neuroscience, 9(10), 1274–1283.

Rosoff, W. J., Urbach, J. S., Esrick, M. A., McAllister, R. G., Richards, L. J., Goodhill, G. J. (2004). A new chemotaxis assay shows the extreme sensitivity of axons to molecular gradients. Nature Neuroscience, 7(6), 678–682.

Ross, A. F., Oleynikov, Y., Kislauskis, E. H., Taneja, K. L. (1997). Characterization of a beta-actin mRNA zipcode-binding protein. Molecular and Cellular Biology, 17(4), 2158-2165.

Rossoll, W., Jablonka, S., Andreassi, C., Kröning, A.-K., Karle, K., Monani, U. R., Sendtner, M. (2003). Smn, the spinal muscular atrophy-determining gene product, modulates axon growth and localization of beta-actin mRNA in growth cones of motoneurons. The Journal of Cell Biology, 163(4), 801–812.

Rotty, J. D., Wu, C., Bear, J. E. (2013). New insights into the regulation and cellular functions of the ARP2/3 complex. Nature Reviews. Molecular Cell Biology, 14(1), 7–12.

Sabatier, C., Plump, A. S., Le Ma, Brose, K., Tamada, A., Murakami, F., Tessier-Lavigne, M. (2004). The divergent Robo family protein rig-1/Robo3 is a negative regulator of slit responsiveness required for midline crossing by commissural axons. Cell, 117(2), 157–169.

Sakurai, T., Gil, O. D., Whittard, J. D., Gazdoiu, M., Joseph, T., Wu, J., Felsenfeld, D. P. (2008). Interactions between the L1 cell adhesion molecule and ezrin support traction-force generation and can be regulated by tyrosine phosphorylation. Journal of Neuroscience Research, 86(12), 2602–2614.

Sarmiere, P. D., Bamburg, J. R. (2004). Regulation of the neuronal actin cytoskeleton by ADF/cofilin. Journal of Neurobiology, 58(1), 103–117.

Sasaki, Y., Welshhans, K., Wen, Z., Yao, J., Xu, M., Goshima, Y., Bassell, G. J. (2010). Phosphorylation of zipcode binding protein 1 is required for brain-derived neurotrophic factor signaling of local beta-actin synthesis and growth cone turning. The Journal of Neuroscience, 30(28), 9349–9358.

Schaefer, A. W., Kabir, N., Forscher, P. (2002). Filopodia and actin arcs guide the assembly and transport of two populations of microtubules with unique dynamic parameters in neuronal growth cones. Journal of Cell Biology, 158(1), 139-152.

Seeger, M., Tear, G., Ferres-Marco, D., Goodman, C. S. (1993). Mutations affecting growth cone guidance in Drosophila: genes necessary for guidance toward or away from the midline. Neuron, 10(3), 409–426.

Serafini, T., Kennedy, T. E., Galko, M. J., Mirzayan, C., Jessell, T. M., Tessier-Lavigne, M. (1994). The netrins define a family of axon outgrowth-promoting proteins homologous to C. elegans UNC-6. Cell, 78(3), 409–424.

Serrano-Castro, P. J., Garcia-Torrecillas, J. M. (2012). Cajal's first steps in scientific research. Neuroscience, 217, 1–5.

Shamah, S. M., Lin, M. Z., Goldberg, J. L., Estrach, S., Sahin, M., Hu, L., Greenberg, M. E. (2001). EphA receptors regulate growth cone dynamics through the novel guanine nucleotide exchange factor ephexin. Cell, 105(2), 233–244.

Sharma, A., Lambrechts, A., Hao, L. T., Le, T. T., Sewry, C. A., Ampe, C., Morris, G. E. (2005). A role for complexes of survival of motor neurons (SMN) protein with gemins and profilin in neurite-like cytoplasmic extensions of cultured nerve cells. Experimental Cell Research, 309(1), 185–197.

Shekarabi, M., Moore, S. W., Tritsch, N. X., Morris, S. J., Bouchard, J.-F., Kennedy, T. E. (2005). Deleted in colorectal cancer binding netrin-1 mediates cell substrate adhesion and recruits Cdc42, Rac1, Pak1, and N-WASP into an intracellular signaling complex that promotes growth cone expansion. The Journal of Neuroscience, 25(12), 3132–3141.

Shestakova, E. A., Singer, R. H., Condeelis, J. (2001). The physiological significance of beta -actin mRNA localization in determining cell polarity and directional motility. Proceedings of the National Academy of Sciences, 98(13), 7045–7050.

Shewan, D., Dwivedy, A., Anderson, R., Holt, C. E. (2002). Age-related changes underlie switch in netrin-1 responsiveness as growth cones advance along visual pathway. Nature Neuroscience, 5(10), 955–962.

Shim, S., Goh, E. L., Ge, S., Sailor, K., Yuan, J. P., Roderick, H. L., Ming, G. (2005). XTRPC1-dependent chemotropic guidance of neuronal growth cones. Nature Neuroscience, 8(6), 730–735.

Shirasaki, R., Katsumata, R., Murakami, F. (1998). Change in chemoattractant responsiveness of developing axons at an intermediate target. Science, 279(5347), 105–107.

Simpson, J. H., Kidd, T., Bland, K. S., Goodman, C. S. (2000). Short-range and long-range guidance by slit and its Robo receptors. Robo and Robo2 play distinct roles in midline guidance. Neuron, 28(3), 753–766.

Song, H. (1998). Conversion of neuronal growth cone responses from repulsion to attraction by cyclic nucleotides. Science, 281(5382), 1515–1518.

Song, H., Ming, G., Poo, M., Shiro, M., Tomb, J., White, O., Bergman, M. I. (1997). cAMP-induced switching in turning direction of nerve growth, Nature, 388, 1211–1212.

Sperry, R., (1963). Chemoaffinity in the orderly growth of nerve fiber patterns and connections, Proceedings of the National Academies of Science, 50, 703-710.

Stein, E., Tessier-lavigne, M. (2001). Hierarchical organization of guidance receptors: silencing of netrin attraction by slit through a Robo/DCC receptor complex. Science, 291(5510), 1928–1938.

Stein, E., Zou, Y., Poo, M., Tessier-Lavigne, M. (2001). Binding of DCC by netrin-1 to mediate axon guidance independent of adenosine A2B receptor activation. Science, 291(5510), 1976–1982.

Stiess, M., Bradke, F. (2011). Neuronal polarization: the cytoskeleton leads the way. Developmental Neurobiology, 71(6), 430–444.

Stiles, J., Jernigan, T. L. (2010). The basics of brain development. Neuropsychology Reviews, 20, 327-348.

Strochlic, L., Dwivedy, A., van Horck, F. P. G., Falk, J., Holt, C. E. (2008). A role for S1P signalling in axon guidance in the *Xenopus* visual system. Development, 135(2), 333–342.

Stuermer, A. (1988). Retinotopic organization of the developing retinotectal projection in the zebrafish embryo. The Journal of Neuroscience, 8(12), 4513-4530.

Sun, Y. E., Wu, H. (2006). The ups and downs of BDNF in Rett syndrome. Neuron, 49(3), 321–323.

Swiercz, J. M., Kuner, R., Behrens, J., Offermanns, S. (2002). Plexin-B1 directly interacts with PDZ-RhoGEF/LARG to regulate RhoA and growth cone morphology. Neuron, 35(1), 51–63.

Tamagnone, L., Artigiani, S., Chen, H., He, Z., Ming, G. I., Song, H., Comoglio, P. M. (1999). Plexins are a large family of receptors for transmembrane, secreted, and GPI-anchored semaphorins in vertebrates. Cell, 99(1), 71–80.

Tanaka, E., Sabry, J. (1995). Making the connection: cytoskeletal rearrangements during growth cone guidance. Cell, 83, 171-176.

Taylor, A. M., Berchtold, N. C., Perreau, V. M., Tu, C. H., Li Jeon, N., Cotman, C. W. (2009). Axonal mRNA in uninjured and regenerating cortical mammalian axons. The Journal of Neuroscience, 29(15), 4697–4707.

Tcherkezian, J., Brittis, P. A., Thomas, F., Roux, P. P., Flanagan, J. G. (2010). Transmembrane receptor DCC associates with protein synthesis machinery and regulates translation. Cell, 141(4), 632–644.

Tennyson, V. M. (1970). The fine structure of the axon and growth cone of the dorsal root neuroblast of the rabbit embryo. The Journal of Cell Biology, 44(1), 62–79.

Tessier-Lavigne, M., Goodman, C. S. (1996). The molecular biology of axon guidance. Science, 274, 1123-1133.

Tobias, G. S., Koenig, E. (1975). Influence of nerve cell body and neurolemma cell on local axonal protein synthesis following neurotomy. Experimental Neurology, 49(1 Pt 1), 235–245.

Torres, E., Rosen, M. K. (2003). Contingent phosphorylation/dephosphorylation provides a mechanism of molecular memory in WASP. Molecular Cell, 11(5), 1215–1227.

Trowe, T., Klostermann, S., Baier, H., Granato, M., Crawford, A D., Grunewald, B., Bonhoeffer, F. (1996). Mutations disrupting the ordering and topographic mapping of axons in the retinotectal projection of the zebrafish, *Danio rerio*. Development, 123, 439–450.

Tsai, N.-P., Bi, J., Wei, L.-N. (2007). The adaptor Grb7 links netrin-1 signaling to regulation of mRNA translation. The EMBO Journal, 26(6), 1522–1531.

Turney, S. G., Bridgman, P. C. (2005). Laminin stimulates and guides axonal outgrowth via growth cone myosin II activity. Nature Neuroscience, 8(6), 717–719.

Vainer, G., Vainer-Mossel, E., Pikarsky, A., Chenoy, S. M., Obermean, F., Yeffet, A., Singer, R. H., Pikarsky, E. (2008). A role for VICKZ proteins in the progression of colorectal carcinomas: regulating lamellipodia formation. Journal of Pathology, 215, 445-465.

Van Kesteren, R. E., Carter, C., Dissel, H. M. G., van Minnen, J., Gouwenberg, Y., Syed, N. I., Smit, A. B. (2006). Local synthesis of actin-binding protein beta-thymosin regulates neurite outgrowth. The Journal of Neuroscience, 26(1), 152–157.

Västrik, I., Eickholt, B. J., Walsh, F. S., Ridley, A., Doherty, P. (1999). Sema3A-induced growth-cone collapse is mediated by Rac1 amino acids 17-32. Current Biology, 9(18), 991–998.

Vicente-manzanares, M., Choi, C. K., Horwitz, A. R. (2009). Integrins in cell migration - the actin connection. Journal of Cell Science, 122(9), 1473–1473.

Vitriol, E. A, Zheng, J. Q. (2012). Growth cone travel in space and time: the cellular ensemble of cytoskeleton, adhesion, and membrane. Neuron, 73(6), 1068–1081.

Wan, Y., Otsuna, H., Chien, C-B., Hansen, C. (2013). FluoRender: an application of 2D image space methods for 3D and confocal microscopy data visualization in neurobiology research, IEEE Pac Vis Symp, 2012, 201-208.

Wang, G. X., Poo, M.-M. (2005). Requirement of TRPC channels in netrin-1-induced chemotropic turning of nerve growth cones. Nature, 434(7035), 898–904.

Wang, K. H., Brose, K., Arnott, D., Kidd, T., Goodman, C. S., Henzel, W., Tessier-Lavigne, M. (1999). Biochemical purification of a mammalian slit protein as a positive regulator of sensory axon elongation and branching. Cell, 96(6), 771–784.

Welshhans, K., Bassell, G. J. (2011). Netrin-1-induced local β-actin synthesis and growth cone guidance requires zipcode binding protein 1. The Journal of Neuroscience, 31(27), 9800–9813.

Wen, Z., Han, L., Bamburg, J. R., Shim, S., Ming, G., Zheng, J. Q. (2007). BMP gradients steer nerve growth cones by a balancing act of LIM kinase and Slingshot phosphatase on ADF/cofilin. The Journal of Cell Biology, 178(1), 107–119.

Wilkinson, D. G. (2001). Multiple roles of EPH receptors and ephrins in neural development. Nature Reviews Neuroscience, 2(3), 155–164.

Willis, D., Li, K. W., Zheng, J.-Q., Chang, J. H., Smit, A. B., Smit, A., Twiss, J. L. (2005). Differential transport and local translation of cytoskeletal, injury-response, and neurodegeneration protein mRNAs in axons. The Journal of Neuroscience, 25(4), 778–791.

Winberg, M. L., Mitchell, K. J., Goodman, C. S. (1998). Genetic analysis of the mechanisms controlling target selection: complementary and combinatorial functions of netrins, semaphorins, and IgCAMs. Cell, 93(4), 581–591.

Wizenmann, A., Brunet, I., Lam, J. S. Y., Sonnier, L., Beurdeley, M., Zarbalis, K., Prochiantz, A. (2009). Extracellular engrailed participates in the topographic guidance of retinal axons *in vivo*. Neuron, 64(3), 355–366.

Wu, K. Y., Hengst, U., Cox, L. J., Macosko, E. Z., Jeromin, A., Urquhart, E. R., Jaffrey, S. R. (2005). Local translation of RhoA regulates growth cone collapse. Nature, 436(7053), 1020–1024.

Yam, P. T., Langlois, S. D., Morin, S., Charron, F. (2009). Sonic hedgehog guides axons through a noncanonical, Src-family-kinase-dependent signaling pathway. Neuron, 62(3), 349–362.

Yao, J., Sasaki, Y., Wen, Z., Bassell, G. J., Zheng, J. Q. (2006). An essential role for beta-actin mRNA localization and translation in Ca2+-dependent growth cone guidance. Nature Neuroscience, 9(10), 1265–1273.

Yarmola, E. G., Bubb, M. R. (2009). How depolymerization can promote polymerization: the case of actin and profilin. BioEssays: News and Reviews in Molecular, Cellular and Developmental Biology, 31(11), 1150–1160.

Yee, K. T., Simon, H. H., Tessier-Lavigne, M., O'Leary, Dennis D. M. (1999). Extension of long leading processes and neuronal migration in the mammalian brain directed by the chemoattractant netrin-1. Neuron*,* 24, 607-622.

Yoon, B. C., Jung, H., Dwivedy, A., O'Hare, C. M., Zivraj, K. H., Holt, C. E. (2012). Local translation of extranuclear lamin B promotes axon maintenance. Cell, 148(4), 752–764.

Yuan, X., Jin, M., Xu, X., Song, Y., Wu, C., Poo, M., Duan, S. (2003). Signalling and crosstalk of Rho GTPases in mediating axon guidance. Nature Cell Biology, 5(1), 38–45.

Zallen, J. A., Yi, B. A., Bargmann, C. I. (1998). The conserved immunoglobulin superfamily member SAX-3/Robo directs multiple aspects of axon guidance in *C. elegans*. Cell, 92(2), 217–227.

Zhang, H. L., Singer, R. H., Bassell, G. J. (1999). Neurotrophin regulation of β-actin mRNA and protein localization within growth cones, The Journal of Cell Biology 147(1), 59–70.

Zhang, H. L., Eom, T., Oleynikov, Y., Shenoy, S. M., Liebelt, D. A., Dictenberg, J. B., Bassell, G. J. (2001). Neurotrophin-induced transport of a beta-actin mRNP complex increases beta-actin levels and stimulates growth cone motility. Neuron, 31, 261-275.

Zheng, J. Q., Kelly, T. K., Chang, B., Ryazantsev, S., Rajasekaran, A. K., Martin, K. C., Twiss, J. L. (2001). A functional role for intra-axonal protein synthesis during axonal regeneration from adult sensory neurons. The Journal of Neuroscience, 21(23), 9291–9303.

Zivraj, K. H., Tung, Y. C. L., Piper, M., Gumy, L., Fawcett, J. W., Yeo, G. S. H., Holt, C. E. (2010). Subcellular profiling reveals distinct and developmentally regulated repertoire of growth cone mRNAs. The Journal of Neuroscience, 30(46), 15464–15478.

CHAPTER 2

NEV (CYFIP2) IS REQUIRED FOR RETINAL LAMINATION AND AXON GUIDANCE IN THE ZEBRAFISH RETINOTECTAL SYSTEM

Andrew J. Pittman, John A. Gaynes, Chi-Bin Chien

Developmental Biology 344:784-794 (2010)

The following paper was published in Developmental Biology, and is reprinted with permission*. The first author, Andrew Pittman, wrote this as part of his dissertation in Chi-Bin Chien's lab. I contributed the data presented in Figure 8 and all parts of the paper associated with it, including data analysis, figure preparation, and writing the text associated with the methods, results and interpretation. This experiment required extensive trouble shooting and persistence in order to adapt the *in vivo* focal electroporation method to express DNA constructs in single cells or small groups of cells in the zebrafish dorsonasal retina. Isaac Bianco had applied it to zebrafish as a postdoctoral fellow in Jon Clarke's lab, and published a paper using the technique in 2008 (Bianco et al. 2008). The Clarke lab provided their protocol and Isaac provided technical assistance over the phone. With the help of Chi-Bin, I optimized this technique to reliably express cDNA constructs in single RGCs in the retina and I was able to rescue the axon missorting phenotype seen in dorsonasal RGCs of the *nevermind* mutant. My work demonstrated that *Cyfip2* function is required cell-autonomously for correct sorting of dorsonasal RGC axons in the zebrafish optic tract.

* Pittman, A. J., Gaynes, J. A., Chien, C.-B. (2010). Nev (cyfip2) is required for retinal lamination and axon guidance in the zebrafish retinotectal system. Developmental Biology, 344, 784-794.

Contents lists available at ScienceDirect

Developmental Biology

journal homepage: www.elsevier.com/developmentalbiology

nev (*cyfip2*) is required for retinal lamination and axon guidance in the zebrafish retinotectal system

Andrew J. Pittman, John A. Gaynes, Chi-Bin Chien *

Program in Neuroscience, Department of Neurobiology and Anatomy, and Brain Institute, University of Utah Medical Center, 20 North 1900 East, Salt Lake City, UT 84132, USA

ARTICLE INFO

Article history:
Received for publication 2 May 2010
Accepted 26 May 2010
Available online 9 June 2010

Keywords:
Axon pathfinding
Retinal development
Retinotectal topography
CYFIP2/PIR121
WAVE
FMRP

ABSTRACT

In the zebrafish retinotectal system, retinal ganglion cells (RGCs) project topographically along anterior–posterior (A-P) and dorsal–ventral (D-V) axes to innervate their primary target, the optic tectum. In the *nevermind* (*nev*) mutant, D-V positional information is not maintained by dorsonasal retinal axons as they project through the optic tract to the tectum. Here we present a detailed phenotypic analysis of the retinotectal projection in *nev* and show that dorsonasal axons do eventually find their correct location on the tectum, albeit after taking a circuitous path. Interestingly, *nev* seems to be specifically required for retinal axons but not for several non-retinal axon tracts. In addition, we find that *nev* is required both cell autonomously and cell nonautonomously for proper lamination of the retina. We show that *nev* encodes Cyfip2 (Cytoplasmic FMRP interacting protein 2) and is thus the first known mutation in a vertebrate Cyfip family member. Finally, we show that CYFIP2 acts cell autonomously in the D-V sorting of dorsonasal RGC axons in the optic tract. CYFIP2 is a highly conserved protein that lacks known domains or structural motifs but has been shown to interact with Rac and the fragile-X mental retardation protein, suggesting intriguing links to cytoskeletal dynamics and RNA regulation.

Introduction

A major focus in developmental neurobiology is to understand the mechanisms by which axons navigate through their environment and ultimately identify their appropriate target cells. One system well suited for studying axon pathfinding is the zebrafish retinotectal system, where the axons of RGCs project to their primary target, the optic tectum, along two topographic axes. RGCs located along the A-P axis of the retina distribute their axons along the posterior-anterior axis of the tectum; likewise, RGCs along the D-V axis distribute their axons along the ventral–dorsal axis of the tectum (Stuermer, 1988). *In vitro* and *in vivo* studies have identified several molecules important for topographic mapping on the tectum (reviewed in McLaughlin and O'Leary, 2005).

Before reaching the tectum, axons are segregated in the optic tract depending on RGC position within the retina. Dorsal axons project through the ventral branch of the optic tract, while ventral axons project through the dorsal branch (Stuermer, 1988). Little is known about the molecular mechanisms controlling topographic order within the tract, and the ligands and receptors involved remain elusive. However, a large-scale forward genetic screen isolated several zebrafish mutants that display mistakes in tract sorting and topographic mapping of retinal axons (Baier et al., 1996; Karlstrom et al., 1996; Trowe et al., 1996), potentially providing insight into this process. Indeed, analysis of the *boxer* and *dackel* mutants shows that heparan sulfate proteoglycans (HSPGs) are required for sorting dorsal axons into the ventral tract (Lee et al., 2004). In the *nevermind* (*nev*) mutant described here, dorsonasal axons missort with ventral axons in the optic tract, and also project inappropriately through the dorsal tectum (Trowe et al., 1996). We show here that *nev* encodes a cytoplasmic protein, CYFIP2, likely involved in growth cone guidance.

The intracellular signaling pathways that mediate signals from cell surface receptors to ultimately change the growth cone's behavior are quite complex. The Rho family of small GTPases, including Rac, Rho, and Cdc42, regulate the cytoskeletal structure of the growth cone and have been shown to act downstream of axon guidance receptors (reviewed in Govek et al., 2005). One function of Rac is to signal through the WAVE/SCAR complex to cause actin nucleation by Arp2/3 activation (Miki et al., 1998; Machesky et al., 1999). The WAVE/SCAR complex consists of five proteins including CYFIP2 [cytoplasmic FMRP interacting protein 2; also known as PIR121 (Saller et al., 1999)], which Rac binds directly (Eden et al., 2002). CYFIP1 [also known as Sra-1; (Kobayashi et al., 1998)] and CYFIP2 were also identified independently through their interaction with FMRP (fragile-X mental retardation protein) (Schenck et al., 2001). FMRP is an mRNA binding protein thought to bind as many as 4% of all brain mRNAs (reviewed in Bardoni and Mandel, 2002).

* Corresponding author. Fax: +1 801 581 4233.
E-mail address: chi-bin.chien@neuro.utah.edu (C.-B. Chien).

Genetic studies in *Drosophila* have shown that CYFIP acts as a Rac1 effector upstream of FMRP (Schenck et al., 2003); more recently, biochemical studies have shown that mammalian CYFIP1 can mediate FMRP's translational repression activity (Napoli et al., 2008).

In *Drosophila*, mutations in *cyfip* give rise to defects in synaptogenesis and axon guidance (characterized by midline crossing errors and ectopic branching) (Schenck et al., 2003). Mutations in any of the three components of the WAVE complex, *cyfip*, *kette*, or *scar*, give rise to similar defects in axon guidance, demonstrating a role for Cyfip and the WAVE complex in mediating axon guidance decisions (Schenck et al., 2004). Furthermore, loss of Cyfip specifically in photoreceptor neurons leads to targeting errors once their axons enter the brain (Bogdan et al., 2004). However, it is not known whether Cyfip has a conserved role in axon guidance in vertebrates.

Here we show that *nev* encodes Cyfip2 and is thus the first known mutant in a vertebrate Cyfip family member. Allele sequencing of both alleles of *nev*, *tr230b* and *ta229f*, identified premature stop codons that likely represent null alleles. *cyfip2* is broadly expressed in the CNS during development, including the eye and brain. We show that cell autonomous function of *cyfip2* is required for maintaining positional information by dorsonasal axons as they project through the optic tract and on the tectum. While *nev* is larval lethal, the overall morphology of the body, brain, and eye are grossly normal, as is the D-V polarity of the eye. However, the lamination of the eye is disrupted in *nev*, apparently independently of the axon guidance phenotype. These data suggest that Cyfip2 is an important regulator of cytoskeletal dynamics and/or RNA translation that acts during retinal lamination and axon pathfinding.

Materials and methods

Mapping and cloning of nev/cyfip2

nev had previously been rough-mapped to LG14 (S. Neuhauss, personal communication). To fine-map *nev*, heterozygotes in the Tü background were crossed to a polymorphic strain, WIK. F1 heterozygotes were incrossed to collect F2 mutant embryos, which were identified by topographically labeling the dorsonasal and ventrotemporal retina (see below). Tightly linked simple sequence length polymorphisms (SSLPs) and single nucleotide polymorphisms (SNPs) were identified by PCR. A total of 588 meioses were analyzed to place *nev* within a 0.51 cM interval flanked by an SSLP, zAJP18 (primers zAJP18F 5′-CAGAATGCTGCAGGGAAATA-3′ and zAJP18R 5′-TGATGGAGTAGGTCCTGGATG-3′) with 2 recombinations/588 and a SNP, zK183B13 (zk183B13sp61F 5′-GGCCACTTTCCAACACAATC-3′ and zk183B13sp61R 5′-CAAACTGAGGGGAGCAGAAA-3′) with 1 recombination/588. To identify candidate genes within this interval, sequenced BACs (Sanger Institute) were analyzed. One candidate of particular interest was pursued further: the zebrafish homolog of human CYFIP2 (Genbank EF531617). A novel SSLP marker, zAJP12 (zAJP12F 5′-CTGACAGATCTGGAAAGGTCAA-3′ and zAJP12R 5′-TGCTCTAAATTAGTATCTTTGGTCAGA-3′), located between the 2nd and 3rd exons of cyfip2, showed 0 recombinations/588 meioses.

Allele sequencing

To search for the molecular defect in *nev*, cDNA was generated from WT and mutant embryos at 54hpf and *cyfip2* RT-PCR products were directly sequenced as previously described (Lee et al., 2004). This led to the identification of premature stop codons in both alleles of *nev* (*tr230b* and *ta229f*). Genomic DNA (gDNA) from the two founder fish (a generous gift from S. Rudolph, MPI Tübingen) was PCR amplified and sequenced to confirm that these mutations were induced by the mutagenesis; neither founder displayed the stop codon mutations. For genotyping *nev*^{tr230b}, the following dCAPS primers (Neff et al., 2002) were used on gDNA: FP 5′-TTGGGTGAATTCCATTTTTCA-3′ and RP 5′-CTCCAGGTGTACAACATGACAGC-3′, which amplify a 213 bp product with an AluI restriction site introduced in *nev* but not wt. AluI digests were run on a 3% Metaphor gel to resolve wt (213 bp) and *nev* (190 bp) bands. We have found no phenotypic differences between the two *nev* alleles, and all of the functional analysis described here used *tr230b*.

Lipophilic labeling of retinal axons

An injection set-up for topographically labeling retinal axons was modeled after that used in the Tübingen screen for retinotectal pathfinding mutants (Baier et al., 1996). Three day postfertilization (dpf) and five dpf embryos from a heterozygote incross were collected and fixed in 4% paraformaldehyde (PFA). Small populations of RGCs in the dorsonasal and ventrotemporal retina were labeled with the lipophilic dyes DiI and DiO, respectively, and the dye was allowed to diffuse anterogradely for at least 15 h at room temperature. To label even smaller numbers of axons, DiI was diluted in 100% ethanol and pressure injected into the dorsonasal retina of live 5dpf embryos. The following day, embryos were fixed in 4% PFA. The retinotectal projections were analyzed using an Olympus confocal microscope.

In situ hybridization and Fc fusion staining

WT embryos and embryos from a *nev* heterozygous intercross were raised at 28.5 °C in 0.1 mM phenylthiourea and staged according to hours postfertilization (hpf) and morphology (Kimmel et al., 1995). Embryos were fixed in 4% PFA in PBS overnight at 4 °C. The following day, embryos were washed in PBST (PBS with 0.1% Tween-20) and dehydrated through a series of MeOH washes and stored at −20 °C. *In situ* hybridization was carried out according to Lee et al. (2001). *cyfip2* antisense riboprobes were generated from a cDNA clone (GenBank accession no. BI879132). *ephrin-B2a*, *EphB3*, *aldh1a2*, *TAG-1*, and *tbx5a* plasmids were generous gifts from S. Wilson, H. Grandel, J. Kuwada, and D. Yelon, respectively. For staining with EphB2-Fc or ephrin-B1-Fc fusion proteins (Supplemental Table 1) embryos were fixed in ice-cold 100% MeOH, washed in PBST, then incubated in the affinity reagent (10 ng/μl; R&D Systems catalog# 467-B2-200 and 473-EB-200) overnight at 4 °C, washed again in PBS, fixed again in 4% PFA, washed in PBST, then incubated in biotin-conjugated goat anti-human Fc (1:200; Jackson Immunoresearch catalog# 109-065-098) and stained with the Vectastain ABC kit (Vector Laboratories). Stained larvae were genotyped for *nev*, prepared for sectioning or cleared in 100% glycerol, and photographed using an Olympus (BX50WI) compound microscope with an Olympus Magnafire SP camera.

Immunofluorescence

For whole-mount immunostaining, embryos from a *nev* heterozygous intercross, with or without a *Tg(isl2b:GFP)*^{zc7} reporter (Pittman et al., 2008), were raised at 28.5 °C in 0.1 mM phenylthiourea and staged as above. Embryos were dechorionated and fixed at 24hpf, 30hpf, 36hpf, or 5dpf in 4% PFA in PBS overnight at 4 °C, washed in PBST, dehydrated through a MeOH series, stored at −20 °C for at least 12 h, rehydrated, washed in PBST and permeabilized with 0.1% collagenase. For retinal lamination experiments, *isl2b:GFP* larvae were incubated in the following primary antibodies overnight at 4 °C: rabbit anti-GFP (1:400; Invitrogen catalog #A11122), and mouse anti-parvalbumin (1:400; Chemicon catalog #MAB1572). They were then washed in PBST and incubated in goat anti-rabbit Alexa 488 (1:200; Invitrogen catalog# A11008) and goat anti-mouse Cy3 (1:200; Jackson Immunoresearch catalog# 115-165-003). Finally, embryos were incubated in Hoechst 33342 (Molecular Probes catalog# H-3570) to visualize cell nuclei. For visualizing axon tracts, embryos were incubated in the following primary antibodies overnight at 4 °C: anti-acetylated tubulin (1:500; Sigma catalog# T6793), znp-1 (1:1000; Iowa DSHB), 3A10 (1:25; Iowa DSHB). They were then washed in PBST and incubated in either goat

anti-mouse Cy3 (1:200; Jackson Immunoresearch catalog# 115-165-003) or goat anti-mouse GFP (1:200; Invitrogen catalog# A11029). For cell transplant studies, larvae were fixed at 5dpf and stained with a rabbit anti-GFP antibody (1:400; Invitrogen catalog# A11222) and goat anti-rabbit Alexa 488 (1:200; Invitrogen catalog# A11008) and streptavidin-Alexa 546 (1:200; Invitrogen catalog# S11225). After immunostaining, larvae were genotyped and some were prepared for sectioning.

Sectioning

After immunostaining or *in situ* hybridization, embryos were dehydrated in MeOH and infiltrated in 1:1 Immuno-Bed:MeOH for 30 min at 4 °C, followed by 100% Immuno-Bed overnight at 4 °C. Embryos were then embedded in a solution of Immuno-Bed: Immuno-Bed Solution B (EMS catalog# 14260-04: 20:1) and sectioned at 8 μm on a Reichert-Jung 2050 Supercut microtome with a glass knife.

Cell transplants

Transplants were performed as described by Ho and Kane (1990). Donor embryos from a *nev*/+;*Tg(isl2b:GFP)*^{zc7}/+ incross were collected at the one-cell stage and injected with a 1:1 mixture of rhodamine-dextran (10,000 MW, 5% in H_2O; Invitrogen catalog# D1817) and biotin dextran (3000 MW, 5% in H_2O; Invitrogen catalog# D7135) to visualize donor cells. At 4hpf, 10–50 cells were transplanted from donor embryos to the animal pole of embryos from a *nev* heterozygote incross. At 24hpf, GFP+ donors were fixed and digested to collect gDNA for genotyping. At 5dpf, host embryos were fixed and processed for immunohistochemistry and subsequently genotyped. Host embryos were then prepared for sectioning. Donor cells misplaced in the IPL of host embryos were counted from 12 serial sections centered on the section containing the optic nerve.

Morpholino injections

Lyophilized morpholinos were solubilized in 1x Danieau's buffer and stored at −20 °C. To block the splicing of *cyfip2*, a morpholino antisense oligonucleotide (Gene Tools) was designed against the exon1-intron1 boundary (5′-agtgcattaggacgtgtacCTGGTA-3′) of *cyfip2* (see Supplemental Fig. 1). The injection volume was calculated using a calibrated eyepiece. 3 nl of morpholino (2.5 μg/μl) was injected into the yolk/cell interface of one-cell embryos. Embryos were collected at 24hpf and 3dpf and cDNA prepared as above. RT-PCR using cyfip2 FP (5′-GATGCGCTGTCCAATGTG-3′) and cyfip2 RP (5′-CTTCAGTTCGTC-CAGCACAG-3′) was performed to confirm knockdown of *cyfip2* (see Supplemental Fig. 1).

Plasmid constructs

CMV:*cyfip2*-pA was constructed using the Tol2kit (Kwan et al., 2007) by recombining p5E-CMV/SP6, pME-*cyfip2*, and p3E-pA into pDestR4-R3; reporter constructs driven by the CMV promoter were pCS2-GAP43-GFP (gift of Jon Clarke), pCS2-mCherryCAAX, and pCS2-EGFP-CAAX (both gifts of Kristen Kwan).

In vivo focal electroporation

Embryos from a *nev* heterozygous incross carrying a *Tg(isl2b:mCherryCAAX)*^{zc23} reporter were dechorionated at 22–28 hpf, anesthetized with 0.02% tricaine, and mounted right side up on a glass slide in a drop of 1% low-melt agarose in E2/gentamycin. The agarose was windowed to expose the eye. The embryo was covered with E3 with 0.1 mM PTU to inhibit pigment formation, and mounted under a 40x water immersion objective. Co-electroporation tests used an equimolar mixture of EGFP-CAAX and mCherryCAAX constructs. Rescue experiments used an equimolar mixture of GAP43-GFP and Cyfip2 constructs (or GAP43-GFP only for controls). A glass microelectrode with a 1–3 μm diameter fire-polished tip was backfilled with 2 μl of DNA (1–3 μg/μl in 10 mM Tris-Cl, pH 8.5), and positioned into dorsonasal retina using a micromanipulator, with a Ag/AgCl cathode placed in the overlying buffer near the head of the embryo. A Grass stimulator was used to deliver 1 s trains of 2 ms negative-going square pulses at 200 Hz, 30–50 V. Several cells were targeted in each eye with 3–5 trains/cell. Embryos were then removed from the agarose and raised in E3 + PTU at 28.5 °C until 5 dpf. *nev* homozygotes were selected by their lack of swim bladders and confirmed by PCR genotyping after imaging.

Most electroporated larvae were imaged live, after tricaine anesthesia and mounting in a drop of 1.5% low-melt agarose, dorsal down, on a Petriperm dish (Greiner Bio-One, Monroe, NC). An Olympus FV300 confocal with 40x/W objective was used to take z-stacks of the left tectum and optic tract in the EGFP and mCherry channels. One to six arbors were imaged per embryo.

A few larvae carried a *Tg(isl2b:GFP)*^{zc7} reporter instead of *Tg(isl2b:mCherryCAAX)*^{zc23} and were electroporated using an mCherryCAAX construct, then imaged live. Two nontransgenic larvae were imaged in 80% glycerol after fixing in 4% PFA, counterstaining the tectal neuropil with mAb zn-8 (1:20, DSHB), and staining electroporated axons with rabbit anti-GFP (1:1000).

Analysis of electroporation experiments

Larvae with GFP-positive RGCs in dorsonasal retina, whose axons terminated in the posteroventral quadrant of the contralateral tectum (as expected for dorsonasal RGCs; Fig. 8B) were chosen for analysis. Using ImageJ (http://rsb.info.nih.gov/ij/; Wayne Rasband, NIH), a maximum-intensity view of the confocal stack was rotated around the y-axis to select a broadside (dorsolateral) view of the tectum. The D-V position of each axon as it left the optic tract to enter the tectum was then quantified relative to the ventralmost (0%) and dorsalmost (100%) fascicles. Tectal images in Fig. 8D–F were generated using FluoRender visualization software (Wan et al., 2009).

Results

nev affects the sorting and targeting of dorsonasal axons

nev was originally isolated in a screen for mutations affecting retinotectal axon pathfinding (Baier et al., 1996; Trowe et al., 1996). Fig. 1 shows the projections of dorsonasal and ventrotemporal axons in WT and *nev*. At 3 and 5dpf, WT dorsal and ventral axons are topographically sorted in the ventral and dorsal branches of the optic tract, respectively (Fig. 1A and E) and project into the tectum where they terminate topographically from the outset (Stuermer, 1988) (Fig. 1B and F; $n>50$). In some WT embryos, a few dorsonasal axons are missorted in the dorsal branch of the tract and on the tectum at 3dpf (Fig. 1A), but these missorted axons are not present at 5dpf (Fig. 1E and F). This could reflect either correction of a transient sorting error, or merely the difficulty of labeling topographically at 3dpf.

In *nev*, a subset of dorsonasal axons are missorted with ventrotemporal axons in the dorsal branch of the optic tract and enter the tectum from an abnormal direction (Trowe et al., 1996; Fig. 1C and G). At 3dpf, a greater number of dorsonasal axons in *nev*, as compared to WT, are missorted in the dorsal branch of the optic tract (Fig. 1C, C′) and project through the dorsal tectum (Fig. 1D, D′). By 5dpf, there are more dorsal axons missorted in the tract, and they appear to have disrupted topography on the tectum (Fig. 1G and H; but see below). Interestingly, ventral axons are unaffected in *nev* (Fig. 1). These results show that *nev* is required for the topographic

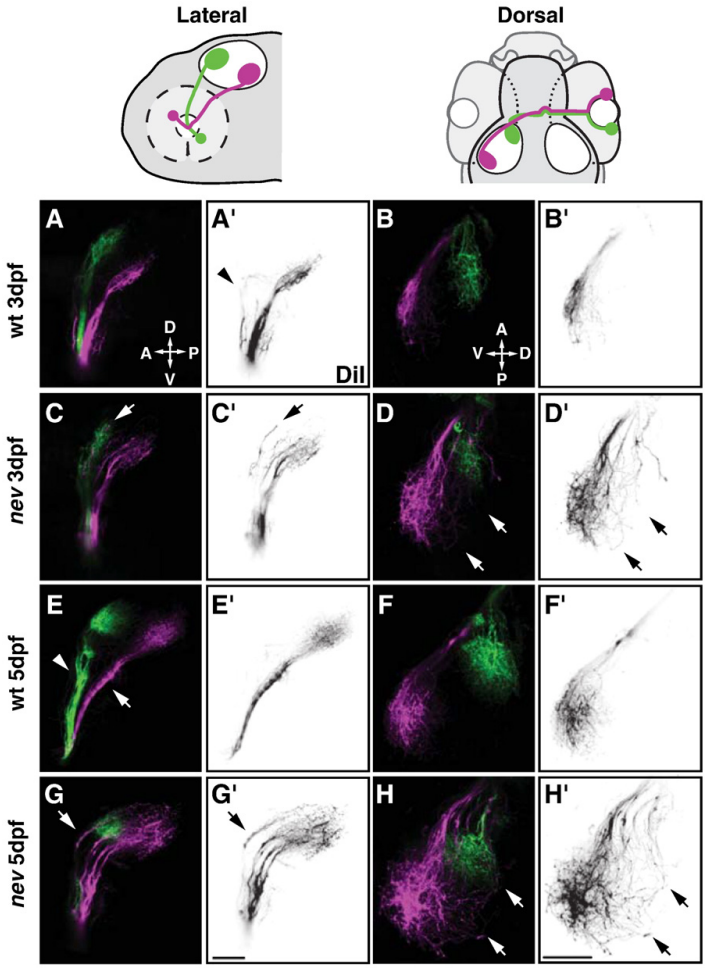

Fig. 1. *nevermind/cyfip2* is required for axon sorting and targeting of dorsonasal retinal axons. Confocal projections of dorsonasal axons (in magenta) and ventrotemporal axons (in green) in WT (A, B, E, F) and *nev* (C, D, G, H) at 3dpf (A–D) and 5dpf (E–H). (A′–H′) show only DiI injected dorsonasal axons in reverse contrast. Cartoons above show orientation of lateral views (A, C, E, G) and dorsal views (B, D, F, H). WT axons (A and E) from dorsonasal and ventrotemporal retina are topographically sorted in the ventral branch (arrow in E) and dorsal branch (arrowhead in E) of the optic tract, respectively. Arrowhead in A′ shows a few dorsal axons in WT projecting in the dorsal branch but turning before entering the tectum. Once on the tectum, WT axons project topographically to their target (B and F). However, in *nev*, dorsonasal axons are missorted in the dorsal branch of the optic tract (arrows in C and G), and project through the dorsal half of the optic tectum (arrows in D and H). Scale bars = 50 μm.

sorting and targeting of dorsonasal axons throughout the development of the retinotectal projection.

Dorsoventral retinal polarity is unaffected in nev

One possible explanation for this phenotype might be that the D-V polarity of the eye (Koshiba-Takeuchi et al., 2000) is disrupted in *nev* such that dorsal RGCs are misspecified as ventral RGCs. To test this, we examined the expression of markers expressed either in the dorsal retina (*tbx5a* [formerly *tbx5*], *aldh1a2* [formerly *raldh2*], and *ephrin-B2a in situs*, and EphB2-Fc affinity reagent staining) or ventral retina (*EphB2*, *EphB3*, and *TAG-1*, and ephrin-B1-Fc) between 24-48hpf (Supplemental Table 1). However, none of these genes showed a detectable reduction or alteration in their D-V pattern (Supplemental Fig. 2), suggesting that *nev* is not important for the development of D-V retinal polarity.

nev dorsonasal axons take circuitous routes to their targets

The conclusion that the topographic mapping of dorsonasal axons on the optic tectum is disrupted in *nev* (Trowe et al., 1996) was based on using a focal injection apparatus (Baier et al., 1996) to label ~100 RGCs. *nev* larvae, focally labeled in dorsonasal retina, show dye in roughly the right position in the ventral tectum, but also show labeled axons in the dorsal tectum (Fig. 1H). Using this method, it is not possible to discern where *individual* axons terminate on the optic tectum and whether they arborize topographically.

To further understand the pathfinding of dorsonasal axons on the optic tectum, we labeled small numbers of dorsonasal RGCs in live embryos at 5dpf with DiI. In WT, dorsonasal axons enter the tectum correctly through the ventral branch of the optic tract and project directly to their topographic location in the ventral tectum where they then arborize (Fig. 2A and B; $n = 21/23$ embryos). In the 2/23 WT

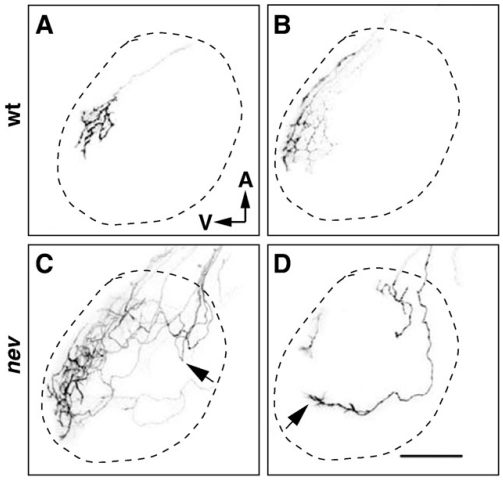

Fig. 2. Dorsonasal axons take circuitous routes on the tectum in *nev*. (A–D) Confocal images of the left optic tectum after DiI labeling of a few RGCs in the dorsal retina of wt (A and B) or *nev* (C and D) at 5dpf. Dashed line indicates approximate outline of tectum. In WT, dorsonasal axons enter the tectum through the ventral branch of the optic tract, project directly to their topographic target and arborize (A and B). In *nev*, dorsonasal axons that enter through the dorsal branch of the optic tract meander around the dorsal tectum, sometimes turning back anteriorly after entering the tectum (arrow in C) but appear to orient toward the ventral tectum (arrow in D). Scale bar in D = 50 μm.

embryos that had axons entering the tectum more dorsally than expected, these axons navigated directly to an appropriate ventral tectal position on the tectum (data not shown). However, in *nev*, dorsonasal axons often enter the dorsal tectum through the dorsal branch of the optic tract and then follow circuitous routes (Fig. 2C and D; $n = 8/12$). Interestingly, some axons turn back in an anterior direction after entering the tectum (arrow in Fig. 2C). Ultimately, most of the axons that enter on the dorsal side do orient towards the ventral tectum and eventually appear to terminate correctly (arrow in Fig. 2D). In *nev* embryos in which dorsonasal axons enter correctly through the ventral branch of the optic tract, almost all axons behave like WT and arborize in the ventral tectum, with only very rare cases of axons extending away from the ventral tectum (data not shown). These data, and similar results obtained by Trowe (2000) suggest that dorsonasal axons in *nev* are still able to project topographically to the ventral tectum but take an indirect route to their target.

nev encodes Cyfip2

To identify the gene encoded by *nev*, we used PCR-based methods to genetically map *nev* by screening for tightly linked SSLPs and SNPs. *nev* had previously been assigned to LG14 (S. Neuhauss, personal communication). We fine-mapped *nev* to a 0.51 cM interval on LG14 by identifying an SSLP, zAJP18, 0.34 cM (2 recombination/588 meioses) on one side of *nev* and an SNP, zK183B13, 0.17 cM (1 recombinations/588 meioses) on the other side (Fig. 3A). By BLAST analysis of several BACs that overlapped this interval, one BAC was identified (GenBank accession no. BX088721), which contained the zebrafish ortholog of human CYFIP2.

Human CYFIP1 and CYFIP2 are 92% and 98% identical to zebrafish Cyfip1 (Schenck et al., 2001) and Cyfip2, respectively. This conservation is evident throughout the entire protein, suggesting that it contains many domains that are structurally and/or functionally important. Furthermore, Cyfip1 and Cyfip2 are very similar to each other (86% identical in zebrafish). CYFIP1 and CYFIP2 do not contain any known functional domains or motifs, but have been shown to bind several other proteins. Both CYFIP1 and CYFIP2 interact with Rac1 (Kobayashi et al., 1998; Eden et al., 2002) and FMRP (Schenck et al., 2001), while CYFIP1 interacts with CRMP2 (collapsin response mediating protein 2) (Kawano et al., 2005), and *Drosophila* CYFIP binds Nap1/Kette (Bogdan et al., 2004). Fig. 3B summarizes the CYFIP fragments implicated in these interactions.

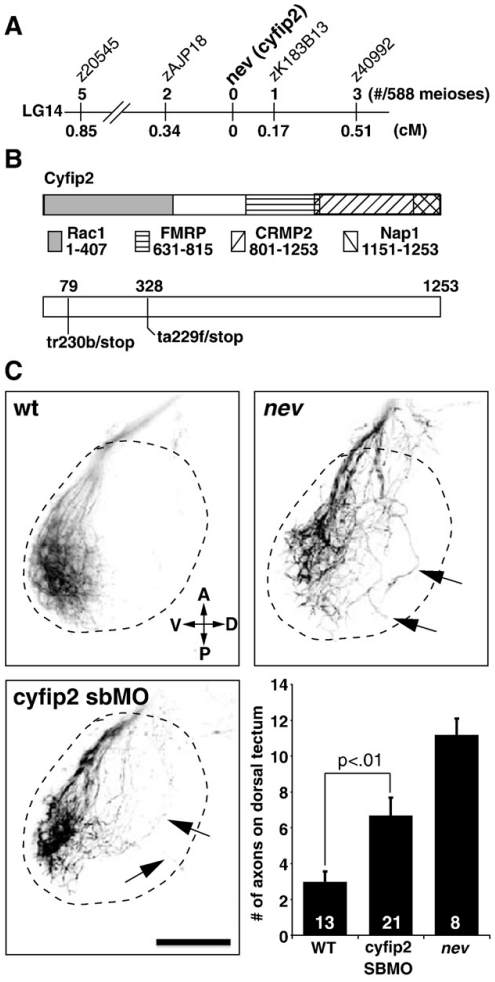

Fig. 3. *nevermind* encodes Cyfip2. (A) Meiotic map of *nev*/*cyfip2*. Using a combination of SSLPs and SNPs, *nev* was fine-mapped to a 0.51 cM interval on LG14. Numbers above show recombinations in 588 meioses; numbers below indicate distance in cM. (B) Structure of Cyfip2. Domains known to be important for protein interactions with Cyfip1 and Cyfip2 are shown (see text for references). cDNA sequencing from *tr230b* and *ta229f* mutant embryos identified premature stop codons 79 amino acids (*tr230b*) and 328 amino acids (*ta229f*) into the protein. (C) A *cyfip2* splice-blocking morpholino phenocopies *nev*. Dorsal views showing dorsonasal axons projecting onto the optic tectum. Dashed lines indicate approximate outline of the tectum. Dorsonasal axons in *nev* project inappropriately onto the dorsal half of the optic tectum, as do dorsonasal axons in embryos injected with a splice-blocking morpholino (SBMO) to *cyfip2* (arrows). To quantify these errors, the number of axons projecting through the dorsal optic tectum was counted in wt, *cyfip2 SBMO*, and *nev* at 3dpf. Numbers of embryos shown inside bars. Scale bar = 50 μm.

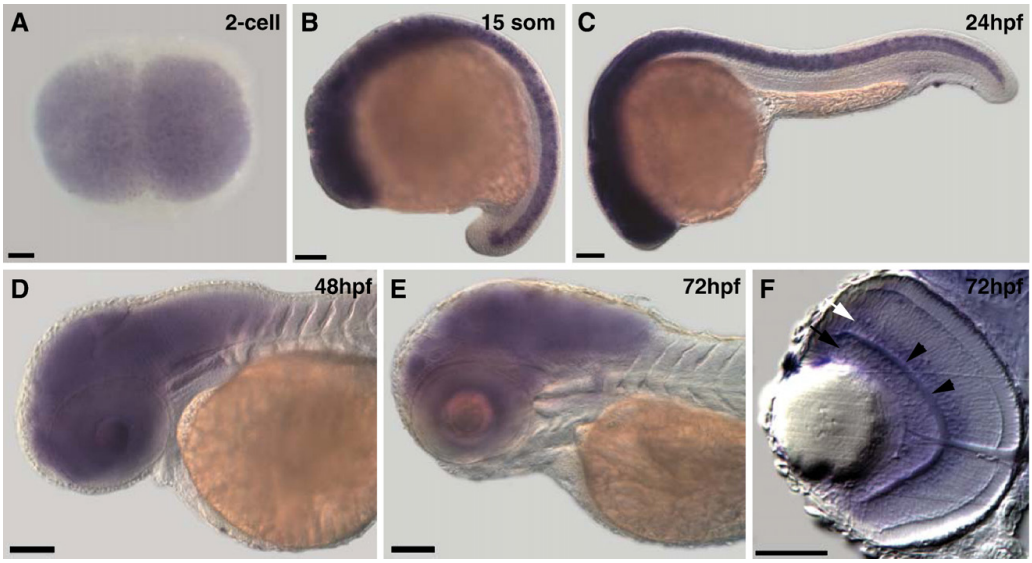

Fig. 4. *cyfip2* is broadly expressed in the CNS. (A) Animal pole view of a two-cell embryo showing maternal expression of *cyfip2*. (B and C) Lateral views of a 15 somite and 24hpf embryo, respectively. *cyfip2* is broadly expressed in the CNS. (D and E) From 48hpf to 72hpf, when axons first arrive at the optic tectum and begin to innervate it, *cyfip2* is still broadly expressed in the brain and retina. (F) Coronal section through a 72hpf eye. *cyfip2* is expressed in the RGC layer (black arrow), the inner plexiform layer (black arrowheads), and the inner nuclear layer (white arrow). Scale bars = 100 μm (A–E), 50 μm (F).

Because it had been shown in *Drosophila* that CYFIP is required for axon pathfinding in the ventral nerve cord (Schenck et al., 2003), we hypothesized that *nev* might encode Cyfip2. To search for a molecular defect in this gene, RT-PCR allele sequencing was performed for *tr230b* and *ta229f*. This analysis identified premature stop codons in Cyfip2 at amino acid 79 (Tyr>Stop) in *tr230b* and at amino acid 328 (Lys>stop) in *ta229f* (Fig. 3B). In addition, gDNA from the corresponding founder fish was sequenced to confirm that the mutations were induced by the mutagenesis (data not shown). Because of the early stop codon in *tr230b* and because both alleles show similar phenotypes (data not shown), we believe that both *tr230b* and *ta229f* are null alleles. Furthermore, *cyfip2* mRNA expression is reduced in *nev* homozygotes (data not shown), consistent with nonsense-mediated decay.

To further confirm that the *cyfip2* mutation is causative for *nev*, we designed a morpholino antisense oligonucleotide (MO) to *cyfip2* that interferes with the splicing of *cyfip2* mRNA. Injecting this SBMO into embryos at the one-cell stage prevented proper Cyfip2 splicing (Supplemental Fig. 1) and phenocopies *nev* (Fig. 3C). To quantify these phenotypes, we counted the number of axons projecting inappropriately through the dorsal optic tectum in WT, *nev,* and embryos injected with *cyfip2* SBMO at 3dpf. While in WT a few axons are present on the dorsal tectum (2.9 ± 0.6, mean ± SEM), the *cyfip2* SBMO significantly increases the number of dorsonasal axons making mistakes (6.6 ± 1.1; $p < 0.01$, unpaired *t* test with Welch correction). In *nev*, the number of dorsonasal axons making mistakes is $11.1 \pm .1.0$ (Fig. 3C). Therefore, the *cyfip2* SBMO partially phenocopies *nev*, further confirming that *nev* is *cyfip2*.

cyfip2 is broadly expressed in the CNS

We next tested whether *cyfip2* is expressed in the developing visual system. *In situ* hybridization for *cyfip2* showed maternal expression at the 2-cell stage (Fig. 4A). From 15 somites to 24hpf, *cyfip2* is broadly expressed in the CNS (Fig. 4B and C). At 48hpf and 72hpf, *cyfip2* is still strongly expressed in the brain and retina (Fig. 4D and E). Thus, *cyfip2* could act in the eye and/or the brain to control proper sorting and targeting of dorsonasal axons. In the 72hpf eye, *cyfip2* is expressed in the RGC layer, inner plexiform layer (IPL), and inner nuclear layer (INL) (Fig. 4F). The expression of *cyfip2* in the IPL, which contains connections between dendrites of RGCs and processes from amacrine cells and bipolar cells, suggests that the translation of *cyfip2* mRNA at synapses could play a role in cytoskeletal remodeling or synaptic plasticity. The broad expression of *cyfip2* in the zebrafish CNS is similar to that of *cyfip* in the *Drosophila* CNS (Schenck et al., 2003; Bogdan et al., 2004).

Other axon tracts appear normal in nev

Given the broad expression pattern of *cyfip2* in the developing brain and spinal cord, we asked whether other axon tracts were affected in *nev*. To examine early axon tracts in the brain, we stained for anti-acetylated tubulin at 24hpf (Fig. 5A and B). All the major tracts formed at this stage appear unaffected in *nev* ($n = 6$ mutant embryos, genotyped by PCR). We also used znp-1 to stain primary motor neurons at 30hpf and found their axonal projections to be normal in *nev* (Fig. 5C and D; $n = 7$). The Mauthner neurons, which are located in the hindbrain, project an axon across the midline that extends down the spinal cord; this projection is normal in *nev* (Fig. 5E and F; $n = 6$). Thus, zygotic *cyfip2* appears to be required quite specifically for dorsonasal retinal axons but not for these non-retinal axon tracts.

Retinal lamination is disrupted in nev

Because *cyfip2* is expressed in the eye throughout development, we asked whether its lamination is normal in *nev*. To visualize lamination, cell nuclei in both WT and *nev* were labeled with Hoechst 33342 at 5dpf. In WT, the eye is well laminated and the RGC layer, IPL, INL, outer plexiform layer (OPL), and outer nuclear layer (ONL) are all clearly visible (Fig. 6A). At 5dpf, the IPL normally contains only processes from

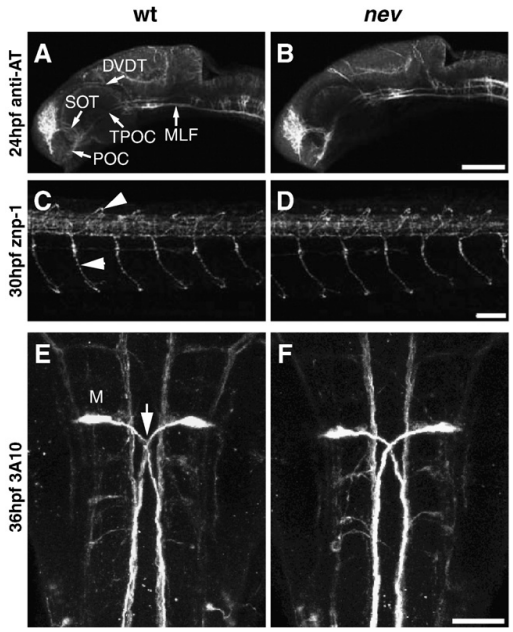

Fig. 5. Early axon pathfinding appears normal in *nev*. Confocal projections in WT (A, C, E) and *nev* (B, D, F) stained with anti-acetylated tubulin (A and B), znp-1 (B and E), and 3A10 (C and F). Lateral views (A–D) and dorsal views (E and F). Anti-acetylated tubulin labels early axon pathways at 24hpf including the anterior commissure (AC), post-optic commissure (POC), supra-optic tract (SOT), tract of the post-optic commissure (TPOC), dorso-ventral diencephalic tract (DVDT), and medial longitudinal fasciculus (MLF). No differences are detectable between WT (A) and *nev* (B). Axon trajectories of primary motor neurons at 30hpf are normal in *nev* (D) compared to WT (C), including middle primary motor neurons (MiPs, upper arrowhead) and caudal primary motor neurons (CaPs, lower arrowhead). (E and F) Mauthner neurons and their axons (arrow in E) project normally in *nev* (F) as compared to WT (E) at 36hpf. Scale bar in B = 100 μm, D, F = 50 μm.

RGCs, amacrine cells, and bipolar cells; very rarely is a displaced cell body found here (only 1 cell in 10 eyes examined). However, in *nev*, there are consistently cell bodies displaced in the IPL ($n = 11/11$ eyes examined, ≥10 cells/eye; Fig. 6B). A similar phenotype was also observed at 3 dpf (data not shown). Unlike the retinotectal projection phenotype, which affects only a subset of dorsal RGCs, displaced IPL cells are found in the dorsal, central, and ventral retina. This suggests that the axon guidance and lamination phenotypes are independent.

To determine the identity of these displaced cells, *nev* heterozygotes were crossed into a transgenic line, *Tg(isl2b:GFP)^{zc7}*, which labels all (or nearly all) RGCs with GFP (Pittman et al., 2008). *nev* embryos and WT siblings at 5dpf were double-stained with antibodies to GFP and to parvalbumin, which is expressed in a subset of amacrine cells in both the RGC layer and the INL (Malicki et al., 2003; Avanesov and Malicki, 2004), and counterstained with Hoechst 33342 (Fig. 6A and B‴). In *nev*, a mixture of RGCs (GFP+) and amacrine cells (parvalbumin+) are intermingled in the IPL (Fig. 6B–B‴). Thus, *cyfip2* is required for the proper segregation of both RGCs and amacrine cells during the lamination of the retina.

To determine whether *cyfip2* acts cell autonomously in retinal lamination, we transplanted cells from donor embryos collected from a *nev/+;Tg(isl2b:GFP)^{zc7}/+* incross (injected with a rhodamine:biotin dextran solution to label donor cells) into host embryos collected from a *nev* heterozygote incross, then stained with streptavidin-Alexa 546 and anti-GFP to identify donor cells and Hoechst 33342 to visualize the cell layers. WT donor cells were found in the IPL of *nev* eyes (4/24 eyes; Fig. 7A and B–B‴) and *nev* donor cells in the IPL of WT eyes (2/37 eyes; Fig. 7C and D–D‴). In *nev* to *nev* control transplants, we found *nev* donor cells in the IPL of *nev* eyes at similar rates (3/17 eyes; Fig. 7E and F–F‴). WT donor cells were never displaced in the IPL of WT eyes (0/24 eyes; data not shown). Thus, *nev* acts both cell autonomously and cell nonautonomously during retinal lamination.

CYFIP2 functions cell autonomously in dorsonasal RGC axon sorting

We hypothesized that CYFIP2 acts in the retinal growth cones during their pathfinding. In this case, restoring wildtype CYFIP2 function in *nev* axons should rescue their sorting in the axon tract. To do so, we adapted focal *in vivo* electroporation (Bianco et al., 2008) to introduce DNA constructs into dorsonasal RGCs (Materials and Methods). Co-electroporation was efficient: when co-electroporating EGFP and mCherry constructs, 90% of RGC arbors were double-labeled ($n = 10$; Fig. 8A). Dorsonasal RGCs were electroporated with *gap43-gfp* alone, or with a wildtype *cyfip2* construct together with a *gap43-gfp* marker (Fig. 8); correct targeting in the retina was confirmed by selecting arbors that terminated in the posteroventral quadrant of the tectum (Fig. 8B). Dorsonasal *nev* axons marked with *gap43-gfp* (Fig. 8E) showed similar paths to those previously labeled with DiI (Fig. 2). They were often missorted in the dorsal brachium of the optic tract; both missorted and properly sorted axons sometimes took "meandering" routes on the tectum. Individual *nev* arbors appeared to be properly restricted to a single tectal lamina (data not shown), but were often less branched than WT and showed abnormal self-crossing (Fig. 8E); however, we did not attempt to quantitate this arborization defect.

To quantitate the tract sorting error, the position at which axons entered the tectum was quantified using a coordinate system in which the ventralmost retinal fascicle was 0% and the dorsalmost, 100% (Fig. 8C and D). Dorsonasal axons in WT labeled with GFP sorted in the ventral brachium and entered the tectum ventrally, with mean position 23.5 ± 1.8% (mean ± SEM, $n = 54$ arbors/22 larvae; Fig. 8C and D). While some dorsonasal axons in *nev* sorted correctly, others sorted in the dorsal brachium and entered the tectum dorsally (Fig. 8C and E). Their mean position was 43.6 ± 4.8% ($n = 26/12$), significantly more dorsal than WT ($p = 0.0005$, two-tailed Mann-Whitney U test). When *nev* axons were co-electroporated with *cyfip2*, their sorting was rescued (Fig. 8C and F), with a mean position of 27.1 ± 3.2% ($n = 22/13$), significantly more ventral than control *nev* ($p = 0.015$), and not significantly different than WT ($p = 0.72$). Therefore, we conclude that CYFIP2 acts cell autonomously in optic tract sorting for dorsonasal RGCs.

Discussion

Here we describe the phenotypic analysis and cloning of the zebrafish retinotectal mutant, *nev*. We show that *nev* encodes Cyfip2 and is thus the first known vertebrate mutation in this gene family. Through a combination of axon labeling methods, we show that specific mistakes are made by a subset of dorsonasal retinal axons, which missort in the optic tract and wander through the dorsal tectum before appearing to terminate topographically. The optic tract sorting defect could be rescued cell autonomously by electroporation of wildtype *cyfip2*. Interestingly, the axon guidance phenotype is specific to retinal axons, as all the non-retinal axons that we analyzed were unaffected. In addition, we show that the lamination of the retina is disrupted in *nev*, so that a mixture of RGCs and amacrine cells are displaced in the IPL. This lamination defect requires both cell-autonomous and nonautonomous *nev* function.

Role of CYFIP2 in tract sorting and tectal targeting

When might *cyfip2* act? *cyfip2* is expressed broadly in the retina and brain at 24hpf, just prior to RGC differentiation (Hu and Easter, 1999); at 36hpf, when axons have begun exiting the eye (Stuermer,

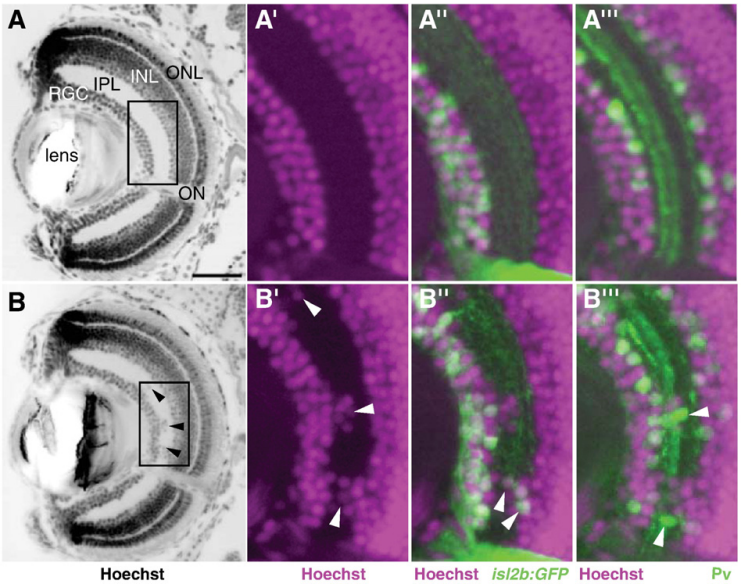

Fig. 6. Retinal lamination is disrupted in *nev*. Coronal sections through a WT eye (A–A‴) and a *nev* eye (B–B‴) at 5dpf. (A and B) Hoechst 33342 stain to visualize lamination. The retinal ganglion cell (RGC) layer, inner plexiform layer (IPL), inner nuclear layer (INL), and outer nuclear layer (ONL) are all clearly visible at this stage. Arrowheads in B show displaced cells in the IPL of *nev*. Boxed regions are magnified in A′–A‴ and B′–B‴ and show nuclei labeled with Hoechst 33342 (magenta; A′–A‴, B′–B‴), RGCs labeled with *isl2b:GFP* (green; A″, B″), and a subset of amacrine cells labeled with anti-parvalbumin (green; A‴, B‴). In *nev*, RGCs and amacrine cells are intermingled in the IPL. Arrowheads in B″ and B‴ show displaced RGCs and amacrine cells in the IPL, respectively. ON, optic nerve. Scale bar = 50 μm.

1988; Burrill and Easter, 1994); and continuing through at least 72hpf, when the first axons have reached the posterior tectum (Stuermer, 1988). *cyfip2* expression is thus consistent with a role in retinal axons as they first sort topographically in the optic tract and then project topographically on the tectum. Indeed, we find both tract sorting and tectal projection phenotypes in *nev* at 3 and 5dpf. By labeling a few RGCs in the dorsonasal retina, we could analyze rather precisely the paths taken by misrouted axons in *nev*. Dorsonasal axons take circuitous routes in the tectum but do appear to direct themselves towards the ventral tectum, suggesting that they are able to respond to topographic cues. Single-axon labeling with DNA electroporation in *nev* showed defects in tract sorting, pathfinding across the tectum, and arborization on the tectum at 5dpf.

We were able to determine that *cyfip2* acts autonomously during retinal axon sorting in the optic tract, consistent with the demonstration by Bogdan et al. (2004) that in *Drosophila*, CYFIP is required eye autonomously for photoreceptor axons to find their appropriate targets in the brain. In *nev*, electroporation with wildtype *cyfip2* caused dorsonasal RGC axons to be sorted ventrally in the optic tract, similar to wildtype. Expression of CYFIP2 in a single dorsonasal RGC in *nev* is sufficient for correct axon sorting in the optic tract. This demonstrates that *cyfip2* acts cell autonomously in the D-V sorting of dorsonasal RGC axons in the optic tract.

Neither the tectal pathfinding nor the arborization phenotypes of *nev* were rescued by *cyfip2* electroporation. In addition, *cyfip2* electroporation appeared to interfere with both processes in wildtype (data not shown), likely due to abnormally high levels of CYFIP2. Because of this, we cannot conclude from the electroporation experiments whether *cyfip2* has autonomous function in these two processes; indeed, it is possible that *cyfip2* acts autonomously for tract sorting and nonautonomously for the tectal phenotypes. We do not believe that the *nev* tectal pathfinding behavior is a secondary consequence of tract missorting. While it has been suggested that pretarget order might influence topographic mapping in the target (Plas et al., 2005), the phenotypes of *nev*, *boxer* (*box*), and *dackel* (*dak*) do not support this idea. In all three mutants, dorsal axons are missorted in the dorsal branch of the optic tract, enter the tectum incorrectly, but then eventually navigate to their correct topographic target in ventral tectum. While *nev* axons take meandering paths on the tectum, *box* and *dak* axons take more direct paths, never turning back on themselves (Lee et al., 2004). Thus in all three mutants, dorsal axons clearly have access to topographic information, although in *nev* they seem to have difficulty translating this into directed growth. *nev* axons electroporated with wildtype *cyfip2* showed tectal pathfinding defects while having largely normal tract sorting, further dissociating these two behaviors.

At present, little is known about the molecules that control sorting in the optic tract. One strategy for uncovering them is to clone the retinotectal mutants found in the Tübingen screen, and indeed many of the affected genes have been cloned (Fricke et al., 2001; Parsons et al., 2002; Lee et al., 2004; D'Souza et al., 2005; Pollard et al., 2006; Seth et al., 2006). In particular, the cloning of *nev*, *box*, and *dak* shows that HSPGs and Cyfip2 play key roles in tract sorting, providing clues that may lead to the responsible ligands and receptors.

In contrast, for D-V topographic targeting on the tectum, work from mouse and *Xenopus* has implicated ephrin-B/EphB forward and reverse signaling, as well as Wnt/Ryk signaling (Hindges et al., 2002; Mann et al., 2002; Schmitt et al., 2006). In zebrafish, recent data has suggested a role for semaphorins (Liu et al., 2004) and *esrom/PAM* (D'Souza et al., 2005). Our analysis of EphB and ephrin-B expression in *nev*, both at the mRNA and protein levels (Supplemental Table 1) suggests that loss of Cyfip2 does not affect their transcriptional or translational regulation. Instead, lack of Cyfip2 might reduce the fidelity of growth responses to topographic signals, by compromising signaling through Rac and the WAVE complex or through FMRP.

Because Cyfip proteins interact with FMRP (Schenck et al., 2001), we tried to determine whether knocking down FMRP with antisense

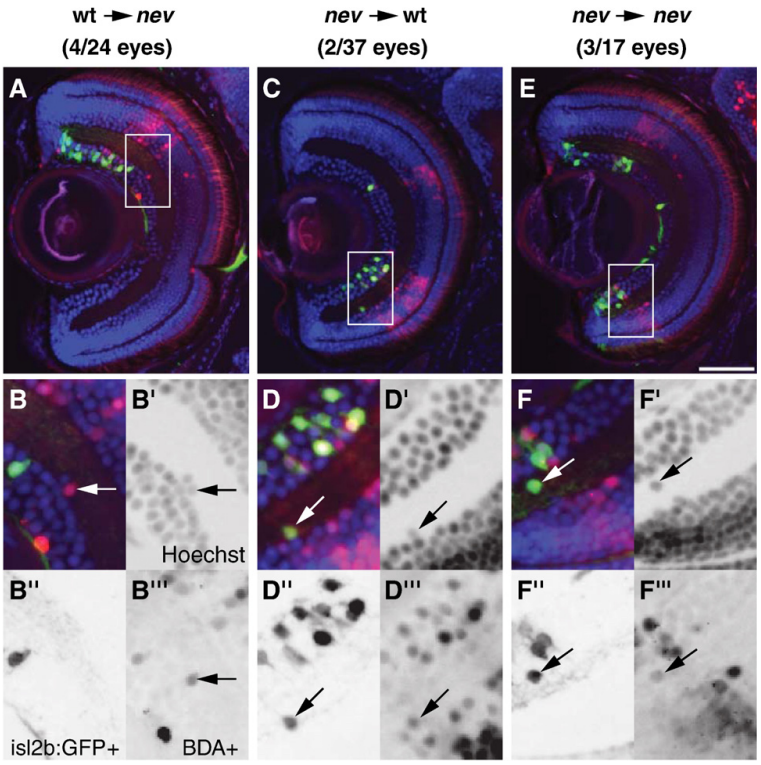

Fig. 7. *cyfip2* acts both cell autonomously and cell nonautonomously in lamination. Representative coronal sections through a *nev* eye with WT donor cells (A–B‴), a WT eye with *nev* donor cells (C–D‴), and a *nev* eye with *nev* donor cells (E-F‴). (A, C, E) Hoechst 33342 stain (blue), biotin dextran-positive (BDA+) donor cells (red), and *isl2b:GFP*+ donor RGCs (green). Insets are shown magnified below. (B–B‴) WT donor cells in a *nev* host are misplaced in the IPL, showing *nev* can act cell nonautonomously. Arrows show a BDA+ donor cell next to a BDA− cell in the IPL. (D–D‴) *nev* donor cells in a WT host are misplaced in the IPL, showing that *nev* can also act cell autonomously. Arrows show a BDA+/*isl2b:GFP*+ cell in the IPL. (F–F‴) Control transplants show *nev* donor cells in a *nev* host that are misplaced in the IPL. Arrow shows a BDA+/*isl2b:GFP*+ cell misplaced in the IPL. Scale bar = 50 μm.

morpholinos affects retinal axons, either in WT or in a *nev* background. Zebrafish *fmr1* is expressed broadly in the retina and brain during development of the retinotectal projection (data not shown; Tucker et al., 2004). When we injected either translation- or splice-blocking antisense *fmr1* morpholinos into WT or *nev*, we could find no effect on the topographic projections of retinal axons (data not shown).

Potential redundancy between Cyfip1 and Cyfip2

As with mammals, zebrafish have two *cyfip* genes. Although the CYFIP proteins do not contain any recognizable protein domains, they are evolutionarily highly conserved: zebrafish Cyfip2 is 98% identical to human CYFIP2, while zebrafish Cyfip1 (Schenck et al., 2001) and Cyfip2 are 86% identical to each other. The single *Drosophila* CYFIP is 67% identical to human CYFIP1 and CYFIP2 (Schenck et al., 2003). As with zebrafish *cyfip2*, fly *cyfip* is expressed broadly in the CNS at both the level of RNA and protein (Schenck et al., 2003; Bogdan et al., 2004).

Given the broad expression of *cyfip2* in the developing zebrafish CNS and the variety of phenotypes observed in *Drosophila*, it interesting that we have only been able to identify subtle phenotypes in the retinotectal system and not in any other axon tracts. One explanation is that maternal *cyfip2* is able to compensate for the loss of zygotic *cyfip2* early in development; the non-retinal axon tracts analyzed in Fig. 5 develop much earlier than retinal axons. In *Drosophila*, removing both maternal and zygotic *cyfip* greatly enhanced the axon pathfinding errors (Schenck et al., 2003). We have tried knocking down both maternal and zygotic *cyfip2* with a translation-blocking morpholino against *cyfip2*, but found a delay in overall development of the embryos and thus the retinotectal projection, which precluded analysis of the retinal axons (data not shown). This does, however, suggest that maternal *cyfip2* functions early in development.

A second explanation for the subtle *nev* phenotype is that Cyfip1 may compensate for the loss of Cyfip2. Zebrafish *cyfip1* is expressed broadly throughout the entire embryo at 24hpf (data not shown). However, from 36hpf and beyond, *cyfip1* is expressed in the brain and retina at very low levels, if at all. Nevertheless, we designed both splice-blocking morpholinos and translation-blocking morpholinos to *cyfip1* and injected them into WT embryos. Similar to the *cyfip2* translation-blocking morpholinos, we found an overall delay in the development of embryos injected with either morpholino, and a delay in the growth of axons to the tectum (data not shown). Thus, *cyfip1* seems also to have required functions in early development, and we were unable to conclude whether Cyfip1 acts redundantly with Cyfip2 in the retinotectal system.

Role of Cyfip2 in retinal lamination

In *nev* mutants, we found both RGCs and amacrine cells displaced in the IPL. We saw lamination defects at both 3 and 5 dpf (data not shown; Fig. 6), and *cyfip2* is expressed in the eye at least through 3 dpf. When we performed cell transplants between *nev* and wt, misplaced

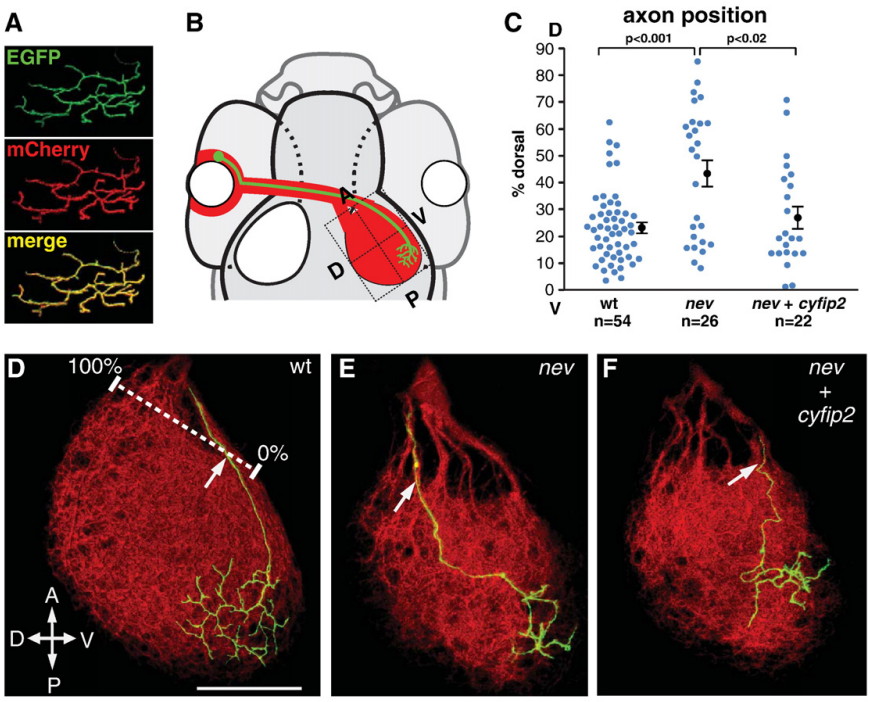

Fig. 8. *cyfip2* acts cell autonomously in dorsonasal RGC axon sorting in the optic tract. (A) Co-electroporation yields consistent co-labeling with EGFP and mCherry. (B) Diagram of rescue experiments: electroporated dorsonasal RGCs project to the posteroventral quadrant of the tectum. (C) Quantification of D-V sorting of dorsonasal axons in the optic tract as they enter the right optic tectum, relative to the ventralmost (0%) and dorsalmost (100%) fascicles (*white ruler* in D). A subset of *nev* axons missorts into the dorsal brachium; electroporation with *cyfip2* yields significant rescue. Error bars show mean ± SEM. (D–F) Confocal projections of single dorsonasal axons (GAP43-GFP, *green*) in the tectal neuropil (mCherryCAAX, *red*) at 5 dpf. (D) WT axons enter the tectum ventrally. (E) *nev* axons often enter dorsally. (F) *cyfip2*-co-electroporated *nev* axons are rescued and enter ventrally. Scale bar, 50 μm.

donor cells were found in the IPL in both wt-to-*nev* and *nev*-to-wt transplants, suggesting that *nev* acts *both* cell autonomously and nonautonomously for proper sorting of cells into their appropriate positions. These results are not necessarily surprising if, for example, *nev* were to act downstream of molecules that act either through homophilic *or* heterophilic interactions (e.g., cell adhesion molecules).

Interestingly, hypomorphic mutations in zebrafish *n-cadherin* show similar retinal lamination phenotypes to *nev* but do not show retinal pathfinding errors (Masai et al., 2003) or topographic mapping mistakes (data not shown). Whether Cyfip2 interacts with N-cadherin during lamination or axon pathfinding is not yet known. In other species, disrupting the cell adhesion molecule NCAM (neural cell adhesion molecule) also causes a phenotype strikingly similar to *nev*. Mice lacking NCAM-180, a specific variant of NCAM, show an increase in cells displaced in the IPL (Tomasiewicz et al., 1993) even though the overall morphology of the retina is similar to WT. Disrupting polysialic acid (PSA), a carbohydrate modification of NCAM, affects the fasciculation of axons in the chick optic tract, and causes axons on the tectum to "wander," sometimes projecting anteriorly (Yin et al., 1995), very similar to what we observe in *nev*. Thus, it is also possible that *cyfip2* may act downstream of NCAM to regulate sorting of cells and axons in the zebrafish retinotectal system.

In summary, we have shown that *nev* encodes Cyfip2, which is required for the lamination of the retina and axon pathfinding in the retinotectal system. Given that *cyfip2* is required only by dorsonasal axons in the tract and tectum but is required for lamination of cells throughout the dorsal, central and ventral retina, these processes appear to function independently. However, in both lamination and axon guidance, *cyfip2* may have a similar function in aiding cells to sort from one another. The known interactions of CYFIP proteins with the Rac pathway as well as with the FMRP family suggest intriguing links to cytoskeletal dynamics as well as with RNA regulation. Thus, the molecular identification of *nev* adds to our understanding of cytoplasmic signaling events mediating both retinal lamination, where Cyfip2 could potentially act downstream of cell adhesion molecules, and axon pathfinding, where Cyfip2 could potentially act through Rac to translate extracellular signals into actin regulation and growth cone turning.

Acknowledgments

We thank members of the Chien lab for helpful discussions, Isaac Bianco for advice on *in vivo* electroporation, and Jude Rosenthal, Louis Ross, and Amy Kugath for excellent technical assistance. We also thank Monica Vetter for helpful comments on the manuscript. This work was supported by an NIH Predoctoral Fellowship F31 NS46189 and an NIH Developmental Biology Training Grant 5T32HD07491 to A. J.P. and grants from the NIH/NEI (EY12873) and the University of Utah Research Foundation to C.B.C.

Appendix A. Supplementary data

Supplementary data associated with this article can be found, in the online version, at doi:10.1016/j.ydbio.2010.05.512.

References

Avanesov, A., Malicki, J., 2004. Approaches to study neurogenesis in the zebrafish retina. Meth. Cell Biol. 76, 333–384.

Baier, H., Klostermann, S., Trowe, T., Karlstrom, R.O., Nusslein-Volhard, C., Bonhoeffer, F., 1996. Genetic dissection of the retinotectal projection. Development 123, 415–425.

Bardoni, B., Mandel, J.L., 2002. Advances in understanding of fragile X pathogenesis and FMRP function, and in identification of X linked mental retardation genes. Curr. Opin. Genet. Dev. 12, 284–293.

Bianco, I.H., Carl, M., Russell, C., Clarke, J.D., Wilson, S.W., 2008. Brain asymmetry is encoded at the level of axon terminal morphology. Neural Dev. 3, 9.

Bogdan, S., Grewe, O., Strunk, M., Mertens, A., Klambt, C., 2004. Sra-1 interacts with Kette and Wasp and is required for neuronal and bristle development in Drosophila. Development 131, 3981–3989.

Burrill, J.D., Easter Jr., S.S., 1994. Development of the retinofugal projections in the embryonic and larval zebrafish (Brachydanio rerio). J. Comp. Neurol. 346, 583–600.

D'Souza, J., Hendricks, M., Le Guyader, S., Subburaju, S., Grunewald, B., Scholich, K., Jesuthasan, S., 2005. Formation of the retinotectal projection requires Esrom, an ortholog of PAM (protein associated with Myc). Development 132, 247–256.

Eden, S., Rohatgi, R., Podtelejnikov, A.V., Mann, M., Kirschner, M.W., 2002. Mechanism of regulation of WAVE1-induced actin nucleation by Rac1 and Nck. Nature 418, 790–793.

Fricke, C., Lee, J.S., Geiger-Rudolph, S., Bonhoeffer, F., Chien, C.B., 2001. astray, a zebrafish roundabout homolog required for retinal axon guidance. Science 292, 507–510.

Govek, E.E., Newey, S.E., Van Aelst, L., 2005. The role of the Rho GTPases in neuronal development. Genes Dev. 19, 1–49.

Hindges, R., McLaughlin, T., Genoud, N., Henkemeyer, M., O'Leary, D.D., 2002. EphB forward signaling controls directional branch extension and arborization required for dorsal–ventral retinotopic mapping. Neuron 35, 475–487.

Ho, R.K., Kane, D.A., 1990. Cell-autonomous action of zebrafish spt-1 mutation in specific mesodermal precursors. Nature 348, 728–730.

Hu, M., Easter, S.S., 1999. Retinal neurogenesis: the formation of the initial central patch of postmitotic cells. Dev. Biol. 207, 309–321.

Karlstrom, R.O., Trowe, T., Klostermann, S., Baier, H., Brand, M., Crawford, A.D., Grunewald, B., Haffter, P., Hoffmann, H., Meyer, S.U., Muller, B.K., Richter, S., van Eeden, F.J., Nusslein-Volhard, C., Bonhoeffer, F., 1996. Zebrafish mutations affecting retinotectal axon pathfinding. Development 123, 427–438.

Kawano, Y., Yoshimura, T., Tsuboi, D., Kawabata, S., Kaneko-Kawano, T., Shirataki, H., Takenawa, T., Kaibuchi, K., 2005. CRMP-2 is involved in kinesin-1-dependent transport of the Sra-1/WAVE1 complex and axon formation. Mol. Cell. Biol. 25, 9920–9935.

Kimmel, C.B., Ballard, W.W., Kimmel, S.R., Ullmann, B., Schilling, T.F., 1995. Stages of embryonic development of the zebrafish. Dev. Dyn. 203, 253–310.

Kobayashi, K., Kuroda, S., Fukata, M., Nakamura, T., Nagase, T., Nomura, N., Matsuura, Y., Yoshida-Kubomura, N., Iwamatsu, A., Kaibuchi, K., 1998. p140Sra-1 (specifically Rac1-associated protein) is a novel specific target for Rac1 small GTPase. J. Biol. Chem. 273, 291–295.

Koshiba-Takeuchi, K., Takeuchi, J.K., Matsumoto, K., Momose, T., Uno, K., Hoepker, V., Ogura, K., Takahashi, N., Nakamura, H., Yasuda, K., Ogura, T., 2000. Tbx5 and the retinotectum projection. Science 287, 134–137.

Kwan, K.M., Fujimoto, E., Grabher, C., Mangum, B.D., Hardy, M.E., Campbell, D.S., Parant, J. M., Yost, H.J., Kanki, J.P., Chien, C.B., 2007. The Tol2kit: a multisite gateway-based construction kit for Tol2 transposon transgenesis constructs. Dev. Dyn. 236, 3088–3099.

Lee, J.S., Ray, R., Chien, C.B., 2001. Cloning and expression of three zebrafish roundabout homologs suggest roles in axon guidance and cell migration. Dev. Dyn. 221, 216–230.

Lee, J.S., von der Hardt, S., Rusch, M.A., Stringer, S.E., Stickney, H.L., Talbot, W.S., Geisler, R., Nusslein-Volhard, C., Selleck, S.B., Chien, C.B., Roehl, H., 2004. Axon sorting in the optic tract requires HSPG synthesis by ext2 (dackel) and extl3 (boxer). Neuron 44, 947–960.

Liu, Y., Berndt, J., Su, F., Tawarayama, H., Shoji, W., Kuwada, J.Y., Halloran, M.C., 2004. Semaphorin3D guides retinal axons along the dorsoventral axis of the tectum. J. Neurosci. 24, 310–318.

Machesky, L.M., Mullins, R.D., Higgs, H.N., Kaiser, D.A., Blanchoin, L., May, R.C., Hall, M.E., Pollard, T.D., 1999. Scar, a WASp-related protein, activates nucleation of actin filaments by the Arp2/3 complex. Proc. Natl. Acad. Sci. U. S. A. 96, 3739–3744.

Malicki, J., Jo, H., Pujic, Z., 2003. Zebrafish N-cadherin, encoded by the glass onion locus, plays an essential role in retinal patterning. Dev. Biol. 259, 95–108.

Mann, F., Ray, S., Harris, W., Holt, C., 2002. Topographic mapping in dorsoventral axis of the Xenopus retinotectal system depends on signaling through ephrin-B ligands. Neuron 35, 461–473.

Masai, I., Lele, Z., Yamaguchi, M., Komori, A., Nakata, A., Nishiwak, Y., Wada, H., Tanaka, H., Nojima, Y., Hammerschmidt, M., Wilson, S.W., Okamoto, H., 2003. N-cadherin mediates retinal lamination, maintenance of forebrain compartments and patterning of retinal neurites. Development 130, 2479–2494.

McLaughlin, T., O'Leary, D.D., 2005. Molecular gradients and development of retinotopic maps. Annu. Rev. Neurosci. 28, 327–355.

Miki, H., Suetsugu, S., Takenawa, T., 1998. WAVE, a novel WASP-family protein involved in actin reorganization induced by Rac. EMBO J. 17, 6932–6941.

Napoli, I., Mercaldo, V., Boyl, P.P., Eleuteri, B., Zalfa, F., De Rubeis, S., Di Marino, D., Mohr, E., Massimi, M., Falconi, M., Witke, W., Costa-Mattioli, M., Sonenberg, N., Achsel, T., Bagni, C., 2008. The fragile X syndrome protein represses activity-dependent translation through CYFIP1, a new 4E-BP. Cell 134, 1042–1054.

Neff, M.M., Turk, E., Kalishman, M., 2002. Web-based primer design for single nucleotide polymorphism analysis. Trends Genet. 18, 613–615.

Parsons, M.J., Pollard, S.M., Saude, L., Feldman, B., Coutinho, P., Hirst, E.M., Stemple, D.L., 2002. Zebrafish mutants identify an essential role for laminins in notochord formation. Development 129, 3137–3146.

Pittman, A.J., Law, M.Y., Chien, C.B., 2008. Pathfinding in a large vertebrate axon tract: isotypic interactions guide retinotectal axons at multiple choice points. Development 135, 2865–2871.

Plas, D.T., Lopez, J.E., Crair, M.C., 2005. Pretarget sorting of retinocollicular axons in the mouse. J. Comp. Neurol. 491, 305–319.

Pollard, S.M., Parsons, M.J., Kamei, M., Kettleborough, R.N., Thomas, K.A., Pham, V.N., Bae, M.K., Scott, A., Weinstein, B.M., Stemple, D.L., 2006. Essential and overlapping roles for laminin alpha chains in notochord and blood vessel formation. Dev. Biol. 289, 64–76.

Saller, E., Tom, E., Brunori, M., Otter, M., Estreicher, A., Mack, D.H., Iggo, R., 1999. Increased apoptosis induction by 121F mutant p53. EMBO J. 18, 4424–4437.

Schenck, A., Bardoni, B., Langmann, C., Harden, N., Mandel, J.L., Giangrande, A., 2003. CYFIP/Sra-1 controls neuronal connectivity in Drosophila and links the Rac1 GTPase pathway to the fragile X protein. Neuron 38, 887–898.

Schenck, A., Bardoni, B., Moro, A., Bagni, C., Mandel, J.L., 2001. A highly conserved protein family interacting with the fragile X mental retardation protein (FMRP) and displaying selective interactions with FMRP-related proteins FXR1P and FXR2P. Proc. Natl. Acad. Sci. U. S. A. 98, 8844–8849.

Schenck, A., Qurashi, A., Carrera, P., Bardoni, B., Diebold, C., Schejter, E., Mandel, J.L., Giangrande, A., 2004. WAVE/SCAR, a multifunctional complex coordinating different aspects of neuronal connectivity. Dev. Biol. 274, 260–270.

Schmitt, A.M., Shi, J., Wolf, A.M., Lu, C.C., King, L.A., Zou, Y., 2006. Wnt-Ryk signalling mediates medial-lateral retinotectal topographic mapping. Nature 439, 31–37.

Seth, A., Culverwell, J., Walkowicz, M., Toro, S., Rick, J.M., Neuhauss, S.C., Varga, Z.M., Karlstrom, R.O., 2006. belladonna/(lhx2) is required for neural patterning and midline axon guidance in the zebrafish forebrain. Development 133, 725–735.

Stuermer, C.A., 1988. Retinotopic organization of the developing retinotectal projection in the zebrafish embryo. J. Neurosci. 8, 4513–4530.

Tomasiewicz, H., Ono, K., Yee, D., Thompson, C., Goridis, C., Rutishauser, U., Magnuson, T., 1993. Genetic deletion of a neural cell adhesion molecule variant (N-CAM-180) produces distinct defects in the central nervous system. Neuron 11, 1163–1174.

Trowe, T., 2000. Analyse von Mutationen mit Einfluss auf die topographische Ordnung von Axonen im retinotektalen System des Zebrabaerblings, Danio rerio. Fakultaet fuer Biologie. University of Tuebingen, Tuebingen, Germany, p. 120.

Trowe, T., Klostermann, S., Baier, H., Granato, M., Crawford, A.D., Grunewald, B., Hoffmann, H., Karlstrom, R.O., Meyer, S.U., Muller, B., Richter, S., Nusslein-Volhard, C., Bonhoeffer, F., 1996. Mutations disrupting the ordering and topographic mapping of axons in the retinotectal projection of the zebrafish, Danio rerio. Development 123, 439–450.

Tucker, B., Richards, R., Lardelli, M., 2004. Expression of three zebrafish orthologs of human FMR1-related genes and their phylogenetic relationships. Dev. Genes Evol. 214, 567–574.

Wan, Y., Otsuna, H., Chien, C.B., Hansen, C., 2009. An interactive visualization tool for multi-channel confocal microscopy data in neurobiology research. IEEE Trans. Vis. Comput. Graph. 15, 1489–1496.

Yin, X., Watanabe, M., Rutishauser, U., 1995. Effect of polysialic acid on the behavior of retinal ganglion cell axons during growth into the optic tract and tectum. Development 121, 3439–3446.

CHAPTER 3

IGF2BP1/ZBP1 FUNCTION IS REQUIRED FOR ZEBRAFISH RGC AXON GUIDANCE *IN VIVO*

Introduction

Axon guidance is a critical process during nervous system development. Proper function in the mature nervous system is highly dependent on the formation of very specific long distance connections between neurons, which depends on precise navigation of growing axons. The direction and rate of axon growth are determined by growth cone behavior in response to extracellular guidance cues (Tessier-Lavigne and Goodman 1996, Marsh and Letourneau 1984, Lafont 1993). The growth cone can respond very rapidly to guidance cues, which regulate actin dynamics that drive attractive or repulsive growth cone turning (Lewis and Bridgman 1992, Vitriol and Zheng 2012, Wu et al. 2005). Regulators of actin dynamics are the targets of signaling within the growth cone (Quinn and Wadsworth 2008). Changes in actin dynamics that initiate growth cone turning occur very rapidly in the presence of guidance cues, suggesting that the growth cone reacts autonomously from the cell body (Campbell and Holt 2001). Local translation of mRNA in the growth cone provides a mechanism for genetic control over growth cone behavior that is not delayed by transport of signals and materials along the axon between the cell body and the growth cone (Lin and Holt 2008). Therefore, local mRNA translation in the growth cone is crucial for an undelayed response to guidance cues.

The turning response of a growth cone depends on the translation of specific subsets of mRNAs (Lin and Holt 2007). Attractive guidance cues such as netrin1 and BDNF activate local translation of β-actin on the side of the growth cone closest to the source (Leung et al. 2006, Yao et al. 2006). Repulsive guidance cues such as Sema3A and Slit2 activate local translation of proteins involved in actin depolymerization (Wu et al. 2005, Piper et al. 2006). Changes in the cytoskeletal structure that result from actin

regulation are responsible for growth cone dynamics (Gundersen and Barrett 1980, Isbister and O'Connor 2000). Therefore, the regulation of β-actin translation in the growth cone is a critical process during pathfinding.

RNA-binding proteins (RBPs) are essential for proper mRNA transport to the growth cone and are targets of growth cone signaling that activates translation (Sotelo-Silveira 2006). ZBP1 binds directly to β-actin mRNA (Welshans and Bassell 2011, Leung et al. 2006, Yao et al. 2006, Ross et al. 1997, Huttelmaier et al. 2005, Zhang et al. 2001, Chao et al. 2010) and is required for its localization to growth cones (Donnelly et al. 2011, Welshans and Bassell 2011). ZBP1 also represses translation of β-actin mRNA until activated through signaling in response to attractive guidance cues (Hüttelmaier et al. 2005, Sasaki et al. 2010), such as BDNF or netrin1 (Tcherkezian et al. 2010, Sasaki et al. 2010). Src tyrosine kinase phosphorylates the Y396 residue in ZBP1, which disrupts the interaction with β-actin mRNA (Hüttelmaier et al. 2005).

The mechanism through which ZBP1 mediates transport and local translation of β-actin mRNA has been studied extensively. ZBP1 binds to a region in the β-actin 3'UTR called the zipcode, which contains the bipartite element (GGACT)-n_{13}-(ACA) required for ZBP1 binding (Ross et al. 1997, Chao et al. 2010). This interaction is required for transport of β-actin mRNA to the growth cone and local β-actin translation is required for growth cone turning in response to attractive guidance cues, but not repulsive guidance cues (Welshans and Bassell 2011, Huttelmaier et al. 2005, Leung et al. 2006, Yao et al. 2006, Wu et al. 2005, Piper et al. 2006).

Although the mechanism for ZBP1-dependent local β-actin translation and its importance for growth cone behavior is well understood *in vitro*, very few studies have

looked directly at the requirement for ZBP1 function *in vivo*. ZBP1$^{-/-}$ mice die as embyros. While adult ZBP1$^{+/-}$ do not have visible defects in axon guidance, axon regeneration in response to induced injury is slower with less branching (Welshans and Bassell 2011). Anti-sense oligonucleotides and dominant negative Vg1RBP$^{\Delta KH4}$ were used to knockdown Vg1RBP (ZBP1) function in pathfinding RGCs *in vivo* in *Xenopus laevis* (Kalous et al. 2014). This study showed evidence that Vg1RBP function is not required for long-range axon growth and pathfinding, however, significant defects in axon branching and arborization on the tectum were documented (Kalous et al. 2014).

Here, I investigated the requirement for ZBP1 and β-actin mRNA translation during RGC axon guidance *in vivo* in the zebrafish retinotectal system. I used an *in vivo* timelapse assay to show that the β-actin 3'UTR is sufficient to target local translation of Kaede in RGC growth cones and I found a bipartite element in the β-actin3'UTR that has the structure required to interact with the KH34 domains of ZBP1. I identified Igf2bp1 as the ZBP1 ortholog, which was previously uncharacterized in zebrafish, and showed that it is expressed in RGCs during axon guidance. Finally, I show that loss of Igf2bp1 function causes increased retinal cell death, retinal layering defects and failure of RGC axons to grow to the tectum. To date, this is the first evidence that ZBP1 function is required for axon pathfinding *in vivo*.

Materials and methods

Fish

All wild-type embryos were from the Tübingen or TL strains. Transgenic strains used were *Tg(isl2b:egfp)^{zc7}* and *Tg(isl2b:mcherryCaax)^{zc23}* (Pittman et al. 2008). All fish

were raised at 28.5°C. Experimental protocols were approved by the University of Utah Institutional Animal Care and Use Committee and followed NIH guidelines.

DNA constructs

Isl2b-Kaede-βactin3'UTRpA, *Isl2b-Kaede-pA, Isl2b-emGFP-Igf2bp1*^{Y399E} *-pA Isl2b-emGFP-Igf2bp1-pA, Isl2b-emGFP-pA*, and *pBSII-igf2bp1* were all constructed in pDEST-Tol2pA2 with the Tol2 kit (Kwan et al. 2007). Zebrafish Igf2bp1 coding cDNA was obtained from Open Biosystems (Accession EB781185). The emerald-GFP (emGFP) cDNA was a gift from Scott Holly. Fusion PCR was used to make the A207K point mutation to generate monomeric emGFP.

Morpholinos

All morpholino oligonucleotides (MOs) were purchased from Gene Tools. Igf2bp1 splice-blocking oligo (sbMO) (5'-TCTGGTCCTGTAGAGAAAGAAATGA-3') was designed by Gene Tools, standard negative control MO (5'-CCTCTTACCTCAGTT-ACAATTTATA-3') and zebrafish p53 MO (5'-GCGCCATTGCTTTGCAAGAATTG-3'). Lyophilized MOs were resuspended in ddH20 at 1mM stock stored at room temperature (RT).

DNA and morpholino injections

All injections were performed with an ASI pressure injector delivering 1nl into the cytoplasm of 1-cell embryos. Injected embryos were raised in E2/gentamycin for 8 hours and then in E3 (1mM phenylthiourea). DNA was injected into wild-type at 25pg with 25pg transposase RNA in RNAse free ddH2O (0.1% phenol red). MO was injected

into either wild-type, *Tg(isl2b:mCherryCAAX)*^{zc23}, or *Tg(isl2b:egfp)*^{zc7}. MO amounts were: 3ng Igf2bp1 sbMO, 4.5ng p53 MO, 6ng negative control MO.

Reverse transcription polymerase chain reaction

Wild-type embyros injected with 3ng Igf2bp1 sbMO were collected at 48 hpf, and total RNA preps from 20 embryos were used to make cDNA with reverse transcription. Igf2bp1 cDNA was amplified with f-primer in exon1 (5'-CGCCAAGGTTGCTACAGT-GAAGAATATTTACCAC-3') and either r-primer in exon3 (5'-CACTGCAGGTGTGG-TGGAATCTTTCTGATC-3') or r-primer in exon4 (5'-CACAGTTCTCAACAGTTCC-ATATTGGGCAAG-3'). PCR product using the exon4 r-primer was gel purified and Topo-cloned for direct sequencing with M13 primers.

Immunostaining

Embryos were selected for imaging under an Olympus SZX16 fluorescent dissecting microscope at 3dpf and then fixed in 4% paraformaldehyde for 6h at 4°C. Embryos were washed in PBST (0.5% tritonX10), permeabilized with 0.1% collagenase in 2%PBST, blocked with 0.1% NCST and then incubated with primary antibody (1:700 rabbit anti-EGFP or 1:200 rabbit anti-DsRed in NCST) for 2d. Embryos were washed with PBST and incubated with Topro3 (conc.) secondary antibody (1:200 Alexa 488 goat anti-rabbit or Cy3 goat anti-rabbit in NCST). Embryos were washed, incubated in 50% glycerol for 2h then 80% glycerol overnight and stored at -20°C. Embryos were prepared for imaging in 100% glycerol under coverglass.

In situ *hybridization*

In situ hybridization was performed as previously described (Thisse and Thisse 2008), on wild-type using Igf2bp1 antisense probe, made from pBSII-Igf2bp. Embryos were photographed in glycerol on an Olympus SZX16 DIC dissecting scope with SPOT camera software.

Plastic sectioning

After *in situ* hybridization, embryos were incubated in 1:1 immunobed in MeOH for 30 minutes and then 100% immunobed overnight. Embryos were embedded in Immunobed with (1:20) solution B (EMS catalog# 14260-04). Sections of 12.5 um were made using a Reichert-Jung supercut microtome with a glass knife.

Acridine Orange staining

A 10um diameter bolus of acridine orange (Sigma catalog# A6014) suspended in ddH_2O was injected into the yolk of embryos 2 h before imaging. Fluorescent pictures were taken using the GFP excitation and emission filters on an Olympus SZX16 fluorescent dissecting microscope. The eyes of 31 hpf AO stained embryos were imaged with an Olympus FV1000 confocal microscope (20x lens).

Timelapse assay

A previously described local translation timelapse assay was adapted to pathfinding retinal growth cones and axons in the zebrafish optic tract (Leung and Holt 2008). Transient 2 dpf *Tg(isl2b:Kaede-βactin3'UTR)* or *Tg(isl2b:Kaede-pA)* embryos were sorted for bright fluorescence in RGCs, anesthetized with 0.02% tricaine, and mounted dorsally in drops of 1.5% low-melt agarose in E2/gentamycin. The agarose was

windowed to expose eyes and covered with E3+1mM PTU (0.02% tricaine). A pulled glass pipette with a short taper was used to dissect the exposed eye from the embryo. The embryos were removed from the agarose and returned to E3+PTU at 28.5°C (0.02% tricaine). Approximately 50% volume of yolk was drained from embryos by squeezing it out through small hole torn with sharpened tungsten needles. Embryos were then recovered in E3 (1mM PTU). At 2.5 dpf, embryos were mounted laterally in a petri-perm (Sigma) dish in drops of low-melt agarose, with the side without an eye facing down, and covered in E3 (1mM PTU, 0.02% tricaine).

Embryos with isolated RGC axons growing in the optic tract were selected for timelapse, removed from the petri-perm dish and remounted in a dish with a glass coverslip bottom. Fish were pressed gently against the bottom of the dish to maximize availability of the optic tract for imaging. The dish was placed on a heated stage at 28.5°C. RGC axons with visible growth cones were selected and the whole head was photoconverted for 2 minutes with 405 nm laser irradiation at maximum intensity, until green Kaede was undetectable and red Kaede very bright. Timelapse was begun immediately taking a z-stack every 10 minutes ten times, for a total of 90 minutes. A 40x water immersion lens was used with immersol, with a 3x zoom. All file handling and image analysis was done in ImageJ. The macro used for quantitation was written by Hideo Otsuna.

Results

Zebrafish β-actin 3'UTR can target local Kaede translation in growth cones

An *in vitro* Kaede timelapse assay was originally used to demonstrate that the β-actin 3'UTR was sufficient to target Kaede translation in RGC growth cones (Leung et al.

2006, Leung and Holt 2008). I adapted this method to pathfinding RGC axons in the zebrafish optic tract *in vivo*. I generated *Tg(isl2b:Kaede-pA)* and *Tg(isl2b:Kaede-βactin3'UTRpA)* transient transgenic embryos with mosaic expression of Kaede in RGCs, by injecting a DNA construct at 1-cell stage (Figure 3.1A-1). At 2dpf, embryos with strong Kaede expression in the eye were selected (Figure 3.1A-2) and the eye was dissected and 50% volume of the yolk was drained (Figure 3.1A-3). At 2.5 dpf embryos were mounted laterally (Figure 3.1B). Immediately after photoconversion (Figure 3.1A-4, Figure 3.1B), axons were imaged every 10 minutes for a total of 90 minutes (Figure 3.1A-5). A timelapse example of one axon expressing Kaede-pA and one axon expressing Kaede-βactin3'UTR is shown in Figure 3.1C, with a colormap representing the ratio of green kaede/red kaede. The red color in the growth cone of the +UTR axon at 90 minutes demonstrates a more rapid rise in newly translated green Kaede in axons expressing Kaede-βactin3'UTR compared to axons expressing Kaede-pA (Figure 3.1C). In order to quantitate the rate of increase of newly synthesized green Kaede in the axons, a 1 pixel wide, 150 pixel long trace was made of each axon using sum projections of the red channel. This was done for each timepoint of each axon. The pixels defined by each trace were measured for green/red fluorescence intensity for each respective image. Pixels 1-10 were averaged and named the growth cone region and pixels 141-150 were averaged and named the proximal axon region. The growth cone values for all Kaede-β-actin3'UTR-expressing axons were averaged together, and this was repeated for each timepoint, giving the datapoints on the top left graph in Figure 3.1D (average +/- SEM). The same was done for the proximal axon values (bottom graphs), and the growth cone values for Kaede-pA-expressing axons. The average green/red growth cone value from

Figure 3.1: The β-actin 3'UTR can target local mRNA translation in RGC growth cones *in vivo*. A shows a schematic of the *in vivo timelapse assay*: 1-injection of cDNA into 1-cell embryos, 2- at 2dpf embryos with bright Kaede expression in the eye were selected, 3- the right eye was dissected off and yolk was drained, 4- pathfinding axons in the optic tract were photoconverted from green to red, 5-timelapse monitored the return on green Kaede over 90 minutes. B shows an example of the whole optic tract (40x water lens, 1x zoom) of a zebrafish prior to photoconversion, and a single axon before and after photoconversion (both green and red channels shown separately). C shows the intensity of green/red in an axon (represented by colormap), at 0, 30, 60, and 90 minutes after photoconversion. D shows quantitation of green/red intensity as the average of all axons (n=10, Kaede-βactin3'UTR, right panels, n=6, Kaede-pA, left panels), the green/red for the first 10 pixels in the growth cone was averaged for each axon, then the average was averaged for all axons (top left and top right). The same was done with pixels 141-150 (bottom left and bottom right). A Kruskal-Wallis test comparing data for growth cones with Kaede-βactin3'UTR, axons with Kaede-βactin3'UTR and growth cones with Kaede-pA showed a significant difference ($p>0.001$).

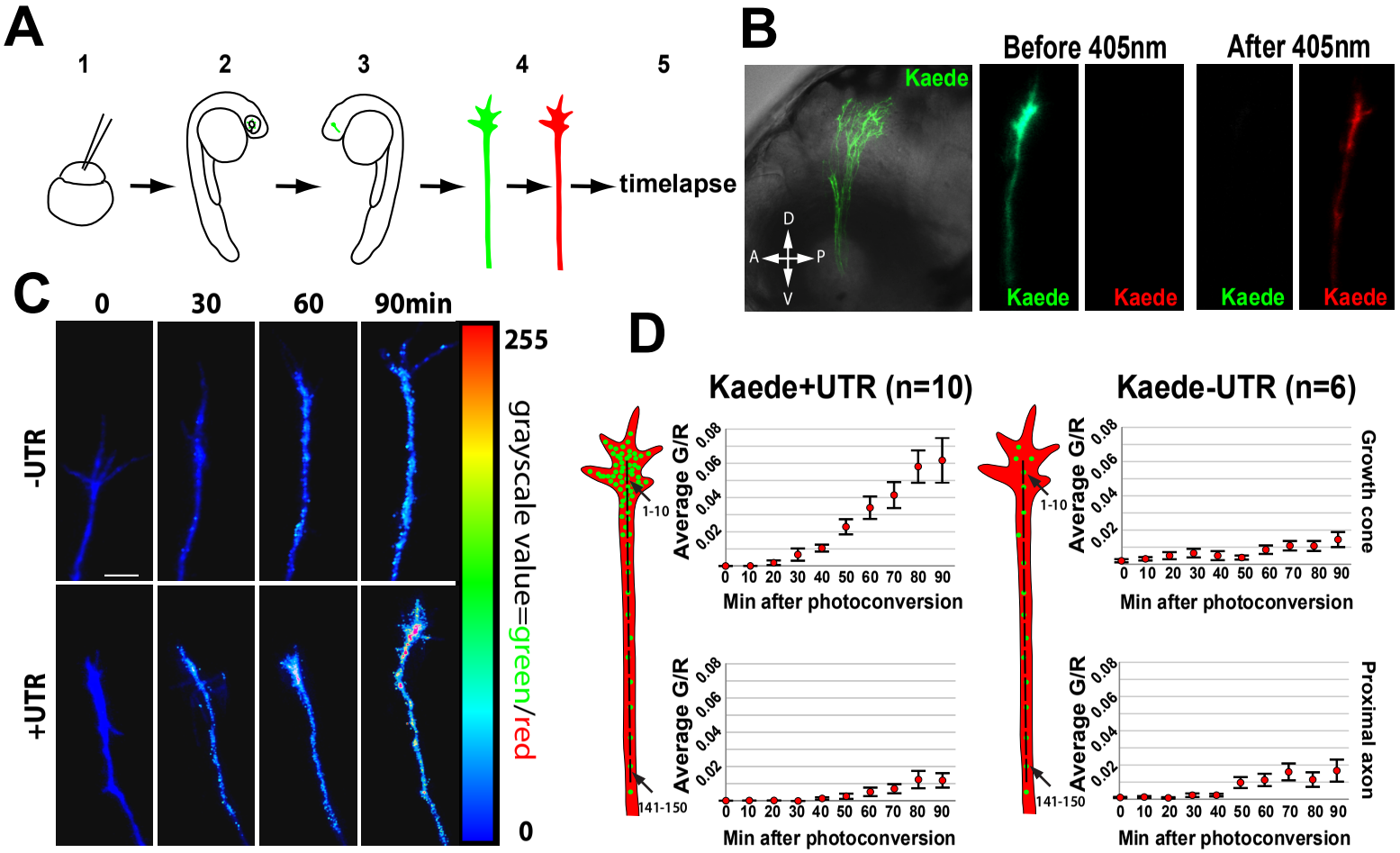
A
1
2
3
4
5
timelapse
B
Before 405nm
After 405nm
Kaede
D
A
P
V
Kaede
Kaede
Kaede
Kaede
C
0
30
60
90min
-UTR
+UTR
255
grayscale value=green/red
0
D
Kaede+UTR (n=10)
Kaede-UTR (n=6)
1-10
141-150
Average G/R
0.08
0.06
0.04
0.02
0 10 20 30 40 50 60 70 80 90
Min after photoconversion
Growth cone
Proximal axon

axons expressing Kaede-βactin3'UTR is significantly different from the average green/red growth cone value from axons expressing Kaede-pA, and the average green/red proximal axon values from axons expressing either form of Kaede ($p<0.001$ Kruskal-Wallace, verified with Mann-Whitney). The Kaede protein in both groups of axons was identical, the only difference was in the mRNA, with the β-actin3'UTR attached 3' to the stop codon. Therefore, the most likely explanation for the more rapid return in green Kaede in the growth cones of axons expressing Kaede-βactin3'UTR is that it is translated locally. Further support of this comes from the observation that green Kaede increases much more slowly in the proximal axon region of axons expressing Kaede-βactin3'UTR, and at a rate similar to both the growth cone region and the proximal axon region of axons expressing Kaede-pA. Therefore, the zebrafish β-actin3'UTR is sufficient to target local Kaede translation in RGC growth cones *in vivo*.

Igf2bp1 is the zebrafish ZBP1 ortholog

A blast search with the Chick ZBP1 amino acid sequence against the zebrafish genome identified Igf2bp1 as the most likely zebrafish ortholog (Figure 3.2B). The Igf2bp1 amino acid sequence is 81% identical to ZBP1. Igf2bp1 also has all six conserved RNA-binding domains, including KH3 and KH4 (KH34) (Figure 3.3A), which interact directly with the β-actin zipcode (Chao et al. 2010). We also found the necessary structure for β-actin mRNA binding to KH34 of ZBP1 in the zebrafish β-actin 3'UTR (Figure 3.2B). In zebrafish, Igf2bp1 is a member of a gene family with three other genes including Igf2bp2a, Igf2bp2b, and Igf2bp3. *Xenopus laevis* only has one homologous gene to ZBP1, Vg1RBP/Igf2bp3. Phylogenic analysis of all genes from the Igf2bp

Figure 3.2: Igf2bp1, the zebrafish ZBP1 ortholog, is expressed in RGCs during axon guidance. The zebrafish β-actin 3'UTR has a bipartite element with the required structure for binding KH34 of ZBP1 (A). B shows a phylogenic tree generated in clustalW, showing that Igf2bp1 is the most closely related to ZBP1 based on amino acid sequence, of the four members in the Igf2bp gene family. C shows a schematic of the proposed Igf2bp1 function: Igf2bp1 binds to β-actin mRNA in the zipcode (1), assembles into an RNA granule (2), which is actively transported along microtubules to the growth cone (3) where β-actin mRNA is translated, which drives attractive growth cone turning by increased polymerization on the side of the growth cone closest to the source (4). D shows wholemount *in situ* hybridization performed on 22 hpf, 48 hpf, 34 hpf, and 72 hpf embryos that show the location of mRNA expression. E shows 15um coronal plastic sections that show Igf2bp1 expression in the RGC layer (white bracket in right panel) in 2dpf embryos.

A

Chick β-actin3'UTR zipcode (54bp)

STOPN_3(GGACTgttaccaacacccACA)N_{30}

Zebrafish β-actin3'UTR (513bp)

STOPN_{200}(GGACTtcaatgtACA)N_{298}

B

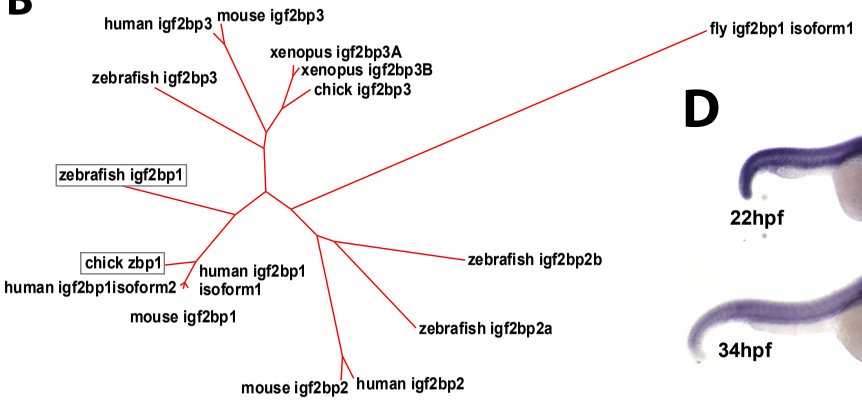

C

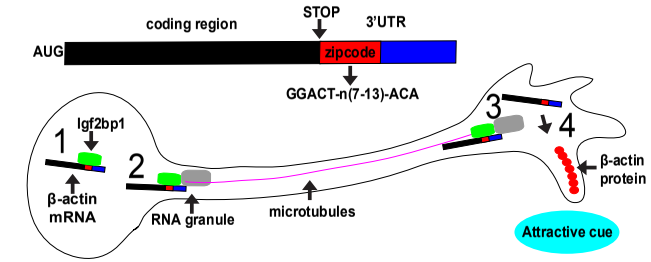

D

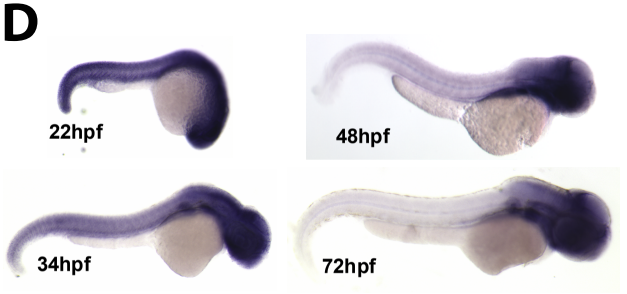

E

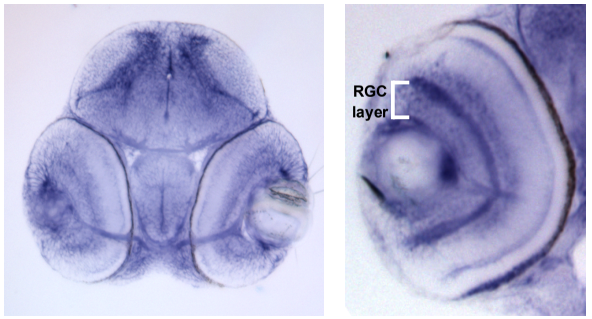

Figure 3.3: Loss of Igf2bp1 function causes underdeveloped retinotectal projection. Igf2bp1 has six conserved RNA-binding domains (A, top). The sbMO targeted to the exon3-intron3 splice junction causes exon3 deletion during mRNA splicing (A, middle), which results in a severely truncated protein (A, bottom). PCR using an f-primer targeted to exon1 and a reverse primer targeted to exon3 shows that the sbMO causes exon 3 deletion form Igf2bp1 mRNA (B). C-D shows four images of *Tg(isl2b-mCherryCAAX)*^{zc23} 3dpf embryos uninjected (C), or injected with negative control MO (D) or Igf2bp1 sbMO (mild (E), moderated (F), severe (G)). The top panel is a transmitted image of the whole embryo, and the bottom three panels are three different views (lateral, coronal, and dorsal) of a 3D-rendered head from a confocal z-stack taken on 1 fish, showing the retinotectal projection (red) and whole counter-stained head (blue). Scale bar=100um

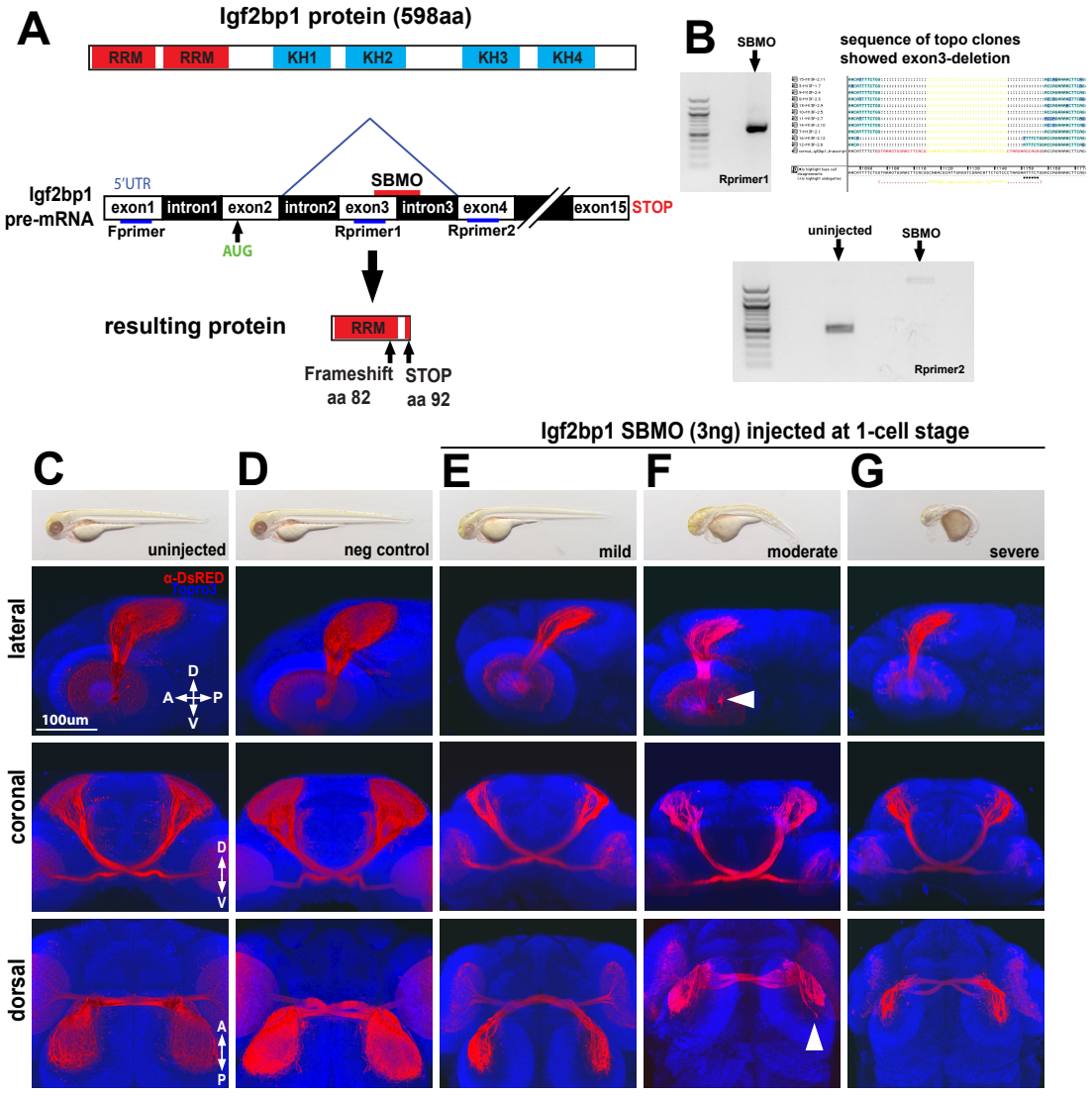
A
Igf2bp1 protein (598aa)
RRM
RRM
KH1
KH2
KH3
KH4
Igf2bp1
pre-mRNA
5'UTR
SBMO
exon1
intron1
exon2
intron2
exon3
intron3
exon4
exon15
STOP
Fprimer
AUG
Rprimer1
Rprimer2
resulting protein
RRM
Frameshift
aa 82
STOP
aa 92
B
SBMO
Rprimer1
sequence of topo clones
showed exon3-deletion
uninjected
SBMO
Rprimer2
Igf2bp1 SBMO (3ng) injected at 1-cell stage
C
D
E
F
G
uninjected
neg control
mild
moderate
severe
α-DsRED
Topro3
lateral
coronal
dorsal
D
A
P
V
100um

family in zebrafish, human, mouse, *Xenopus*, and chick, with *Drosophila* Igf2bp1 as a comparison, showed that zebrafish Igf2bp1 is indeed the ZBP1 ortholog (Figure 3.2B).

Igf2bp1 is expressed in RGCs during pathfinding

I performed wholemount *in situ* hybridization and plastic sectioning to look at Igf2bp1 expression in zebrafish embryos (Figure 3.2D-E). The staining pattern showed quasi-ubiquitous expression of Igf2bp1 mRNA (Figure 3.2D). Staining was very strong throughout the embryo at 22 hpf and became more restricted to the central nervous system with increasing age up to 3 dpf (Figure 3.2D). I also performed *in situ* hybridization on 4-cell embryos, which showed that Igf2bp1 is maternally expressed (data not shown), similar to Igf2bp3 (Zhang et al. 1999). Plastic sections of 3dpf embryos revealed expression in the RGC layer of the retina (Figure 3.2E), suggesting that Igf2bp1 could function in RGCs during pathfinding. Therefore, it is possible that Igf2bp1 does play a role in RGC axon pathfinding, through a mechanism where Igf2bp1 binds to the β-actin3'UTR during transcription in the nucleus (Figure 3.2C-1), exits the nucleus and associates with RNA granules in the cytoplasm (Figure 3.2C-2), is actively transported to the growth cone along microtubules in the axon via molecular motors associated with the RNA granule (Figure 3.2C-3), and stays bound to β-actin mRNA in the growth cone, repressing its translation until an attractive guidance cue is detected, at which point Igf2bp1 dissociates from the β-actin mRNA and translation is activated, therefore increasing polymerization and turning in the direction of the guidance cue source (Figure 3.2C-4).

Loss of Igf2bp1 causes retinotectal defects

Having established that Igf2bp1, the ZBP1 ortholog in zebrafish, is expressed during axon guidance, I next wanted to investigate whether Igf2bp1 function is required during RGC axon guidance. A splice-blocking morpholino oligonucleotide (sbMO) targeted against the exon3-intron3 splice junction (Figure 3.3A) was used to knockdown endogenous Igf2bp1 function. RT-PCR was performed on total RNA extracts from 2 dpf embryos injected with 3 ng Igf2bp1 sbMO or uninjected controls (Figure 3.3B). PCR product made using Rprimer1 (targeted to exon 4) was Topo-TA cloned and sequenced, revealing that 61bp exon3 was deleted from the Igf2bp1 mRNA, which was confirmed with PCR using Rprimer2 targetted to exon 3 which yielded no detectable product (Figure 3.3B). This deletion would cause a frameshift at amino acid 81 and an early in-frame stop codon after amino acid 91. The protein product resulting from exon3 deletion would have the first RRM domain, but would completely lack all of the remaining domains, including KH3 and KH4 (Figure 3.3A).

I predicted that loss of Igf2bp1 function would cause retinal pathfinding errors in embryos injected with 3 ng sbMO. At 3 dpf morphant embryos were grouped into three categories based on severity of gross morphological defects, which included small under-developed eyes and brain, hindbrain swelling, pericardial edema, smaller overall body size and curved tails. Mild embryos had little or no brain and heart swelling and had a normal body shape (Figure 3.3E, top panel). Moderate embryos had more significant swelling in the heart and brain and slight body curvature (Figure 3.3F, top panel). Severe embryos had substantial swelling in the heart and head, and their bodies were noticeably deformed, with severe curvature and tail curling (Figure 3.3G, top panel). At 3 dpf most

RGC axons have reached the optic tectum and the retinotectal projection appears mature. The sbMO was injected into *Tg(isl2b:mCherryCAAX)*^{z23} stable transgenic embryos to allow visualization of the RGCs (Figure 3.3C-D, lateral, coronal, and dorsal). At 3dpf morphant embryos were fixed and immunostained with α-DsRed (red RGC axons) and counterstained with Topro3 (blue). The whole head was imaged with confocal microscopy and reconstructed using Fluorender software to give lateral, coronal, and dorsal views of each head in Figure 3.3. There were a few embryos with axon guidance errors, such as Figure 3.3F (lateral view, white arrow head), with a misrouted axon inside the retina. There were also a few examples of "over-shooting" axons on the tectum (Figure 3.3F, dorsal view, white arrow), which was previously described in *Xenopus laevis* injected with Vg1RBP MO (Kalous et al. 2014). However, the trajectory of the retinotectal projection appeared normal. The most striking defect in morphants was that they had less elaborate arbors on the tectum that filled a much smaller volume compared to wild-type embryos. This could be due to defective branching and arborization of RGC axons on the tectum as previously reported (Kalous et al. 2014). Alternatively it could be the result of fewer axons reaching the tectum.

Loss of Igf2bp1 caused cell death and defects in retinal layers

After observing fewer RGC axons in Igf2bp1 sbMO morphant embryos, I postulated that this decrease might reflect increased cell death in the retina due to loss of Igf2bp1 function. However, morpholino injections commonly cause a ubiquitous increase in cell death, due to toxicity to the embryo or nonspecific effects (Robu et al. 2007). It is generally accepted that cell death that is not dependent on p53 is likely to be specific to the function of the targeted gene (Robu et al. 2007). *Tg(Isl2b:mCherry-*

CAAX)^{Z23} embryos were co-injected with p53 MO and Igf2bp1 sbMO (Figure 3.4D). These embryos were fixed and stained at 3dpf. Lenses were removed and the embryos mounted laterally to image the eyes in order to look more closely for retinal defects, particularly in the RGC layer. RGC axons leave the eye through the optic nerve, making a small hole in the central RGC layer. RGCs were absent in the central domain of the retina in embryos injected with sbMO alone (Figure 3.4C, white arrow). This was based on the absence *eGFP* expression or *Topro3* staining in this area of the eye. Embryos co-injected with p53 MO and Igf2bp1 sbMO were also missing RGCs in the middle of the retina (Figure 3.4D, white arrow), suggesting that this phenotype was not due to p53-dependent cell death (Robu et al. 2007). This suggests that Igf2bp1 may be required for proper formation of the retina. Consistent with this idea, 100% of embryos injected with Igf2bp1 sbMO had holes in *Topro3* staining in the retina, which may reflect excessive cell death. A few embryos had what appeared to be rosette-like defects in the RGC layer (Figure 3.4C', right white arrow), with cells that were not expressing *eGFP* protruding into the RGC layer.

I proposed that the loss of central RGCs in morphant retinas was caused by increased cell death from loss of Igf2bp1 function. We used acridine orange (AO) to visualize dying cells in live embryos. In uninjected embryos and embryos injected with p53 MO, most AO staining appeared in the lens (Figure 3.4A", B"). Embryos injected with Igf2bp1 sbMO alone had a striking increase in AO-positive cells in the brain, eye and retina, including the central RGC layer (Figure 3.4C"). Embryos co-injected with p53 MO and Igf2bp1 sbMO also had an increased number of AO-positive cells throughout the brain, eye, and retina (Figure 3.4D"). However, there appeared to be

Figure 3.4: Loss of Igf2bp1 function increases cell death and layering defects in the retina. *Tg(Isl2b:egfp)*^{zc7} stable transgenic embryos (A-D, A'-D') were injected with p53 MO (B, B'), sbMO (C, C'), or p53MO+sbMO (D, D'). Embryos were fixed and stained with α-egfp (green) and Topro3 (red in A-D, gray in A'-D'). Images are maximum intensity projections (A-D, A"-D") or singles slices (A'-D') of lateral views of eyes with lens removed taken with a confocal microscope (20x lens). Igf2bp1 morphant eyes were missing RGCs in central retina (white arrows) and showed holes and abnormal layers (yellow arrows). Wild-type embryos were stained with acridine orange and imaged with a confocal microscope at 31hpf (A"-D"), with dashed yellow line outline for eye and lens. maximum intensity projections eye, lateral mount). The AO-positive cells in the retina alone (between outer and inner yellow dashed lines) were counted in uninjected (n=10), p53 MO injected (n=9), Igf2bp1 sbMO injected (n=10), and p53+sbMO injected (n=10) embryos (E). A one-way anova ($p<0.0001$) with tukey HSD test demonstrated significant differences between uninjected or p53 injected and either sbMO or p53+sbMO injected ($p<0.01$) and non significant differences between uninjected and p53 injected or sbMO and p53+sbMO injected. Black points on the graph represent mean +/- SEM). Scale bars=50um

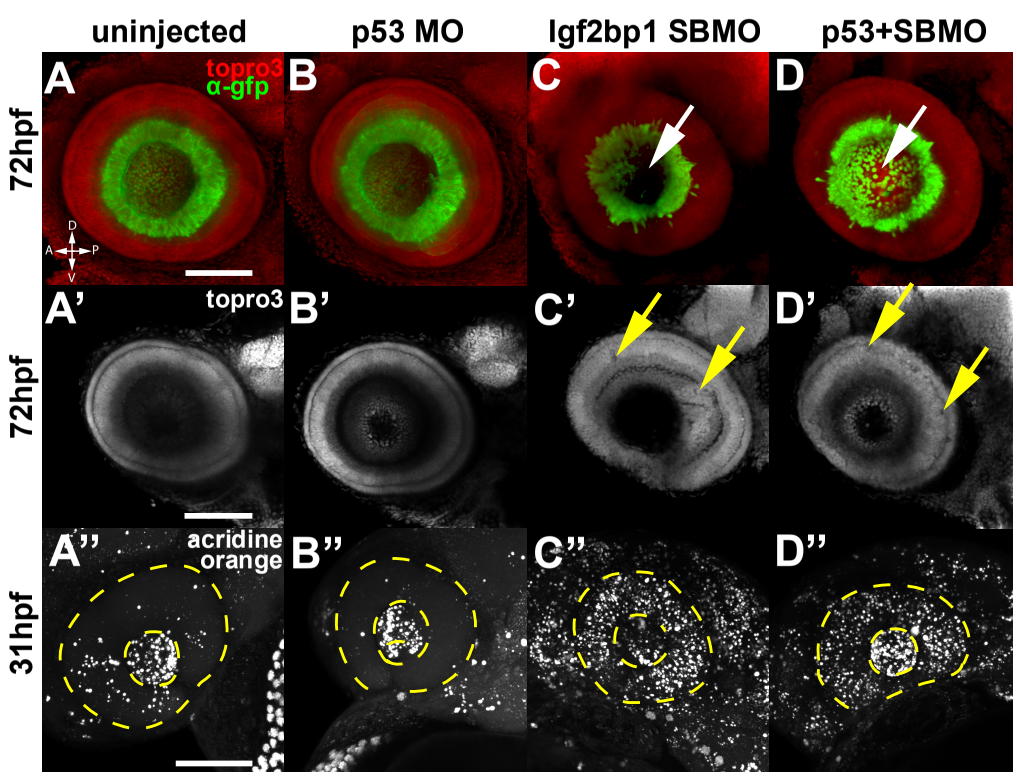
uninjected
p53 MO
lgf2bp1 SBMO
p53+SBMO
72hpf
72hpf
31hpf
A
B
C
D
topro3
α-gfp
A'
B'
C'
D'
topro3
A''
B''
C''
D''
acridine
orange
D
A
P
V

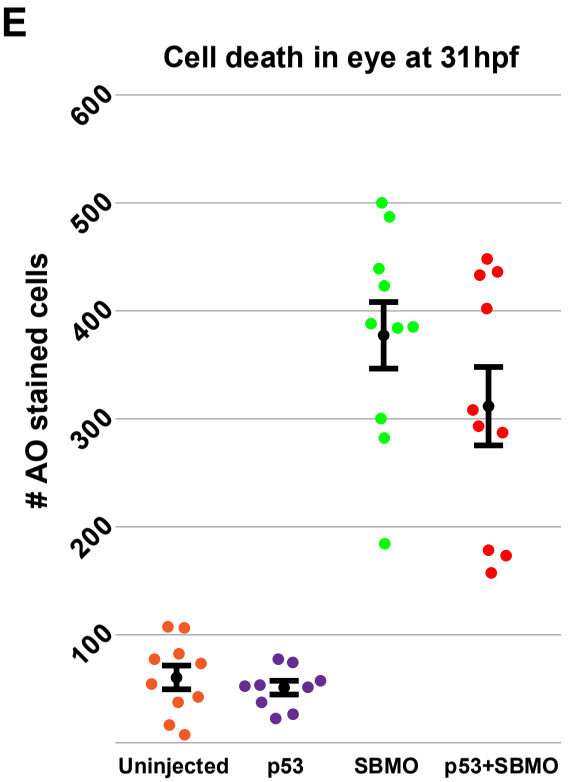
E
Cell death in eye at 31hpf
AO stained cells
600
500
400
300
200
100
Uninjected
p53
SBMO
p53+SBMO

more stained cells in the lens (Figure 3.4D", center circle).

I wanted to quantify cell death in the eye specifically at a time that the first RGC axons have begun pathfinding. Therefore, I used a confocal microscope to image AO-staining in the eyes of 31 hpf embryos (Figure 3.4A"-D"). I used Imaris software to count cells in eyes of uninjected embryos (Figure 3.4A"), embryos injected with p53 MO alone (Figure 3.4B"), sbMO alone (Figure 3.4C"), or co-injected with p53 MO and sbMO (Figure 3.4D"). The results showed that injection of sbMO with and without p53 MO resulted in a significantly higher number of AO-positive cells in the eye compared to uninjected eyes (Figure 3.4E). There was not a significant difference between the number of AO-positive cells in sbMO injected eyes and eyes co-injected with p53 MO and sbMO (Figure 3.4E). These results suggest that loss of Igf2bp1 function causes cell death in the retina that is not p53-dependent and is therefore specific.

Igf2bp1 function is required for retinal axon growth and maintenance
in vivo

While the sbMO effectively knocked down endogenous Igf2bp1 transcript (Figure 3.3B), I was unable to determine if Igf2bp1 function was required specifically in RGCs for axon guidance, or if the decreased number of RGC axons seen in morphants reflected the stunted growth and development. Igf2bp1 morphants were under-developed and the trajectory that the retinotectal projections followed appeared normal. In order to test whether Igf2bp1 function is required specifically in RGCs, I expressed a dominant negative form of Igf2bp1 with the phospho-mimetic Y399E mutation (Igf2bp1^{Y399E}) and an n-terminal emGFP fusion (Figure 3.5). It was previously shown that ZBP1^{Y396E} cannot bind to the β-actin zipcode (Chao et al. 2010), and that phosphorylation of ZBP1

Figure 3.5: Igf2bp1 function is required for RGC axons to reach the tectum. *Tg(isl2b:-emGFP)* (A), *Tg(isl2b:emGFP-Igf2bp1)*^{wt} (B), and *Tg(isl2b:emGFP-Igf2bp1)*^{Y399E} transient transgenics were fixed at 3dpf and stained with α-egfp and counterstained with Topro3. The images are maximum intensity projections from confocal z-stacks. D shows a schematic of the predicted mechanism of how Igf2bp1^{Y399E}interferes with endogenous Igf2bp1 by failing to transport β-actin mRNA to the growth cone and occupying RNA granules to prevent β-actin from localizing to the growth cone and preventing local translation required for growth cone turning. E shows a graph quantitating the ratio of emGFP (green) positive RGCs in the retina to emGFP positive axons on the contralateral tectum per eye/tectum pair (average +/- SEM). The ratio of RGCs in the retina to axons on the tectum was significantly different ($p<0.0001$, two-way ANOVA).

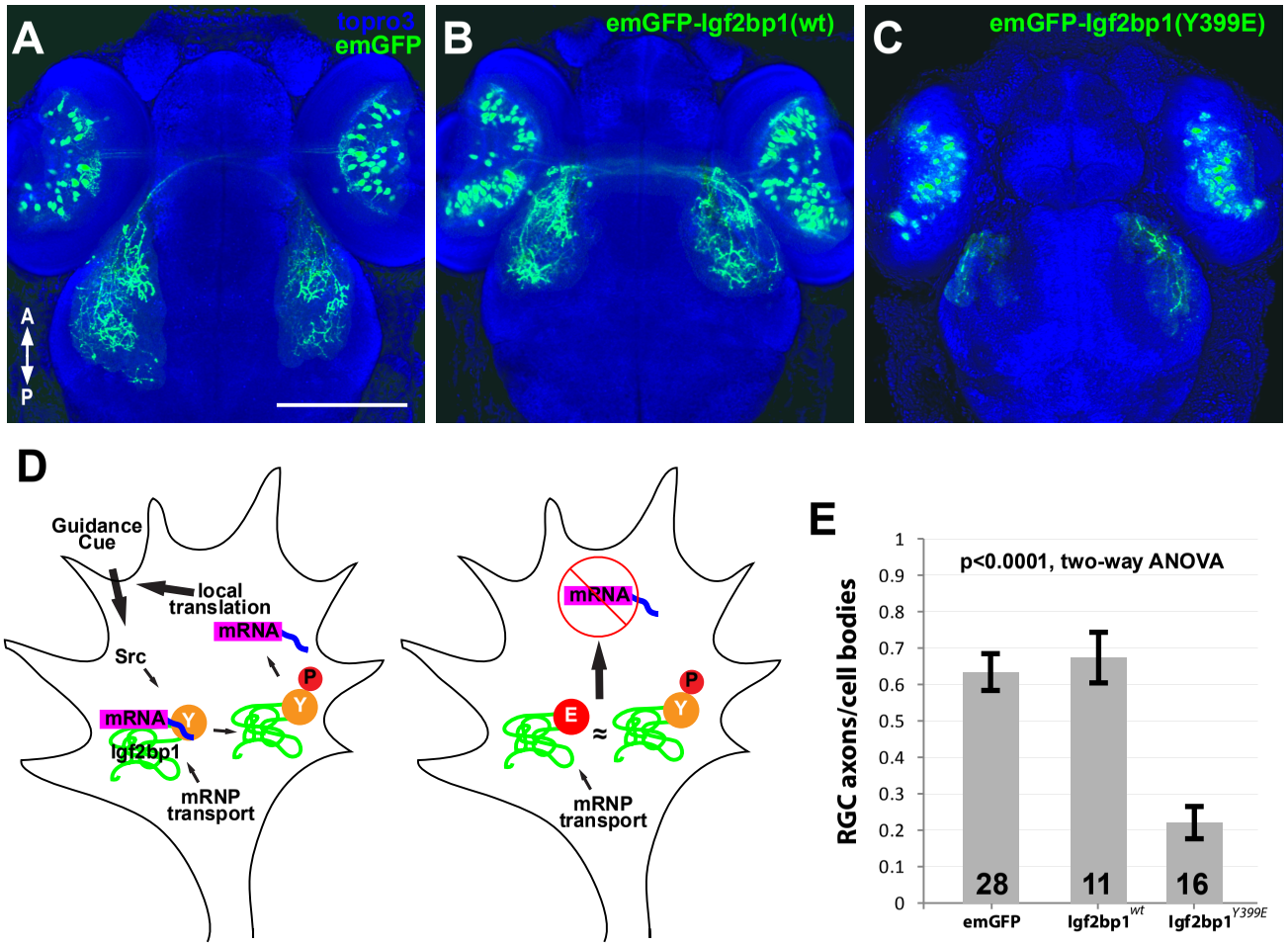
A
topro3
emGFP
A
P
B
emGFP-Igf2bp1(wt)
C
emGFP-Igf2bp1(Y399E)
D
Guidance Cue
local translation
mRNA
Src
P
Y
mRNA
Y
Igf2bp1
mRNP transport
mRNA
P
E
≈
Y
mRNP transport
E
p<0.0001, two-way ANOVA
RGC axons/cell bodies
1
0.9
0.8
0.7
0.6
0.5
0.4
0.3
0.2
0.1
0
28
11
16
emGFP
Igf2bp1wt
Igf2bp1Y399E

at the Y396 residue releases binding between ZBP1 and β-actin mRNA (Hüttelmaier et al. 2005), as is required for local β-actin translation in response to BDNF (Sasaki et al. 2010). I predicted that expression of Igf2bp1^{Y399E} in RGCs would interfere with β-actin mRNA localization to the growth cone, by occupying transport machinery without β-actin mRNA attached, therefore preventing β-actin mRNA transport to growth cones and preventing local β-actin translation (Figure 3.5D). I generated *Tg(isl2b:emGFP-Igf2bp1^{Y399E})* (Figure 3.5C) transient transgenics with mosaic expression of emGFP-Igf2bp1^{Y399E} in RGCs, with *Tg(isl2b:emGFP-Igf2bp1^{wt})* (Figure 3.5B) and *Tg(isl2b:-emGFP)* (Figure 3.5A) as controls. These embryos were fixed and stained at 3dpf with α-EGFP antibodies and *Topro3*. A confocal microscope was used to image the whole head of embryos (Figure 3.5A-C). I noticed a smaller ratio of emGFP-positive RGC axons on the tectum compared to the number of GFP-positive RGC cell bodies in the retinas in *Tg(isl2b:emGFP-Igf2bp1^{Y399E})* (Figure 3.5C), in comparison to the controls (Figure 3.5A, B). However, I did not notice any misguided or stalled axons outside the eye, or inside the retina. I quantitated the ratio of the number of GFP-positive RGC cell bodies in the retina to GFP-positive RGC axons on the contralateral tectum, with each n consisting of a ratio calculated from one eye/tectum pair (Figure 3.5E). The results showed a significant reduction in the number of axons/cell bodies in *Tg(isl2b:emGFP-Igf2bp1^{Y399E})* embryos compared to embryos expressing *isl2b:emGFP* or *isl2b:emGFP-Igf2bp1^{wt}*(Figure 3.5E). I concluded that interference with endogenous Igf2bp1 function through expression of *isl2b:emGFP-Igf2bp1^{Y399E}* reduced the number of RGC axons to grow to the tectum and that Igf2bp1 function is required for RGC axon extension, elongation or maintenance *in vivo*.

Discussion

I identified the zebrafish ZBP1 ortholog as Igf2bp1 and showed that its function is required for RGC axon growth to the tectum. This is the first study that demonstrates that Igf2bp1/ZBP1 function is required for axon pathfinding *in vivo*. Although a similar study in *Xenopus laevis* showed that Vg1RBP function was not required for long-range retinal axon growth and pathfinding *in vivo*, overshooting of axons on the tectum and defective arborization were documented (Kalous et al. 2014). I observed that Igf2bp1 knockdown with an sbMO resulted in what appeared to be fewer RGC axons on the tectum. While I did observe a few obvious axon guidance errors, these were very infrequent and the vast majority of analyzed morphants did not show obvious errors. Igf2bp1 function may be important for early morphogenesis of the embryo. This fits the results of the *in situ* study, which showed ubiquitous mRNA expression in embryos that was particularly strong in the younger 22 hpf embryos. Also, acridine orange staining showed increased cell death in morphant embryos at all ages assayed, including 22 hpf. Since mRNA localization and translation plays an important role in cell polarization (Shestakova et al. 2001) and cell surivival (Cox 2008), it is possible that complete knockdown of Igf2bp1 would cause early embryonic death. Loss of polarity and movement is seen in embryonic fibroblasts when ZBP1 is knocked down (Shestakova et al. 2001). A similar effect is seen when the interaction between ZBP1 and the β-actin zipcode is blocked (Shestakova et al. 2001). If Igf2bp1-dependent polarity is required during early embryonic development, specific loss of Igf2bp1 function early in development may result in early death. In order to look at the retinotectal projection, embryo survival required an injection of no more than 3 ng of sbMO. It is possible that

this prevented full knockdown of Igf2bp1 in RGCs and therefore prevented me from noticing the effect of Igf2bp1 loss on RGC axon guidance. Another possibility is that the other gene family members, Igf2bp2a, Igf2bp2b, or Igf2bp3, may have redundant function in RGCs during axon guidance.

Overexpression of the dominant negative form of Igf2bp1^{Y399E} in RGCs prevented axons from reaching the tectum. Since RGC axon guidance errors were not seen, this suggests that either axons were stalled somewhere along the retinotectal projection, that they were degraded, or that they failed to form in the first place through neurite specification (Stiess and Bradke 2010). The requirement for Igf2bp1 function for axon specification would be novel, however, neurite behavior is highly influenced by actin dynamics similar to growth cones (Stiess and Bradke 2010) and netrin expressed at the optic nerve head (Lauderdale et al. 1997) may be involved in axon specification through a β-actin translation-dependent mechanism that requires Igf2bp1 function. It is possible that early axon formation may require Igf2bp1 function to localize mRNA for local translation at one pole of the cell. The requirement of Igf2bp1 function for axon and growth cone formation might be more apparent *in vivo*. It has been observed *in vitro* that axon elongation does not require local translation (Eng et al. 1999), however, there is also evidence that netrin1 and NGF can promote elongation through local translation (Hengst et al. 2009). RGC axon formation may be more complex in the context of the developing retina.

Another possibility is that RGC axons cannot grow toward netrin1 expressed at the optic disc, where RGC axons exit the eye. Attractive growth cone turning in response to netrin1 is well known to require local β-actin translation *in vitro* (Welshans and

Bassell 2011, Leung et al. 2006, Yao et al. 2006, Campbell and Holt 2001). Axons may either fail to extend or may not form or be degraded very early during axon guidance due to a failure to detect netrin1. It is also possible that axons cannot respond to other intra-retinal guidance cues, resulting in stalled axon growth or degradation. Another intriguing idea is that RGC axons cannot respond to growth factors that are required for survival and maintenance. There is evidence that growth factors such as NGF can activate local translation of survival factors, such as CREB in axons (Andreassi et al. 2010, Cox 2008). After translation in the growth cone, CREB is retrogradely transported to the cell body where it promotes transcription of survival genes in the nucleus. RGC axons may require Igf2bp1-dependent local translation of transcription factors during pathfinding and loss of Igf2bp1 function may cause axons to stall or degrade caused by inability to respond to growth factors.

Embryos expressing *isl2b:emGFP-Igf2bp1* or *isl2b:emGFP* controls had more emGFP-positive cells in the retina than RGC axons on the tectum. Most RGC axons have reached the tectum at 72 hpf, however, a few axons are still growing. Therefore, it is possible that axon growth is delayed, but axons are still actively pathfinding at a slower pace. However, there were some embryos in controls that had a 1:1 ratio of emGFP-positive axons on the tectum and emGFP-positive RGC cell bodies in the retina while none of the *Isl2b:emGFP-Igf2bp1*^{Y399E} expressing embryos had a 1:1 ratio. Furthermore, there were some *Isl2b:emGFP-Igf2bp1*^{Y399E} -expressing embryos that had 0 emGFP-positive axons on the tectum, but still had several emGFP-positive RGC cell bodies in the retina. In these examples, axons were not seen outside the eye, which would have been detected with the imaging protocol that we used. This suggests that axons were not

growing for these RGCs, supporting the idea that Igf2bp1 function is required for axon extension and that loss of Igf2bp1 function prevents axon formation or causes early axon degredation. Regardless of the exact cause, the decreased ratio of axons on the tectum likely reflects a cell-autonomous function for Igf2bp1 in RGCs since the isl2b promoter drives expression specifically in RGCs (Pittman et al. 2008).

The results of the *in vivo* timelapse assay demonstrate that the zebrafish β-actin 3'UTR is sufficient to target local translation of Kaede in pathfinding RGC axons in the optic tract. This result is similar to the results seen in *Xenopus laevis* RGC axons from cultured retinal explants (Leung et al. 2006, Leung and Holt 2008). However, netrin1 was manually applied to the growth cones *in vitro* before photoconversion and timelapse. In our experiment, the analyzed RGCs were growing in purely *in vivo* conditions. The identity of all guidance cues that stimulate local β-actin translation in the zebrafish retinal axons in the optic tract is not known. It is also not clear if the β-actin 3'UTR –dependent local translation of Kaede requires Igf2bp1 function. The interaction of ZBP1 with the β-actin zipcode is well documented in different neuronal types *in vitro*. The requirement for local β-actin translation seems to be conserved as well as its dependence on Igf2bp1/ZBP1 function.

Igf2bp1 is expressed in RGCs during axon guidance and it has all of the structural features of ZBP1 that are required for its known mechanism in local β-actin translation *in vitro*, including the KH3 and KH4 domains which interact directly with the β-actin zipcode (Chao et al. 2010) and a similar tyrosine residue with an adjacent Src recognition site at amino acid 399 compared to 396 in chick ZBP1 (Hüttelmaier et al. 2005). Binding affinity of ZBP1 to β-actin is drastically reduced by the phosphomimetic point mutation

in ZBP1^{Y396E} (Hüttelmaier et al. 2005). Furthermore, the non-phosphorylatable mutation in ZBP1^{Y396F} prevents Src-dependent β-actin translation in growth cones *in vitro* (Hüttelmaier et al. 2005). Therefore, since Igf2bp1^{Y399E} overexpression in RGCs appears to interfere with axon formation and growth, it is likely that phosphorylation of Y399 by Src in the growth cone is a conserved event that activates β-actin translation. Finally, the zebrafish β-actin 3'UTR has the required structure for zipcode function, GGACT (n_{7-13}) ACA (Chao et al. 2010). The zebrafish zipcode is GGACT (n_7) ACA. It was shown biochemically that GGACT and ACA must be separated by at least seven nucleotides in order for the zipcode to form the loop required for interaction with the KH34 domains of ZBP1 (Chao et al. 2010).

References

Andreassi, C., Zimmermann, C., Mitter, R., Fusco, S., De Vita, S., Devita, S., Riccio, A. (2010). An NGF-responsive element targets myo-inositol monophosphatase-1 mRNA to sympathetic neuron axons. Nature Neuroscience, 13(3), 291–301.

Bassell, G. J., Zhang, H., Byrd, A. L., Femino, A. M., Singer, R. H., Taneja, K. L., Kosik, K. S. (1998). Sorting of beta-actin mRNA and protein to neurites and growth cones in culture. The Journal of Neuroscience 18(1), 251–265.

Campbell, D. S., Holt, C. E. (2001). Chemotropic responses of retinal growth cones mediated by rapid local protein synthesis and degradation. Neuron, 32(6), 1013–1026.

Chao, J. A., Patskovsky, Y., Patel, V., Levy, M., Almo, S. C., Singer, R. H. (2010). ZBP1 recognition of beta-actin zipcode induces RNA looping. Genes and Development, 24(2), 148–158.

Cox, L. J., Hengst, U., Gurskaya, N. G., Lukyanov, K. A., Jaffrey, S. R. (2008). Intra-axonal translation and retrograde trafficking of CREB promotes neuronal survival. Nature Cell Biology, 10(2), 149–159.

Donnelly, C. J., Willis, D. E., Xu, M., Tep, C., Jiang, C., Yoo, S.,Twiss, J. L. (2011). Limited availability of ZBP1 restricts axonal mRNA localization and nerve regeneration capacity. The EMBO Journal, 30(22), 4665–4677.

Eng, H., Lund, K., Campenot, R. B. (1999). Synthesis of beta-tubulin, actin, and other proteins in axons of sympathetic neurons in compartmented cultures. The Journal of Neuroscience, 19(1), 1–9.

Gundersen, R. W., Barrett, J. N. (1980). Characterization of the turning response of dorsal root neurites toward nerve growth factor establishing the drug gradient. The Journal of Cell Biology, 87*,* 546-554.

Hengst, U., Deglincerti, A., Kim, H. J., Jeon, N. L., Jaffrey, S. R. (2009). Axonal elongation triggered by stimulus-induced local translation of a polarity complex protein. Nature Cell Biology, 11(8), 1024–1030.

Hüttelmaier, S., Zenklusen, D., Lederer, M., Dictenberg, J., Lorenz, M., Meng, X., Singer, R. H. (2005). Spatial regulation of beta-actin translation by Src-dependent phosphorylation of ZBP1. Nature, 438(7067), 512–515.

Isbister, C. M., Connor, T. P. O. (2000). Mechanisms of growth cone guidance and motility in the developing grasshopper embryo. Neurobiology, 44, 271–280.

Kalous, A., Stake, J. I., Yisraeli, J. K., Holt, C. E. (2014). RNA-binding protein Vg1RBP regulates terminal arbor formation but not long-range axon navigation in the developing visual system. Developmental Neurobiology, 74(3), 303–318.

Kiebler, M. A., Bassell, G. J. (2006). Neuronal RNA granules: movers and makers. Neuron, 51(6), 685–690.

Lafont, F., Rouget, M., Rousselet, A., Valenza, C., Prochiantz, A. (1993). Specific responses of axons and dendrites to cytoskeleton perturbations: an *in vitro* study. Journal of Cell Science, 104 (Pt 2), 433–443.

Lauderdale, J. D., Davis, N. M., Kuwada, J. Y. (1997). Axon tracts correlate with netrin-1a expression. Molecular and Cellular Neuroscience, 9, 293–313.

Leung, K.-M., van Horck, F. P. G., Lin, A. C., Allison, R., Standart, N., Holt, C. E. (2006). Asymmetrical beta-actin mRNA translation in growth cones mediates attractive turning to netrin-1. Nature Neuroscience, 9(10), 1247–1256.

Leung, K.-M., Holt, C. E. (2008). Live visualization of protein synthesis in axonal growth cones by microinjection of photoconvertible Kaede into Xenopus embryos. Nature Protocols, 3(8), 1318–1327.

Lewis, K., Bridgman, C. (1992). Nerve growth cone lamellipodia contain two populations of actin filaments that differ in organization and polarity, The Journal of Cell Biology, 119(5), 1219–1243.

Lin, A. C., Holt, C. E. (2007). Local translation and directional steering in axons. The EMBO Journal, 26(16), 3729–3736.

Lin, A. C., Holt, C. E. (2008). Function and regulation of local axonal translation. Current Opinion in Neurobiology, 18(1), 60–68.

Marsh, L., Letourneau, P. C. (1984). Growth of neurites without filopodial or lamellipodial activity in the presence of cytochalasin B. The Journal of Cell Biology, 99(6), 2041–2047.

Perycz, M., Urbanska, A. S., Krawczyk, P. S., Parobczak, K., Jaworski, J. (2011). Zipcode binding protein 1 regulates the development of dendritic arbors in hippocampal neurons. The Journal of Neuroscience, 31(14), 5271-5285.

Piper, M., Anderson, R., Dwivedy, A., Weinl, C., van Horck, F., Leung, K. M., Holt, C. (2006). Signaling mechanisms underlying Slit2-induced collapse of Xenopus retinal growth cones. Neuron, 49(2), 215–228.

Pittman, A. J., Law, M.-Y., Chien, C.-B. (2008). Pathfinding in a large vertebrate axon tract: isotypic interactions guide retinotectal axons at multiple choice points. Development, 135(17), 2865–2887.

Pyati, U. J., Look, A. T., Hammerschmidt, M. (2007). Zebrafish as a powerful vertebrate model system for *in vivo* studies of cell death. Seminars in Cancer Biology, 17(2), 154–165.

Quinn, C. C., Wadsworth, W. G. (2008). Axon guidance: asymmetric signaling orients polarized outgrowth. Trends in Cell Biology, 18(12), 597–603.

Robu, M. E., Larson, J. D., Nasevicius, A., Beiraghi, S., Brenner, C., Farber, S. A., Ekker, S. C. (2007). P53 activation by knockdown technologies. PLoS Genetics, 3(5), e78.

Ross, A. F., Oleynikov, Y., Kislauskis, E. H., Taneja, K. L. (1997). Characterization of a beta-actin mRNA zipcode-binding protein. Molecular and Cellular Biology, 17(4), 2158-2165.

Sasaki, Y., Welshhans, K., Wen, Z., Yao, J., Xu, M., Goshima, Y., Bassell, G. J. (2010). Phosphorylation of zipcode binding protein 1 is required for brain-derived neurotrophic factor signaling of local beta-actin synthesis and growth cone turning. The Journal of Neuroscience, 30(28), 9349–9358.

Shestakova, E. A., Singer, R. H., Condeelis, J. (2001). The physiological significance of beta -actin mRNA localization in determining cell polarity and directional motility. Proceedings of the National Academy of Sciences, 98(13), 7045–7050.

Sotelo-Silveira, J. R., Calliari, A., Kun, A., Koenig, E., Sotelo, J. R. (2006). RNA trafficking in axons. Traffic, 7(5), 508–515.

Sperry, R., (1963). Chemoaffinity in the orderly growth of nerve fiber patterns and connections, Proceedings of the National Academies of Science, 50, 703-710.

Stiess, M., Bradke, F. (2011). Neuronal polarization: the cytoskeleton leads the way. Developmental Neurobiology, 71(6), 430–444.

Tcherkezian, J., Brittis, P. A., Thomas, F., Roux, P. P., Flanagan, J. G. (2010). Transmembrane receptor DCC associates with protein synthesis machinery and regulates translation. Cell, 141(4), 632–644.

Tessier-Lavigne, M., Goodman, C. S. (1996) The molecular biology of axon guidance. Science, 274, 1123-1133.

Thisse, C., Thisse, B. (2008). High-resolution in situ hybridization to whole-mount zebrafish embryos. Nature Protocols, 3(1), 59–69.

Vitriol, E. A., Zheng, J. Q. (2012). Growth cone travel in space and time: the cellular ensemble of cytoskeleton, adhesion, and membrane. Neuron, 73(6), 1068–1081.

Welshhans, K., Bassell, G. J. (2011). Netrin-1-induced local β-actin synthesis and growth cone guidance requires zipcode binding protein 1. The Journal of Neuroscience, 31(27), 9800–9813.

Wu, K. Y., Hengst, U., Cox, L. J., Macosko, E. Z., Jeromin, A., Urquhart, E. R., Jaffrey, S. R. (2005a). Local translation of RhoA regulates growth cone collapse. Nature, 436(7053), 1020–1024.

Wu, K. Y., Hengst, U., Cox, L. J., Macosko, E. Z., Jeromin, A., Urquhart, E. R., Jaffrey, S. R. (2005b). Local translation of RhoA regulates growth cone collapse. Nature, 436(7053), 1020–1024.

Yao, J., Sasaki, Y., Wen, Z., Bassell, G. J., Zheng, J. Q. (2006). An essential role for beta-actin mRNA localization and translation in Ca2+-dependent growth cone guidance. Nature Neuroscience, 9(10), 1265–1273.

Zhang, H. L., Eom, T., Oleynikov, Y., Shenoy, S. M., Liebelt, D. A, Dictenberg, J. B., Bassell, G. J. (2001). Neurotrophin-induced transport of a beta-actin mRNP complex increases beta-actin levels and stimulates growth cone motility. Neuron, 31(2), 261–275.

CHAPTER 4

DISCUSSION

Summary

As a growth cone navigates through the developing embryonic nervous system, it is able to decipher the correct trajectory that defines an axon tract. The growth cone is able to control the direction of axon growth by turning in response to an established pattern of extracellular guidance cues around the path that it follows. Actin dynamics inside the growth cone are well known as the primary determinant of growth cone morphology and behavior. External guidance cues activate signaling pathways that mediate the activity of actin-binding proteins (ABPs) that regulate actin dynamics. A key feature of growth cone signaling is that it enables external cues to elicit a turning response that is autonomous from the cell body.

The function of the β-actin 3'UTR and zipcode *in vivo*

The ability of a growth cone to respond autonomously eliminates the requirement for the transport of signaling molecules and proteins along the axon. Genetic control over growth cone behavior in response to guidance cues is made possible by local translation of mRNA in the growth cone. Regulation of mRNA translation is achieved through RNA-binding proteins (RBPs), which function in mRNA transport and translation in the growth cone in response to guidance cues. Like ABPs, RBPs are also targets of growth cone signaling in response to guidance cues and the requirement for local translation-dependent growth cone turning has been documented *in vitro* and to a lesser extent *in vivo*. In this dissertation I present evidence that CYFIP2, a protein known to interact directly with regulators of local translation and actin dynamics, has a cell autonomous function in pathfinding RGCs in vivo. I also present the first evidence that Igf2bp1/ZBP1 function is required for correct RGC axon guidance *in vivo*. These

findings contribute evidence that genes involved with local translation play an important role during axon guidance *in vivo*.

The zebrafish β-actin 3'UTR is sufficient to target local translation of Kaede in pathfinding RGC growth cones in the optic tract *in vivo*. This result is similar to that seen in *Xenopus* retinal explants *in vitro*, where netrin1 was applied to growth cones before photoconversion and timelapse (Leung et al. 2006, Leung and Holt 2008). In this case the return of Kaede occurred more quickly in the growth cone after 10 minutes. In my experiment the return of green Kaede did not return as rapidly after photoconversion. This could be due to lower concentrations of guidance cues *in vivo*, or due to exposure to more guidance cues. Based on the differential translation model, the turning response of a growth cone depends on local translation that either promotes actin polymerization in response to positive cues, or proteins that promote actin disassembly in response to negative cues. In my experiment, RGC growth cones in the optic tract were exposed to many external cues. It is likely that these cues include both attractive and repulsive guidance cues. With conflicting guidance signals, it is likely that the net translation of Kaede occurred more slowly due to a less dramatic difference between local translation of polymerizing factors and disassembly factors. Also, since the RGC axons are contained with in the brain, they grow in 3D and skin covers the axons, which causes some light scatter. Nevertheless, application of the local translation timelapse assay establishes an effective tool that can be used to test the ability of other mRNA sequences to target local Kaede translation *in vivo*.

A similar assay was also performed in cultured neurons from ZBP1$^{-/-}$ mice (Welshans and Bassell 2011). This experiment demonstrated that ZBP1 function is

required for β-actin 3'UTR-dependent local translation of heterologous mRNA. It would be good to perform the *in vivo* assay in zebrafish Igf2bp1$^{-/-}$ embryos, or alternatively Igf2bp1 morphants, to directly test the requirement for Igf2bp1 for β-actin 3'UTR-dependent local translation *in vivo* during axon guidance. The zipcode in chick β-actin mRNA is (GGACT)-n_{13}-(ACA) (Chao et al. 2010). There is a similar bipartite signal in the zebrafish β-actin3'UTR, (GGACT)-n_7-(ACA) which meets the requirements for direct interaction with the KH34 domain of ZBP1. The *in vivo* assay could be used with Kaede-βactin3'UTR$^{\Delta zipcode}$ to test whether this "zebrafish zipcode" is the necessary part of the zebrafish β-actin 3'UTR required for local translation.

Igf2bp1 may be required for axon elongation *in vivo*

Overexpression of dominant negative Igf2bp1^{Y399E} in RGCs interfered with the ability of RGC axons to grow to the tectum. This result is the first demonstration that Igf2bp1/ZBP1 is required for axon guidance *in vivo*. Even more interesting is that the axons apparently failed to grow. This may contradict the idea that local translation is not required for axon extension or elongation. Studies in cultured neurons initially showed that axons can still grow after being severed from the cell body and that local translation is only required for growth cone turning in response to a guidance cue (Eng et al. 1999, Campbell and Holt 2001, Leung et al. 2006). There is also evidence that netrin1 and NGF can promote axon elongation (Hengst et al. 2009). While this may have been the case *in vitro*, it is likely that the complex in *vivo* environment of the developing retina exposes axons to more chemical or physical barriers that create resistance to forward growth of the axon. One possibility is that, once again the growth cone is exposed to many cues simultaneously, both positive and negative. Another possibility is that

physical barriers exist in all dimensions around the axon, making it more difficult to grow forward. In either case, the proper response to external growth factors or guidance cues may be sufficient to drive navigation and growth forward. However, the axon may stall more easily with resistance from the *in vivo* environment, in absence of the ability to respond to growth promoting cues. Igf2bp1-dependent local β-actin translation may be required for the response.

A possible requirement of Igf2bp1 for RGC survival or maintenance

Another interesting observation about this experiment is that the axons are not obviously misrouted. If Igf2bp1 function were only required for growth cone turning, then it would be expected that axons would not follow the correct path to the tectum. Instead, axons appear to either grow normally to the tectum or not grow at all. If growth cones cannot respond to the attractive cue, it is likely that they may never reach the optic nerve head where netrin acts as an attractive cue (Lauderdale et al. 1997). However, obvious intraretinal guidance errors were not seen in embryos expressing Igf2bp1^{Y399E}. If axons were misrouted in the eye, they would need to have been degraded to explain why misrouted axons were not seen in the retina, since the imaging would have detected misrouted axons. Degradation could also happen due to the inability of growth cones to respond to growth factors. Transcription factors required for survival may be locally translated in response to survival-promoting external cues and retrogradely transported to the nucleus. An example is CREB local translation in response to NGF, seen in cultured neurons (Cox et al. 2008). It is conceivable that Igf2bp1 could somehow promote local translation of transcription factors, either directly or indirectly. If Igf2bp1 is only required for β-actin local translation, then increased β-actin concentration or

polymerization could promote local translation of survival-promoting transcription factors. Another way Igf2bp1 can be required for translation of transcription factors is through assembly of RNA granules required to transport other RBPs and mRNAs. Consistent with this idea is the observation that ZBP1 and SMN interact with each other in granules that are transported along axons (Fallini et al. 2013). When the interaction between the two proteins is blocked or one protein or the other knocked-down, the level of the other is also reduced in axons. Therefore, in the absence of ZBP1, assembly of RNA granules may be defective, reducing transport of other RBPs and mRNAs important for survival or growth. Without the ability to promote survival, axons may be degraded.

A potential requirement of Igf2bp1 for axon specification

The other explanation for fewer axons on the tectum is that axons cannot extend, which would suggest that Igf2bp1 function may be required for axonogenesis. After differentiation, a neuron extends many neurites from the cell body (Stiess and Bradke 2010). One of these neurites is specified as an axon, which extends and begins pathfinding. The initial neurites have growth cones that are heavily influenced by actin dynamics. Therefore Igf2bp1-dependent local β-actin translation may be required for the dynamics of neurite growth cones. Neurites might fail to form in the absence of Igf2bp1 function. The absence of neurites may destroy the potential for axon formation. Another possibility is that the capability of the cell to specify a neurite as an axon may be lost in the absence of Igf2bp1 function. An intriguing possibility would be that netrin expressed at the optic nerve head normally specifies a neurite as an axon, with the neurite closest to the source becoming the axon. This netrin-dependent specification could require a similar attractive response to that seen in growth cone turning, resulting in local β-actin

translation. Without Igf2bp, local translation of β-actin in the neurite in response to netrin is blocked and axon specification is either blocked or it happens with much lower efficiency (Figure 4.1). This explanation seems to fit the data from my dominant negative experiment. In order to determine what actually happens to the RGC axons expressing Igf2bp1^{Y399E}, this experiment would need to be repeated with imaging aimed at the retina at around 28hpf, the time that RGC axon specification would be occurring. Timelapse confocal microscopy can be used to see if any axons grow within the retina, and if axons are degraded. High magnification, high resolution imaging techniques may be used to observe neurite behavior on RGCs, however, this is likely to be a serious technical challenge. Loss of ZBP1 function or β-actin mRNA translation has been shown to decrease the length of neurites, supporting this idea (Donnelly et al. 2011). The *in vivo* environment may prevent axon extension or growth more effectively than *in vitro*. It would also be informative to determine if netrin receptors are expressed in RGC neurites.

Igf2bp1 function may be required for early embryonic development

A splice-blocking morpholino oligonucleotide (sbMO) against Igf2bp1 gave results that were difficult to interpret. While there were a few embryos that had axon guidance errors in the retina and in the optic tract, the vast majority of morphant embryos had normal retinotectal projections. However, there were apparent defects. Compared to wild-type there appeared to be fewer RGC cell bodies in the retina, the optic nerve had a thinner diameter, and the volume of neuropil from RGC axon arbors was smaller. This is similar to results seen in *Xenopus* embryos injected with Vg1RBP MO from a study that reported that axons grew past the termination zone on the tectum occasionally, but the retinotectal projection looked normal with no sign of misrouted axons (Kalous et al.

Figure 4.1: Proposed model, Igf2bp1 function may be required for axon specification. One of the minor neurites in an RGC may become specified as an axon by higher exposure to netrin expressed at the optic nerve head, compared to the other neurites. This may depend on local translation of β-actin that is Igf2bp1-dependent. When Igf2bp1 function is lost, the neurites cannot respond to netrin and therefore cannot be specified as an axon, and axon extension fails.

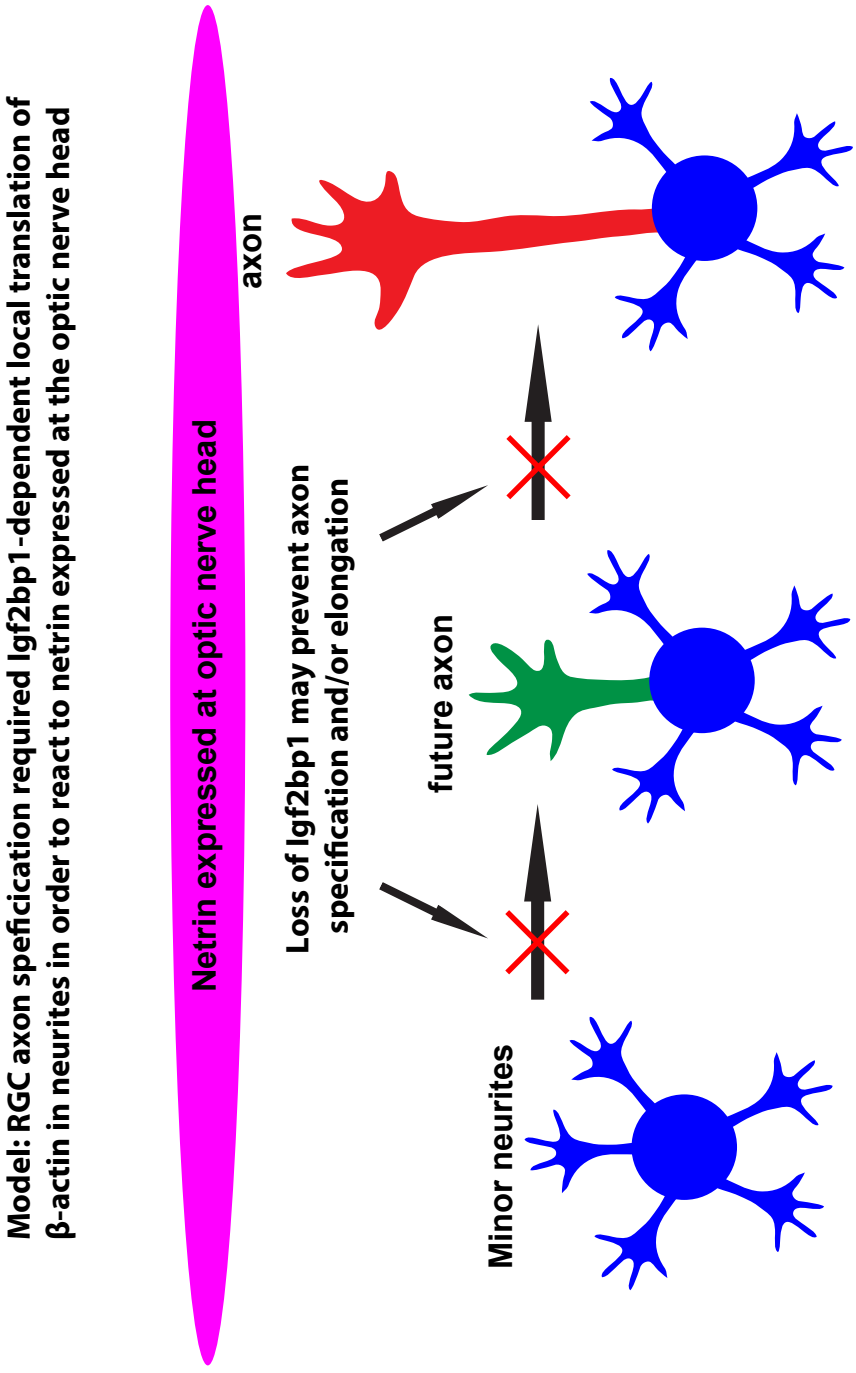
Model: RGC axon specification required Igf2bp1-dependent local translation of β-actin in neurites in order to react to netrin expressed at the optic nerve head
Netrin expressed at optic nerve head
axon
Loss of Igf2bp1 may prevent axon specification and/or elongation
future axon
Minor neurites

2014). The study also used a different dominant negative strategy, with Vg1RBP$^{\Delta KH4}$ to knockdown endogenous function, however, they reported normal RGC axon guidance and growth but defective branching and arbor formation on the tectum. They expressed the dominant negative cDNA construct in RGCs with electroporation after injection into the retina. This resulted in very densely labelled RGCs, which may have masked a decreased ratio of RGC cell bodies to axons on the tectum and made it impossible to count cell bodies or axons. Nevertheless, neither this study nor my experiments showed a noticeable reduction in the amount of axons on the tectum in ratio with cell bodies in the retina of morphant embryos. This is again likely from the pan-RGC labelling used in both studies.

My sbMO injections yielded morphants that had what appeared to be fewer RGCs in the retina and fewer axons in the retinotectal projection. However, the entire embryo was smaller and the eyes were underdeveloped in morphants. Therefore, it is impossible to determine if Igf2bp1 function is required for RGC axon guidance based on the morphants. There are several potential reasons for these results. While the sbMO effectively knocked down Igf2bp1, it is possible that the effect was not specific to Igf2bp1 and that it either knocked down the function of many other genes important for development. Or, it is possible that there was increased cell death in the embryo due to toxicity of the sbMO. While this is a common concern for MO injections, it is likely not the case since co-injection with p53 MO did not rescue the defects in morphology or cell death assayed by acridine orange stain (Robu et al. 2007). Although the sbMO effectively knocked down endogenous Igf2bp1 function, it is possible that there was still mRNA that was not detectable but sufficient for function of Igf2bp1. This could be

explained by an important role for Igf2bp1 function in early development. In order to investigate the retinotectal projection the embryos had to survive until 3 dpf. However, it is possible that a strong loss of Igf2bp1 resulted in early death before 1 dpf as was seen in embryos injected with more than 3 ng of sbMO. Therefore, survival of morphants past 1 dpf may have been enabled by incomplete Igf2bp1 knockdown. In other words, the need to keep morphants alive long enough to see the retinotectal projection prevented complete knockdown of Igf2bp1.

The requirement for Igf2bp1 function in early development throughout the embryo is consistent with the expression of Igf2bp1. *In situ* hybridization showed quasi-ubiquitous expression of embryos with very strong staining, suggesting that Igf2bp1 is expressed strongly throughout the CNS. Also, expression was very strong at 22hpf and throughout the whole embryo. This suggests that loss of Igf2bp1 function may cause early lethality. Igf2bp1 morphants also had very high levels of cell death throughout the brain which was not rescued by p53 MO co-injection. The fact that the cell death was not p53-dependent suggests that it is a result of loss of Igf2bp1 function (Robu et al. 2007). The specificity of the sbMO is further supported by the fact that the pattern of acridine orange staining reflected the expression pattern of Igf2bp1 with the highest levels of cell death occurring in the same regions Igf2bp1 expression was strongest.

A good approach to determine whether Igf2bp1 function is required for early embryonic development and survival would be to generate Igf2bp1$^{-/-}$ zebrafish through a targeted gene knockout strategy (Zu et al. 2013). If homozygous embryos were to die at a very young age, similar to Igf2bp1 morphants, this would confirm the interpretation that Igf2bp1 is required for early embryonic development. This would be similar to

ZBP1$^{-/-}$ mice, which die as embryos, also supporting the idea that Igf2bp1 is required for early embryonic development.

Redundant function of other Igf2bp family members in zebrafish

Another potential reason for the lack of axon guidance errors in Igf2bp1 morphants is redundant function from the other Igf2bp family members in zebrafish: Igf2bp2a, Igf2bp2b, and Igf2bp3. These genes code for very similar proteins that could potentially mask the loss of Igf2bp1 function. In particular, Igf2bp3 is the zebrafish ortholog for Vg1RBP (Zhang et al. 1999). *Xenopus* does not have an ortholog for other Igf2bp genes therefore it is likely to be the ZBP1 functional ortholog. In zebrafish, Igf2bp1 is the ZBP1 ortholog based on phylogenic analysis, however, it is conceivable that Igf2bp3 protein could function redundantly. Igf2bp3 expression in zebrafish is similar to Igf2bp1 expression that I observed. In addition, Igf2bp3 is expressed maternally in zebrafish embryos, suggesting that this gene may have an important function in early development, such as cell polarization. Also, since Igf2bp3 has a similar expression pattern to Igf2bp1 and both are expressed maternally, similar to my own *in situ* study for Igf2bp3 (data not shown). This is further support for the idea that Igf2bp1 function is required in early development.

Igf2bp1 morphants had abnormal layers in the retina that were not clearly defined and underdeveloped. In addition there were small holes in topro3 staining that appeared to resemble cell death. Another intriguing observation was that morphants had a hole in the central region of the RGC layer, which is where the first RGCs are born. These RGCs send out the first RGC axons, or pioneers (Pittman et al. 2008). This may reflect a phenotype in the eye that results from partial loss of Igf2bp1 function.

RGC axon guidance in Igf2bp1$^{-/-}$ genetic mutants

Generation of a conditional mutant would be a way to determine the requirement for Igf2bp1 function in RGC axon guidance (Hans et al. 2011). If Igf2bp1$^{-/-}$ embryos died early, the inducible knockout would be a way to target genetic loss of Igf2bp1 function in the eye. However, if Igf2bp1 function were required for eye development then loss of Igf2bp1 function in the whole eye before RGC differentiation may result in massive amounts of cell death or a severely underdeveloped eye, which may still obfuscate the effect on RGC axon guidance. An alternative approach would be to use a fish line with Cre driven by an RGC specific promoter such as isl2b or Hermes (Appendix B). This would knockout Igf2bp1 function specifically in RGCs. However, this approach may delay the loss of Igf2bp1 function since the isl2b promoter turns on expression when RGCs differentiate since residual mRNA and protein may still persist (Pittman et al. 2008). This may also be useful if loss of Igf2bp1 function prevented axons from being specified from neurites, as predicted from the dominant negative experiment. An alternative would be to express Cre in RGCs by electroporating them with cDNA for Cre at around 22 hpf to achieve a more complete knockdown in RGCs at 28 hpf. Another approach would be to transplant RGCs from a conditional mutant into wild-type and then induce Cre.

Fundamental widespread function for Igf2bp1 in regulation of cellular processes?

The finding that Igf2bp1 may have an important function throughout the entire embryo and early in development is intriguing. This would point to a widespread role in fundamental cellular processes. Igf2bp1 is a known regulator of actin dynamics, through

regulation of β-actin local translation. Igf2bp1 is involved in mRNA transport and as a translation regulator of β-actin, polarizing the distribution of β-actin mRNA and protein within a cell. While Igf2bp1 is known for its role in enabling migration in cells, the underlying mechanism is through asymmetric actin polymerization through regulating β-actin local translation (Vainer et al. 2008, Katz et al. 2012). The actin cytoskeleton has widespread importance as a fundamental component of cell structure and function. Therefore as a key regulator of actin dynamics, it would not be surprising if Igf2bp1 functions to polarize cells during early development. Cell polarization is an important process for specifying tissues and cell-fate, as well as other things such as cell division. This would explain the widespread cell death seen in Igf2bp1 morphants. If genetic loss of Igf2bp1 function caused early lethality as seen in Igf2bp1 morphants, consistent with ZBP1$^{-/-}$ mice, this would fit with the idea that Igf2bp1 is involved in a fundamental cell process such as establishing polarity in cells by distributing materials asymmetrically.

ZBP1 interacts with another RBP involved in local translation, SMN (Fallini et al. 2014). SMN and ZBP1 co-localize in RNA granules that are transported along axons. The finding that loss of either protein in a cell prevents the other from localizing to axons is intriguing and provides a possible mechanism through which Igf2bp1 function may be required for the function of many proteins. In other words, it is possible that loss of Igf2bp1 may cause loss of function for many other proteins and mRNAs. Igf2bp1 may be required for assembly of RNA granules that actively transport other many other RBPs, mRNAs and regulators of translation and cytoskeletal dynamics (Kiebler and Bassell 2006). As suggested by the evidence that loss of ZBP1 causes deficient axonal transport of SMN, loss of Igf2bp1 function may cause mislocalization of other proteins and

therefore be causing mislocalization of a large number molecules rather than β-actin alone. Interdependence of RBPs on each other for assembling RNA granules could cause the loss of protein functions and the functions of the mRNAs that they transport. This may be a cause for widespread cell death early in development. This would also provide an explanation for the possibility that complete loss of Igf2bp1 function causes early death or widespread cell death throughout the embryo that resembles toxicity. It may be that loss of Igf2bp1 causes massive malfunction of cellular processes required during early embryonic development.

Potential interconnection between Igf2bp1 and CYFIP2 functions

Not only does SMN1 interact with ZBP1 in RNA granules, it also is found in FMRP-containing granules (Piazzon et al. 2008). It would be interesting to determine whether all three proteins are contained within the same RNA granules. There is a reasonable chance given the common partner SMN1 and the given size of RNA granules. Also, all three of these proteins are RBPs that are known to co-localize to axons. Furthermore, FMRP interacts with CYFIP2, which is a regulator of actin dynamics similar to ZBP1 and SMN1 (Schenk et al. 2001). Even more interesting is the fact that all three proteins seem to play a role in axon guidance. Therefore it seems that the importance of RBPs and regulators of actin dynamics are closely related in function and they share common widespread signaling mechanisms and functions within cells. This suggests that both processes may be intimately related and each one as crucial as the other for cell function and behavior. This shows the strong importance of local translation and its regulators within neurons.

References

Campbell, D. S., Holt, C. E. (2001). Chemotropic responses of retinal growth cones mediated by rapid local protein synthesis and degradation. Neuron, 32(6), 1013–1026.

Chao, J. A., Patskovsky, Y., Patel, V., Levy, M., Almo, S. C., Singer, R. H. (2010). ZBP1 recognition of beta-actin zipcode induces RNA looping. Genes and Development, 24(2), 148–158.

Cox, L. J., Hengst, U., Gurskaya, N. G., Lukyanov, K. A, Jaffrey, S. R. (2008). Intra-axonal translation and retrograde trafficking of CREB promotes neuronal survival. Nature Cell Biology, 10(2), 149–159.

Donnelly, C. J., Willis, D. E., Xu, M., Tep, C., Jiang, C., Yoo, S., Schanen, N. C., Kirn-Safran, C. B., van Minnen, J., English, A., Yoon, S. O., Bassell, G. J., Twiss, J. L. (2011). Limited availability of ZBP1 restricts axonal mRNA localization and nerve regeneration capacity. The EMBO Journal, 30(22), 1-13.

Eng, H., Lund, K., Campenot, R. B. (1999). Synthesis of beta-tubulin, actin, and other proteins in axons of sympathetic neurons in compartmented cultures. The Journal of Neuroscience, 19(1), 1–9.

Fallini, C., Rouanet, J. P., Donlin-Asp, P. G., Guo, P., Zhang, H., Singer, R. H., Bassell, G. J. (2014). Dynamics of survival of motor neuron (SMN) protein interaction with the mRNA-binding protein IMP1 facilitates its trafficking into motor neuron axons. Developmental Neurobiology, 74(3), 319–332.

Hans, S., Freudenreich, D., Geffarth, M., Kaslin, J., Machate, A., Brand, M. (2011). Generation of a non-leaky heat shock-inducible Cre line for conditional Cre/lox strategies in zebrafish. Developmental Dynamics, 240(1), 108–115.

Hengst, U., Deglincerti, A., Kim, H. J., Jeon, N. L., Jaffrey, S. R. (2009). Axonal elongation triggered by stimulus-induced local translation of a polarity complex protein. Nature Cell Biology, 11(8), 1024–1030.

Huang, Y., Harrison, M. R., Osorio, A., Kim, J., Baugh, A., Duan, C., Lien, C.-L. (2013). Igf signaling is required for cardiomyocyte proliferation during zebrafish heart development and regeneration. PloS One, 8(6), e67266.

Kalous, A., Stake, J. I., Yisraeli, J. K., Holt, C. E. (2014). RNA-binding protein Vg1RBP regulates terminal arbor formation but not long-range axon navigation in the developing visual system. Developmental Neurobiology, 74(3), 303–318.

Katz, Z. B., Wells, A. L., Park, H. Y., Wu, B., Shenoy, S. M., Singer, R. H. (2012). β-actin mRNA compartmentalization enhances focal adhesion stability and directs cell migration. Genes and Development, 26(17), 1885–1890.

Kiebler, M. A., Bassell, G. J. (2006). Neuronal RNA granules: movers and makers. Neuron, 51(6), 685–690.

Lauderdale, J. D., Davis, N. M., Kuwada, J. Y. (1997). Axon tracts correlate with netrin-1a expression, Molecular and Cellular Neuroscience 9, 293–313.

Leung, K.-M., van Horck, F. P. G., Lin, A. C., Allison, R., Standart, N., Holt, C. E. (2006). Asymmetrical beta-actin mRNA translation in growth cones mediates attractive turning to netrin-1. Nature Neuroscience, 9(10), 1247–1256.

Leung, K.-M., Holt, C. E. (2008). Live visualization of protein synthesis in axonal growth cones by microinjection of photoconvertible Kaede into *Xenopus* embryos. Nature Protocols, 3(8), 1318–1327.

Piazzon, N., Rage, F., Schlotter, F., Moine, H., Branlant, C., Massenet, S. (2008). *In vitro* and *in cellulo* evidences for association of the survival of motor neuron complex with the fragile X mental retardation protein. The Journal of Biological Chemistry, 283(9), 5598–5610.

Robu, M. E., Larson, J. D., Nasevicius, A., Beiraghi, S., Brenner, C., Farber, S. A., Ekker, S. C. (2007). P53 activation by knockdown technologies. PLoS Genetics, 3(5), e78.

Schenck, A., Bardoni, B., Moro, A., Bagni, C., Mandel, J. L. (2001). A highly conserved protein family interacting with the fragile X mental retardation protein (FMRP) and displaying selective interactions with FMRP-related proteins FXR1P and FXR2P. Proceedings of the National Academy of Sciences, 98(15), 8844–8849.

Stiess, M., Bradke, F. (2011). Neuronal polarization: the cytoskeleton leads the way. Developmental Neurobiology, 71(6), 430–444.

Vainer, G., Pikarsky, A., Shenoy, S. M., Oberman, F., Yeffet, A., Singer, R. H., Pikarsky, E. (2008). A role for VICKZ proteins in the progression of colorectal carcinomas: regulating lamellipodia formation. Journal of Pathology, 215, 445–456.

Welshhans, K., Bassell, G. J. (2011). Netrin-1-induced local β-actin synthesis and growth cone guidance requires zipcode binding protein 1. The Journal of Neuroscience, 31(27), 9800–9813.

White, Y. A. R., Kyle, J. T., Wood, A. W. (2009). Targeted gene knockdown in zebrafish reveals distinct intraembryonic functions for insulin-like growth factor II signaling. Endocrinology, 150(9), 4366–4375.

Zhang, Q., Yaniv, K., Oberman, F., Wolke, U., Git, A, Fromer, M., Yisraeli, J. K. (1999). Vg1 RBP intracellular distribution and evolutionarily conserved expression at multiple stages during development. Mechanisms of Development, 88(1), 101–106.

APPENDIX A

ANALYZING RETINAL AXON GUIDANCE IN ZEBRAFISH

Fabienne E. Poulain, John A. Gaynes, Cornelia Stacher Horndli, Mei-Yee Law, and Chi-Bin Chien, Methods in Cell Biology 100, The Zebrafish: Cellular and Developmental Biology, Part A Third Edition, Part I, Chapter 1, 3-26 (2010)

This article is Chapter 1 of Methods in Cell Biology Volume 100 3rd edition "The Zebrafish: Cellular and Developmental Biology," Part A, reprinted with permission*. This chapter was written with other members of the Chien Lab in 2010. Fabienne Poulain was the first author. Cornelia Horndli, Mei-Yee Law, and I were middle authors. The focus of the chapter is describing methods for analyzing axon guidance in the zebrafish retinotectal system. My contribution was describing *in vivo* focal electroporation in section II part E, the images and composition of Figure 2E-H and the detailed protocol in section II part G. This is the first detailed protocol for use in zebrafish to have been published.

* Poulain, F. E., Gaynes, J. A., Horndli, C. S., Law, M.-Y., Chien, C.-B. (2010). Analyzing retinal axon guidance in zebrafish, Methods in Cell Biology, 100, The zebrafish: cellular and developmental biology, A, third edition, part I, chapter 1, 3-26.

CHAPTER 1

Analyzing Retinal Axon Guidance in Zebrafish

Fabienne E. Poulain, John A. Gaynes, Cornelia Stacher Hörndli, Mei-Yee Law, *and* Chi-Bin Chien

Department of Neurobiology and Anatomy, University of Utah, Salt Lake City, Utah

Abstract

How neuronal connections are established during development is one of the most fascinating questions in the field of neurobiology. The zebrafish retinotectal system offers distinct advantages for studying axon guidance in an *in vivo* context. Its accessibility and the larva's transparency not only allow its direct visualization, but

also facilitate experimental manipulations to address the mechanisms of its development. Here we describe methods for labeling and visualizing retinal axons *in vivo*, including transient expression of DNA constructs, injection of lipophilic dyes, and time-lapse imaging. We describe in detail the available transgenic lines for marking retinal ganglion cells (RGCs); a protocol for very precise lipophilic dye labeling; and a protocol for single cell electroporation of RGCs. We then describe several approaches for perturbing the retinotectal system, including morpholino or DNA injection; localized heat shock to induce misexpression of genes; a comprehensive list of known retinotectal mutants; and a detailed protocol for RGC transplants to test cell autonomy. These methods not only provide new ways for examining how retinal axons are guided by their environment, but also can be used to study other axonal tracts in the living embryo.

I. Introduction

Axon guidance is an essential process for proper formation of neuronal connections during development. This is certainly true in the visual system, where retinal axons must interpret a large variety of signals to navigate to their brain target and establish precise and ordered connections reflecting our perception of the environment. The accessibility of the visual system not only allows its easy visualization, but also facilitates experimental manipulations to test the mechanisms of its development. Many studies have taken advantage of this accessibility to give a precise description of the visual system's anatomy and identify important factors required for its formation. In the past decade, the zebrafish retinotectal system has drawn attention for its distinct advantages. The optical transparency of zebrafish embryos allows direct visualization of retinal axons and is particularly suited for high-resolution imaging, including time-lapse analysis. Chimeric embryos with retinal neurons of different genetic backgrounds can be easily generated by cell transplants. Finally, the short generation time of zebrafish as well as the recent characterization of its genome are especially suited for genetic analysis and have allowed the generation and identification of many mutants with retinotectal defects. These properties establish zebrafish as an excellent model for studying retinal axon guidance and, more generally, for studying cell biology in an *in vivo* context, as many *in vivo* experiments not possible in other systems can be performed.

Retinal ganglion cells (RGCs) are the primary cell type in the innermost cellular layer of the retina, responsible for carrying visual information from the eye to the brain. In zebrafish, the first RGCs are born at 28 h post-fertilization (hpf) (Hu and Easter, 1999; Masai *et al*., 2005) and immediately extend axons that then must pass several landmarks (Fig. 1A). Retinal axons first grow within the retina to the optic disc, where they exit (30–32 hpf). They then join the optic nerve and elongate toward the ventral midline of the diencephalon, where nerves coming from both eyes meet to form the optic chiasm (34–36 hpf). In zebrafish and other species lacking binocular vision, all axons cross the midline. Retinal axons then

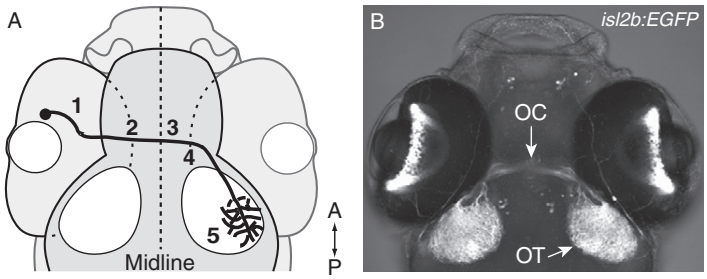

Fig. 1 The zebrafish retinotectal projection. (A) Diagram of the retinal axon pathway. Retinal axons navigate to the optic nerve head (1), pass through the optic nerve and exit the eye (2), cross the midline at the chiasm (3), and grow dorsally along the optic tract (4) to reach the tectum (5). (B) Dorsal view of a Tg(*isl2b:EGFP*)^{zc7} transgenic embryo, which specifically expresses EGFP in all RGCs, allowing a direct visualization of retinal projections. Courtesy of A. Pittman. A: anterior; P: posterior; OC, optic chiasm; OT, optic tectum. *Maximum intensity projection, confocal microscopy.* (A, B): dorsal views, anterior up.

navigate dorsally through the optic tract to reach their main target, the optic tectum (48 hpf), where they establish a topographic map, making connections according to their position in the retina (Fig. 2C–D). Axons originating from the more rostral retina project to the more posterior tectum, and axons from the dorsal retina project to the ventrolateral tectum. Interestingly, this ordering in the tectum can already be observed along the dorso-ventral axis in the optic tract: dorsal axons grow through the ventral branch of the tract, and ventral axons through its dorsal branch. Once in the tectum, retinal axons mature, arborize, and form synapses with their tectal targets.

Retinal axons encounter many guidance decision points along their pathway and respond to various attractive or repulsive cues to choose the right track. Many factors acting as road signs have been identified, but how retinal axons respond to them *in vivo* still remains poorly understood. Many laboratories, including ours, have developed tools for visualizing retinal axons during their navigation and modifying their nature or their environment to test specific functions. We describe here the different methods used for labeling and visualizing retinal axons, as well as several approaches for perturbing the retinotectal system. Many of these methods are also applicable to nonretinal axons. We finish with an overview of methods likely to be important in the future.

II. Visualizing Retinal Axons

Understanding how retinal projections develop requires specific labeling and precise visualization of retinal axons *in vivo*. Several methods can be used, depending on which part of the retinotectal pathway is studied, how many axons are observed, and whether the axons are observed live. Thanks to the optical transparency of zebrafish

embryos, transgenic lines expressing fluorescent proteins in RGCs can be used to visualize retinal axons as they develop. Lipophilic dyes are particularly useful to label specific groups of axons. Finally, transient expression of DNA constructs and *in vivo* electroporation are specially suited for labeling single axons and imaging them as they elongate. For all these approaches, precise imaging is best achieved using confocal microscopy.

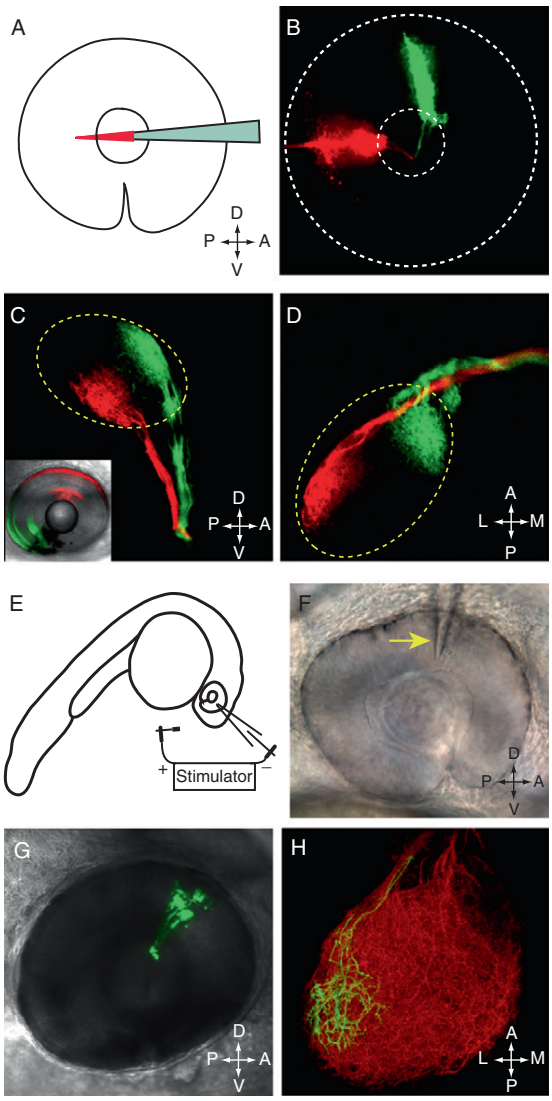

Fig. 2 *(Continued)*

A. Transgenic Lines

Several transgenic lines that express fluorescent proteins (FPs) under the control of RGC-specific promoters have been developed (Table I). Their main advantage is to allow clear and direct visualization of retinal projections in live embryos. Labeled embryos are simply obtained by crossing transgenic carriers. Depending on the promoter used, all RGCs or a subset of them are labeled. Promoters from the *isl2b* and *atoh7* (previously named *isl3* and *ath5*) genes drive transgene expression in all RGCs, allowing the visualization of all retinal axons (Fig. 1B, Masai *et al*., 2003; Pittman *et al*., 2008). In contrast, promoters from the *pou4f3* (previously named *brn3c*) gene can be used to label a subset of RGCs (Neumann and Nüsslein-Volhard, 2000; Xiao *et al*., 2005). For instance, the *pou4f3* promoter drives expression in RGCs that project mainly into one of the four retinorecipient layers of the tectum, allowing characterization of laminar targeting of retinal axons (Xiao *et al*., 2005).

Different FPs can be expressed to label RGCs. Enhanced green fluorescent protein (EGFP) is the most frequently used, as it is stable and particularly bright. RGCs can also be labeled in red using TagRFP or mCherry. Adding specific tags to the FP coding sequence allows labeling of specific cellular compartments such as the nucleus or the plasma membrane. For instance, the N-terminal palmitoylation sequence from GAP-43 (Moriyoshi *et al*., 1996) or the CAAX consensus motif from Ras (Choy *et al*., 1999) can target FPs to the plasma membrane, giving better labeling of axonal arbors.

Finally, other transgenic lines express the strong transcriptional activator Gal4-VP16, which drives the expression of DNA constructs containing a UAS (upstream activation sequence) control element (Köster and Fraser, 2001). These lines can be

---

Fig. 2 Methods for visualizing retinal axons. (A–D) Focal injection of dyes in the retina allows visualization of retinal axons exiting from the retina and making topographic connections in the tectum. (A) After removing lens, a dye-coated glass micropipette is briefly inserted in a peripheral direction into the RGC layer (method described in detail in Section II.G.1). (B) Lateral view of a 48 hpf eye focally injected with DiI (red) and DiO (green). Labeled retinal axons can be observed exiting from the retina. *Maximum intensity projection, confocal microscopy.* (C) Lateral view of a 4 dpf embryo topographically injected with DiI and DiO into the dorsonasal (DN) and ventrotemporal (VT) retina, respectively, using a vibrating-needle injection apparatus (Baier *et al*., 1996). Inset shows the sites of injection in the retina. DN (red) and VT (green) retinal axons navigate through the ventral and dorsal branches of the optic tract, respectively, and terminate topographically in the tectum. Yellow dashed line: tectal border. *Maximum intensity projection, confocal microscopy.* (D) Dorsal view of the projections showed in C. DN axons terminate in the posterolateral tectum, whereas VT axons innervate the antero-medial tectum. Yellow dashed line: tectal border. *Maximum intensity projection, confocal microscopy.* (E–H) *In vivo* single cell electroporation allows visualization of retinal arbors in the tectum. (E) Schematic representation of the electroporation setup: a 22–28 hpf embryo is mounted laterally under a compound microscope. A negatively charged glass microelectrode is filled with DNA solution and placed in the retina, with a positively charged ground electrode placed near the head. (F) DIC picture of the microelectrode (arrow) placed into the DN retina just prior to electroporation. *40× water immersion objective, compound microscope.* (G) Electroporated RGCs expressing GAP43-EGFP (green) in a live 5 dpf embryo mounted laterally with the lens removed. The EGFP image has been merged with a DIC image of the head. *Maximum intensity projection, confocal microscopy.* (H) Dorsal view of the contralateral tectum of the same embryo, with tectal neuropil visualized by *isl2b:mCherry-CAAX* transgene [red; Tg(*isl2b:mCherry-CAAX*)^{zc23}] and electroporated RGC axons and arbors visualized with GAP43-EGFP (green). *3D projection from Fluorender software, 40× water immersion objective, confocal microscopy.* A: anterior; P: posterior; D: dorsal; V: ventral; L: lateral; M: medial. (See Plate no. 1 in the Color Plate Section.)

Table I
Transgenic Lines that Label RGCs

Transgenic line	Previous names, ZFIN allele number	Retinal expression	Other expression	References
atoh7:GFP	*ath5:GFP, rw021*	Newborn RGCs	Forebrain, tectum	Masai *et al*. (2003), Poggi *et al*. (2005)
atoh7:mGFP	*ath5:mGFP, cu1*	"	"	Vitorino *et al*. (2009), Zolessi *et al*. (2006)
atoh7:mRFP	*ath5:mRFP, cu2*	"	"	Vitorino *et al*. (2009), Zolessi *et al*. (2006)
atoh7:Gal4-VP16	*zf138*	"	"	Maddison *et al*. (2009)
pou4f1-hsp70:GFP	*brn3a-hsp70:GFP, rw0110*	RGCs (likely a subset)	Tectum, habenula, cranial sensory ganglia	Aizawa *et al*. (2005), Sato *et al*. (2007)
pou4f3:mGFP	*brn3c:mGFP, s273t, s356t*	Subset of RGCs	Inner ear, lateral line neuromasts	Del Bene *et al*. (2008), Xiao *et al*. (2005)
pou4f3:Gal4VP16	*s311t*	"	"	Xiao and Baier (2007)
isl2b:GFP	*isl3:GFP, zc7*	All RGCs	Cranial ganglia Rohon-Beard neurons, a few cells in forebrain dorsal midbrain	Pittman *et al*. (2008)
isl2b:mGFP	*zc20*	"	"	Law and Chien (unpublished)
isl2b:mCherryCAAX	*zc23, zc25*	"	"	Pittman *et al*. (2008)
isl2b:Gal4VP16	*zc60*	"	"	Ben Fredj *et al*. (2010)
chrnb3b:GFP	*jt0021*	RGCs	Trigeminal ganglion, Rohon-Beard neurons, some tectal cells	Matsuda and Mishina (2004), Tokuoka *et al*. (2002), Yoshida and Mishina (2003)
-2.7shh:GFP	*t10*	RGCs	Amacrine cells, notochord, floor plate, pharyngeal arch endoderm, ventral forebrain	Neumann and Nüsslein-Volhard (2000), Nevin *et al*. (2008), Roeser and Baier (2003)

mGFP, Membrane-targeted GFP; RGCs, retinal ganglion cells.

particularly useful for expressing DNA constructs at high levels in a few RGCs (described in Section II.D).

B. Labeling with Antibodies

Alternately, antibodies can be used to label retinal axons. Although they cannot be employed for live visualization, they provide strong staining that can be useful to examine details or specific aspects of retinal axon navigation. Several antibodies have been widely used to label retinal axons using standard whole-mount antibody staining techniques. Anti-acetylated tubulin (Sigma, St. Louis, Missouri) recognizes a form of tubulin found in stable microtubules, and thus labels all axons. This staining has been used to visualize the earliest axons crossing the chiasm (Karlstrom *et al*., 1996) and to label axon bundles within the retina (Li *et al*., 2005). Zn-5 and zn-8 (Zebrafish International Resource Center, Developmental Studies Hybridoma Bank, Iowa City, Iowa) are two monoclonal antibodies, likely derived from the same hybridoma, that recognize the cell surface adhesion molecule Alcam-a (previously named neurolin/DM-GRASP, Laessing *et al*., 1994). Alcam-a is expressed by newly born RGCs that are added in successive peripheral rings around the retina, but turns off in central RGCs by 48 hpf (Laessing and Stuermer, 1996). Consequently, zn-5/8 staining is particularly appropriate to label retinal axons navigating within the retina to the optic nerve head. Finally, anti-GFP (Invitrogen, Carlsbad, California), anti-DsRed (which also recognizes mCherry, Clontech, Mountain View, California) and anti-TagRFP (Evrogen, Moscow, Russia) antibodies can be used to amplify the signal from FPs.

C. Labeling with Lipophilic Dyes

While transgenic lines and antibodies are appropriate for labeling a large population of axons, they cannot be used to visualize spatially specific sub populations of RGCs. Lipophilic carbocyanine dyes such as DiI, DiO, DiA, or DiD (Invitrogen) offer the great advantage of being easily injected in specific locations within the retina. Structurally, they consist of a fluorophore attached to two long aliphatic alkyl tails responsible for their insertion within membranes. Carbocyanine dyes are highly fluorescent in lipid bilayers, but weakly fluorescent in water. Once applied, they become incorporated into the plasma membrane and diffuse laterally, labeling the entire cell. These properties have made lipophilic dyes the tool of choice for anterograde and retrograde tracing of neurons in both live and fixed tissues (Honig and Hume, 1989).

DiI (red) and DiO (green) are the most commonly used. They can be applied using several methods. The first is to inject DiI or DiO dissolved in chloroform into the eye, which labels the entire projection ("whole eye fills"). This technique is particularly useful for studying guidance at the chiasm, as each eye can be labeled with a different color. It has been described previously (Hutson *et al*., 2004) and is not repeated here.

DiI and DiO can also be delivered into specific regions of the retina, so that only a subset of RGCs is labeled (Fig. 2A–D). In the second method, dyes dissolved in dimethylformamide are focally injected using a vibrating-needle injection apparatus (Baier *et al*., 1996; Trowe, 2000). DiI or DiO is loaded in a reservoir through which

passes a tungsten needle. Fixed larvae are mounted in an agarose form. A small loudspeaker vibrates the needle, transporting dye to its tip, where the dye precipitates in the embedded tissue. This method has the advantage of labeling many embryos reproducibly and has been used to analyze projection topography in the tectum and axon ordering in the tract (Karlstrom *et al*., 1996; Lee *et al*., 2004; Trowe *et al*., 1996). However, the custom-built apparatus is not widely available. The third technique uses a dye-coated microneedle to focally deposit dye into the retina. The needle is coated with dye and can be reused several times. It does not require any specialized apparatus and can be used to label very few cells. We describe this method in Section II.G.1. A final method is to focally inject DiI along the retinal pathway to retrogradely label RGCs. Although it is difficult to inject dye precisely enough, this technique can be used to visualize RGC morphology and organization within the retina (Mangrum *et al*., 2002).

D. Transiently Expressing DNA Constructs

Whereas lipophilic dyes can easily label a subset of RGCs, they are more difficult to use for single axons. These can be better visualized by transiently expressing DNA constructs encoding FPs. Plasmids injected at the one cell stage are expressed mosaically, labeling a few cells randomly. Expression can be targeted to RGCs using the *atoh7* or *isl2b* promoters (Masai *et al*., 2003; Pittman *et al*., 2008). This method has been used to visualize single retinal arbors (Campbell *et al*., 2007) and RGC dendritic outgrowth (Mumm *et al*., 2006). Alternatively, constructs containing a UAS element upstream of an FP coding sequence can be injected into transgenic embryos expressing Gal4-VP16 in RGCs (Table I). The Gal4/UAS system amplifies FP expression and gives better labeling. While DNA methods are very useful for labeling single axons, they cannot yet be used to target specific RGC subtypes or RGCs in particular locations, since the required enhancers have not yet been identified.

E. *In Vivo* Single Cell Electroporation

Another way to label individual axons is *in vivo* single cell electroporation (Fig. 2E–H). Although technically demanding, this powerful approach offers the possibility of delivering DNA constructs or dextran-coupled indicators to individual RGCs or RGCs in specific locations in the retina. We have used it to visualize projections and arborizations of individual dorsonasal RGCs (Pittman *et al*., 2010). In this approach, an applied voltage generates an electric field across cells in the retina, breaking down the plasma membrane and creating transient pores through which negatively charged DNA molecules move into the cell. Briefly, embryos are mounted laterally on a glass slide in agarose that is windowed to expose the eyes, covered with medium, and viewed under a 40× water immersion objective. A glass microelectrode filled with DNA or tracer solution is poked into the retina with a micromanipulator, and a voltage train applied. Embryos are then unmounted and raised. This approach allows coelectroporation of several indicators or constructs into the same cell, allowing both visualization and perturbation experiments. We describe this technique in detail in Section II.G.2.

F. Time-Lapse Imaging

Time-lapse imaging of RGC axons is crucial to understand their response to the environment. It has been used by many investigators to monitor axons' behavior (Campbell *et al*., 2007; Hutson and Chien, 2002; Kaethner and Stuermer, 1992; O'Brien *et al*., 2009; Schmidt *et al*., 2000) and can be used with all the labeling techniques described above, except for antibody labeling. Confocal or two-photon microscopy is most appropriate for time-lapse imaging and can be performed with an upright or inverted microscope. Several protocols have been previously described, so we do not discuss them here (Campbell *et al*., 2007; Hutson and Chien, 2002; Hutson *et al*., 2004; Meyer and Smith, 2006).

G. Protocols for Labeling Methods

Here we describe detailed protocols for focal injections of lipophilic dyes in the retina and for *in vivo* single cell electroporation.

1. Method 1: Precise Labeling with Intraretinal Injection of Lipophilic Dyes

This method uses glass microneedles coated with lipophilic carbocyanine dyes to focally deposit dye into the retina (Fig. 2A–B). It can be used to target specific locations in the retina and label very few cells. It was originally developed by Torsten Trowe (2000).

a. Solutions Needed

- DiI or DiO crystals (Molecular Probes)
- 4% PFA (4% paraformaldehyde in 0.1 M phosphate buffer, pH 7.4)
- 1% low-melt agarose in PBS (phosphate-buffered saline)
- 50% and 80% glycerol in water

b. Protocol

1. Fix zebrafish embryos at required stage in 4% PFA at 4°C for at least 12 h. For growth cone labeling, fix at room temperature for the first 2 h.
2. Use glass capillary with an outer diameter of 1.0 mm and an inner diameter of 0.58 mm to prepare the micropipette for injections. Pull the capillary to a final taper length of 9.0 mm and a tip size of 2 µm. To coat the micropipette with dye, place a few dye crystals on a cover glass and melt them at 100°C on a hot plate. Dip the tip of the micropipette horizontally into the dye paste and roll it to cover the tip equally on all sides. Wipe off as much dye from the tip as possible onto the cover glass.
3. Prepare 30 ml of 1% low-melt agarose and keep on heating block at 45°C to prevent from solidifying. Use a Petri dish lid to embed embryos for dye injection. Coat bottom with a thin layer of 1% low-melt agarose and let solidify. Transfer embryos with as little PFA as possible onto the agarose. Cover embryos with a drop of 1% low-melt agarose and orient them in a lateral position.
4. When the agarose covering is solid, use a sharpened tungsten needle to remove the top-facing lens by carefully cutting the skin covering the eye in a circle along the

border between lens and retina. The lens will become loose and can now be easily removed. The resulting hole should be refilled with 1% low-melt agarose. The embryos are now ready to be injected with the dye.

5. Use a standard pipette holder and three-axis micromanipulator to hold the dye-coated micropipette. Insert it into the RGC layer by placing it in the empty lens cup and advancing in a peripheral direction at a roughly 45° angle (Fig. 2A). Leave the needle in the eye for not more than 2 s to ensure a small injection site and labeling of only a few axons. The coated micropipette can be reused for several injections before it has to be coated again with fresh dye.
6. After finishing the injections, cover embedded embryos with 1× PBS or water to avoid drying. This step also washes off excessive dye. Store the embryos for a few hours at room temperature for fast diffusion of the dye, or keep them at 4°C overnight if slower diffusion is desired. Long incubation times can result in nonspecific diffusion of the dye within the eye, which can prevent clear imaging results later on.
7. Recover embryos from the agarose bed using forceps. Place them in a microfuge tube and wash them in 1× PBS. Transfer embryos to 50% glycerol/H_2O and incubate them for 3 h at 4°C with agitation. Change the medium to 80% glycerol/H_2O, and store embryos at 4°C overnight. Now that they are cleared, embryos can be mounted for confocal imaging in 80% glycerol between two coverslips (Fig. 2B).

2. Method 2: Single Cell *In Vivo* Electroporation

In vivo focal electroporation is used to deliver tracers or transgenes into single RGCs. It can target several or individual cells in precise topographic positions within the retina (Fig. 2E–H). An electric field applied across an RGC progenitor creates transient pores in the plasma membrane through which negatively charged DNA molecules move into the cell. We have used the protocol detailed here to image single RGC arbors in the tectum (Pittman *et al*., 2010); it was slightly modified from a previous method for imaging habenular neurons (Bianco *et al*., 2008).

a. Solutions Needed

- E2 medium (15 mM NaCl, 0.5 mM KCl, 1 mM $CaCl_2$, 1 mM $MgSO_4$, 0.15 mM KH_2PO_4, 1.7 mM $NaHCO_3$)
- 0.1 mM phenylthiourea (PTU) in E3 embryo medium (5 mM NaCl, 0.17 mM KCl, 0.33 mM $CaCl_2$, 0.33 mM $MgSO_4$)
- tricaine stock (0.4% tricaine, 10 mM HEPES, pH 7.4)
- 1% low-melt agarose in E2/GN/tricaine (10 µg/ml gentamicin in E2 medium, 0.02% tricaine)

b. Protocol

1. Raise embryos at 28.5°C in E3 medium containing 0.1 mM PTU to inhibit pigment formation, and dechorionate them between 22 and 28 hpf. Anesthetize embryos by adding tricaine to a final concentration of 0.02%. Mount laterally in a drop of 1% low-melt agarose in E2/gentamycin/ tricaine, in wells built with quick-hardening

epoxy on a glass microscope slide. Expose the eye by cutting a small window in the agarose with forceps, and cover the embryo with E3-PTU + 0.02% tricaine.

2. After mounting the embryo, place the glass slide under a 40× water immersion objective on an upright compound microscope. Place an Ag/AgCl cathode in the overlying buffer near the head of the embryo. Backfill a glass microelectrode (1–3 μm diameter tip) with 2 μl of solution containing the tracer or DNA (final concentration of 1–3 μg/μl in water or 10 mM Tris-HCl, pH 8.5), and place it in the retina using a micromanipulator. Use a stimulator to deliver 1 s trains of 2 ms negative-going square pulses at 200 Hz, 30–50 V (reverse polarity and use 3–5V for positively charged tracers). An effective train will cause a visible rippling effect (tissue response) in the tissue surrounding the microelectrode tip when the voltage train is applied. A clogged needle will result in a less pronounced tissue response. A "pop" will occasionally appear in the tissue in response to a voltage train, resulting in an ineffective electroporation. While the exact cause of the pop is not known, it occurs less often with a lower DNA concentration and a lower voltage. Each cell is targeted with 3–5 trains, and several cells can be targeted per eye. After electroporation, the embryo is removed from the agarose and raised in E3 + PTU at 28.5°C
3. FP expression can be seen in electroporated RGCs in the eye under a fluorescent dissecting microscope by 12 h after electroporation. Corresponding axons can be visualized in the contralateral optic tract and tectum under a 40× water objective on a compound microscope, or by confocal microscopy. Labeled axons are best observed from a dorsal view in the contralateral tectum, or from a lateral view in the contralateral optic tract after removal of the contralateral eye. Time-lapse imaging can also be performed.

III. Perturbing the Retinotectal System

Experimental manipulations perturbing axons or their environment are crucial to understand how and by which molecular mechanisms retinotectal projections develop. Many important factors have been discovered through the generation and characterization of mutants with retinotectal defects isolated in large-scale genetic screens. In addition, several approaches including DNA or antisense morpholino oligonucleotide (MO or "morpholino") injections, heat shock experiments, or transplants can be used to assess the function of a particular protein.

A. Retinotectal Mutants

The first mutants with retinotectal defects were obtained from a large genetic screen performed in Tübingen in the 1990s (Karlstrom *et al*., 1996; Trowe *et al*., 1996). Topographic injections of DiI and DiO in the retina were used as an assay to identify mutants with defects in retinal axon pathfinding, sorting in the tract, and topography in the tectum. Almost all the genes affected in these mutants have now been identified, allowing the discovery of crucial regulators of axon guidance or brain patterning, including the receptors *robo2* and *patched1*, the transcription factor *lhx2*, and the

Table II
Retinotectal Pathfinding Mutants

Mutant name (abbreviation)	Region in which pathfinding affected	Gene	Brain defect?	References
acerebellar (ace)	Chiasm, anterior projection, optic tract, topography	*fgf8*	Yes	Picker *et al*. (1999), Shanmugalingam *et al*. (2000)
astray (ast)	Chiasm, anterior projection, optic tract, tectum aroborization	*robo2*	No	Campbell *et al*. (2007), Fricke *et al*. (2001), Hutson and Chien (2002), Karlstrom *et al*. (1996)
bashful (bal)	Retinal exit, anterior projection	*laminin α1*	Yes	Karlstrom *et al*. (1996), Paulus and Halloran (2006)
belladonna (bel)	Midline crossing	*lhx2*	Yes	Karlstrom *et al*. (1996), Seth *et al*. (2006)
beyond borders (beyo)	Confinement to tectal neuropil	*?*	Yes	Xiao *et al*. (2005)
blind date (blin)	Tectum innervation	*?*	No	Muto *et al*. (2005), Xiao *et al*. (2005)
blowout (blw)	Midline crossing eye shape	*patched 1 (ptc)*	Yes	Karlstrom *et al*. (1996), Lee *et al*. (2008)
blue kite (bluk)	Tectum innervation	*?*	No	Xiao *et al*. (2005)
blumenkohl (blu)	Expanded terminations	*slc17a6b (glutamate transporter)*	No	Smear *et al*. (2007), Trowe *et al*. (1996)
bogus journey (boj)	Midline crossing	*?*	?	Muto *et al*. (2005)
boxer (box)	Tract sorting, crossing in posterior commissure	*extl3*	No	Karlstrom *et al*. (1996), Lee *et al*. (2004), Trowe *et al*. (1996)
breaking up (brek)	Confinement to tectal neuropil	*?*	No	Xiao *et al*. (2005)
chameleon (con)	Retinal exit, midline crossing	*dispatched homolog 1 (dips1)*	Yes	Karlstrom *et al*. (1996), Nakano *et al*. (2004)
clueless (clew)	Tectum innervation	*?*	No	Xiao *et al*. (2005)
coming apart (coma)	Optic tract, tectum innervation	*?*	No	Xiao *et al*. (2005)
cyclops (cyc)	Midline crossing	*nodal related-2 (ndr2)*	Yes	Karlstrom *et al*. (1996), Rebagliati *et al*. (1998), Sampath *et al*. (1998)
dackel (dak)	Tract sorting crossing in posterior commissure	*ext2*	No	Karlstrom *et al*. (1996), Lee *et al*. (2004), Trowe *et al*. (1996)
dark half (darl)	Ventral branch of the optic tract missing, topography	*gdf6a*	No	Gosse and Baier (2009), Muto *et al*. (2005)
detour (dtr)	Midline crossing	*gli1*	Yes	Karlstrom *et al*. (1996, 2003)
dragnet (drg)	Laminar specificity in the tectum	*collagen IVa5 (col4a5)*	No	Xiao and Baier (2007), Xiao *et al*. (2005)
esrom (esr)	Midline crossing, termination	*MYC binding protein 2 (mycbp2) or PAM*	No	D'Souza *et al*. (2005), Karlstrom *et al*. (1996), Trowe *et al*. (1996)
excellent adventure (exa)	Targeting defect in the tectum	*?*	?	Muto *et al*. (2005)

fuzz wuzzy (fuzz)	Confinement to tectal neuropil	*?*	No	Xiao *et al.* (2005)
gnarled (gna)	Tectal entry, tectal misrouting	*?*	Yes	Trowe *et al.* (1996), Wagle *et al.* (2004)
grumpy (gup)	Anterior projection, midline crossing	*laminin β1*	Yes	Karlstrom *et al.* (1996), Parsons *et al.* (2002)
iguana (igu)	Midline crossing	*DAZ interacting protein 1 (dzip1)*	Yes	Karlstrom *et al.* (1996), Sekimizu *et al.* (2004), Wolff *et al.* (2004)
late bloomer (late)	Delayed innervation of the tectum	*?*	No	Xiao *et al.* (2005)
no isthmus (noi)	Chiasm, anterior projection, tectal bypass	*pax2a*	Yes	Brand *et al.* (1996), MacDonald *et al.* (1997), Trowe *et al.* (1996)
macho (mao)	Expanded terminations	*?*	No	Gnuegge *et al.* (2001), Trowe *et al.* (1996)
michikusa (mich)	Ectopic arbor after crossing the midline	*?*	?	Muto *et al.* (2005)
missing link (miss)	Pretectal targets (AF4, AF9) absent or reduced	*?*	?	Muto *et al.* (2005)
nevermind (nev)	Tract sorting, D-V topography	*cyfip2*	No	Pittman *et al.* (2010), Trowe *et al.* (1996)
odysseus (ody)	Intraretinal guidance defects	*cxcr4b*	No	Knaut *et al.* (2003), Li *et al.* (2005)
parachute (pac)	Ipsilateral projection\; entering chiasm area	*N-cadherin*	Yes	Lele *et al.* (2002), Masai *et al.* (2003)
pinscher (pic)	Tract sorting, crossing in posterior commissure	*papst1 (sulfate transporter)*	No	Clément *et al.* (2008), Karlstrom *et al.* (1996), Trowe *et al.* (1996)
shirli-myrli (shir)	Delayed innervation of the tectum	*?*	No	Muto *et al.* (2005)
sleepy (sly)	Anterior projection; midline crossing	*laminin γ1*	Yes	Karlstrom *et al.* (1996), Parsons *et al.* (2002)
smooth muscle omitted (smu)	Midline crossing	*smoothened (smo)*	Yes	Chen *et al.* (2001), Varga *et al.* (2001)
sonic-you (syu)	Retinal exit, midline crossing	*sonic hedgehog (shh)*	Yes	Brand *et al.* (1996), Schauerte *et al.* (1998)
space cadet (spc)	Retinal exit, midline crossing	*?*	No	Karlstrom *et al.* (1996), Lorent *et al.* (2001)
tarde demais (tard)	Delayed innervation of the tectum	*?*	No	Xiao *et al.* (2005)
umleitung (uml)	Midline crossing	*?*	Yes	Karlstrom *et al.* (1996)
vertigo (vrt)	Delayed innervation of the tectum	*?*	No	Xiao *et al.* (2005)
walkabout (walk)	Pretectal target AF4 overinnervated	*?*	?	Muto *et al.* (2005)
who cares (woe)	Tract sorting, D-V topography	*?*	No	Trowe *et al.* (1996)
you-too (yot)	Midline crossing	*gli2*	Yes	Karlstrom *et al.* (1996, 1999)

?=not known

adhesion molecule *N-cadherin* (see Table II for a complete listing of these mutants). While some genes such as *astray (robo2)* primarily affect axon navigation, others such as *ace (fgf8)* disrupt brain patterning, resulting in mispresented axon guidance cues. More recently, a new screen has been performed using the *pou4f3:mGFP* transgenic line expressing membrane-targeted GFP (mGFP) in a subset of RGCs (Xiao *et al*., 2005). This approach allowed the identification of novel mutants with various defects in tectum innervation (Table II). Two mutants from this screen have been cloned, revealing new functions for *gdf6a* and *collagenIVa5* in regulating eye dorso-ventral patterning and tectum laminar targeting, respectively (Gosse and Baier, 2009; Xiao and Baier, 2007). Finally, a recent screen using behavioral assays identified mutants with disrupted response to visual motion and/or impaired background adaptation (Muto *et al*., 2005). Some of these mutants also have abnormal retinotectal projections or a lack of RGCs that are likely responsible for their phenotype. Identifying the mutations generated in these newer screens will give new clues about the factors involved in retinal axon guidance.

B. Injecting DNA or Morpholinos

A common approach to characterize protein function in zebrafish is to inject stable MOs into one-cell stage embryos. MOs inhibit either protein translation when targeted near the start codon of mRNAs (Nasevicius and Ekker, 2000) or splicing of the pre-mRNAs when they are targeted to exon–intron or intron–exon boundaries (Draper *et al*., 2001). Under good conditions, MOs can quickly reveal required functions for a targeted gene, though their use is subject to several caveats, including loss of efficacy as they are diluted during development (Eisen and Smith, 2008). We took advantage of this dilution with an MO against the transcription factor *atoh7* to specifically block differentiation of early- but not late-born RGCs, allowing the functional analysis of isotypic interactions between pioneer and follower axons during navigation (Pittman *et al*., 2008).

Alternatively, DNA constructs encoding dominant negative forms of the protein of interest can be transiently or stably expressed. Temporal or spatial control can be provided by the *hsp70l* heat shock promoter (see following section) or cell-specific promoters, respectively. Similarly, gain-of-function experiments can be performed by misexpressing genes of interest at specific times or locations. For greater precision, DNA constructs or MOs can be delivered to individual RGCs by *in vivo* cell electroporation (described in Section II.E), allowing functional studies at single-cell resolution (Pittman *et al*., 2010).

C. Using Heat Shock to Induce Misexpression

A powerful technique to misexpress genes in a temporally or spatially controlled manner is to use heat shock. This approach is particularly useful for studying genes with both early and late roles during development. Heat shocks can be performed after transient injection of DNA constructs or on stable transgenic lines. The *hsp70l* promoter

is an inducible element that drives strong gene expression in response to a temperature shift from 28.5°C (normal rearing temperature) to 37–40°C (Halloran *et al*., 2000). Global heat shocks have been widely used to induce ubiquitous gene expression in embryos at specific times. The exact heat shock duration and temperature depend on the age of the embryo, the transgene to be expressed, and the level of expression desired. For instance, raising the temperature to 42°C for 5 min can induce detectable transgene expression in 20 hpf embryos (Thummel *et al*., 2005).

Recently, we developed a technique using a sharpened soldering iron to induce focal heat shocks in restricted regions of the embryo (Hardy *et al*., 2007). For this approach, a copper soldering iron tip with a diameter of 15 μm is heated to 60°C and put directly in contact with the embryo for 3 min. A perfusion chamber keeps fluid flowing over the embryo during heat shock, thereby preventing heating of the medium and restricting the area of activation. This method is rapid and easy, allows the targeting of ~100 μm patches of tissue, and can be used in a variety of tissues and stages. A detailed protocol has been described (Hardy *et al*., 2007). Even more recently, Rolf Karlstrom's group developed another focal heat shock method using an optical fiber to deliver energy to a localized region (Placinta *et al*., 2009).

D. Transplanting to Test Cell Autonomy of Gene Function

Transplanting cells or tissues is a powerful approach to test cell autonomy of gene function. Different types of transplant can be performed depending on the question (e.g., transplanting all RGCs, or RGCs in specific parts of the retina; labeling donors, hosts, or both labeled). A tricky but elegant approach is to transplant entire eye primordia, yielding mosaic embryos in which the whole eye comes from the donor while the rest of the embryo is derived from the host. A main advantage of this approach is that all retinal axons coming from the transplanted eye share the same genotype and are not influenced by interactions with host retinal axons, as these have been removed. We used eye transplants to demonstrate that *robo2* acts eye-autonomously to regulate retinal axon guidance (Fricke *et al*., 2001). A detailed protocol has been previously described (Hutson *et al*., 2004).

Alternatively, early transplants at blastula stage can be used to test cell autonomy (Ho and Kane, 1990). These are easy to perform and allow quite effective targeting of the retina (Moens and Fritz, 1999). Cells are removed from donor embryos between 4 and 6 hpf and replaced into the animal pole of host embryos. The resulting mosaic embryos display clones of RGCs in the retina, as well as some clones of cells in the brain. An abbreviated protocol is given below. While the presence of donor cells in the brain may make results harder to interpret, this approach is the easiest way to generate mosaic embryos with RGCs from different genetic backgrounds. However, it cannot be employed to target RGCs from or to specific regions within the retina.

Instead, transplants at a later stage are required. We have recently begun to use a technique for transplanting RGCs in a topographic manner (Fig. 3; inspired by Masai *et al*., 2003). Donor and host embryos labeled with different transgenes are grown to 30–33 hpf, when the first RGCs are specified. After mounting embryos laterally in

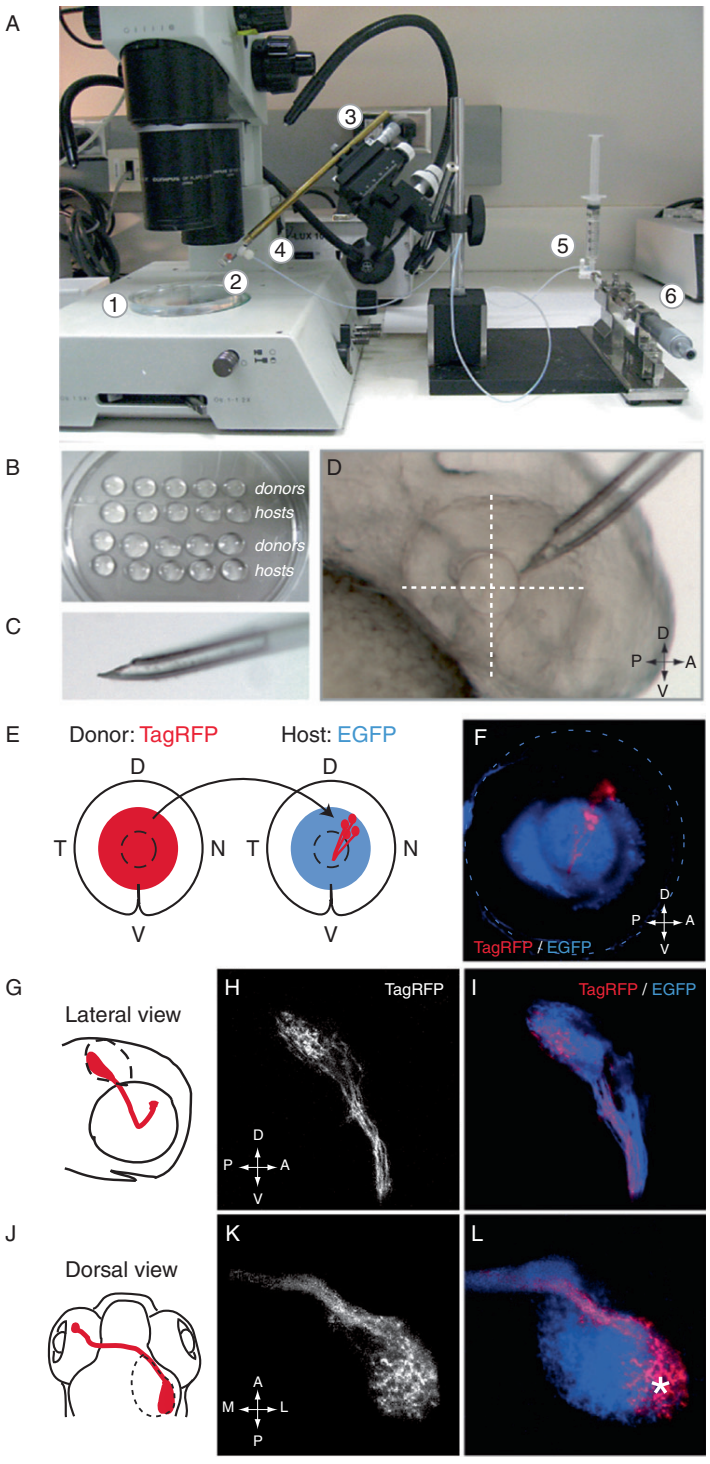

Fig. 3 *(Continued)*

agarose, donor RGCs are precisely removed from a specific location in the retina with a 40 µm glass micropipette and replaced at the same position in the host retina. The transplant is considered successful if, after raising the host, the transplanted RGCs are observed in the correct area of the retina (from a lateral view), and if in control conditions their arbors terminate in the appropriate part of the tectum (from a dorsal view). We obtain ~25% successful transplants with this approach and provide a detailed protocol below.

E. Protocols for Transplants

1. Method 3: Blastula Transplants

Since blastula stage transplants have been explained in detail elsewhere (Ho and Kane, 1990; Kemp *et al*., 2009), only a succinct description of the method is provided here.

1. Donor embryos are injected at the one-cell stage with 5% Alexa-488 dextran or rhodamine dextran (10,000 MW) as a lineage marker. The light color from the dextran helps to distinguish donors from hosts during later steps. We use agarose-groove dishes for the injections (mold TU-1, Adaptive Science Tools, Worcester, Massachusetts; 1% agarose w/v in E2 or E3 embryo medium). Donor and host embryos are raised at 28.5°C until the sphere (4 hpf) or shield stage (6 hpf).
2. While waiting for the embryos to develop, pull and bevel standard wall, non-filament capillaries for use as transplant needles and prepare an agarose transplant dish (single-well mold; mold PT-1, Adaptive Science Tools; Kane and Kishimoto, 2002).
3. Dechorionate donor and host embryos. Use a clean fire-polished large-bore Pasteur pipette to transfer one donor and four hosts into each row of the transplant dish using an air-filled syringe and fire-polished transplantation pipette. Remove cells

Fig. 3 Perturbing the retinotectal system with late topographic transplants. (A) Embryos are mounted laterally in drops of low-melt agarose deposited on a dish lid that is then placed under a dissecting microscope (1). The transplant needle is mounted in a micropipette holder (2), itself mounted onto a three-axis micromanipulator (3) placed next to the microscope. The micropipette holder is connected via a tube filled with mineral oil (4) to an oil-filled Hamilton syringe with a micrometer drive (6). The syringe is attached by a three-way stopcock to a reservoir filled with mineral oil (5). (B) Donor and host embryos mounted laterally in low-melt agarose drops. Embryos are arranged so that each donor is close to its respective host. (C) The transplant needle has a 40 µm diameter opening with a sharp tip that is slightly bent (around 20°). (D) The transplant needle is inserted into the dorsonasal retina, close to the lens, at a 45° angle. The bend of the needle tip is facing upward, so that ventral RGCs cannot be drawn up. (E) Dorsonasal (DN) RGCs from an *isl2b:TagRFP* donor are isotopically transplanted into the DN retina of an *isl2b:EGFP* host between 30 and 33 hpf. Their axonal projections are then visualized at 4 dpf by live confocal microscopy. (F) Lateral view of a WT *isl2b:EGFP* host eye in which WT TagRFP-positive RGCs have been transplanted. GFP is shown as blue for the best visualization. (G, J) Projections of DN donor axons observed in transplants in lateral (G) and dorsal (J) views. (H, I) Lateral view of TagRFP-positive projections at 4 dpf. DN donor axons navigate along the ventral branch of the tract to reach the tectum. (K, L) Dorsal view of the same projections. DN donor axons project to the posterolateral part of the host tectum (asterisk). *F, H, I, K, L: confocal maximum intensity projections*. (See Plate no. 2 in the Color Plate Section.)

from each donor embryo and transplant 20–50 cells into the animal pole of each corresponding host. While the origin of the transplanted cells is not important, the location where they are placed into the host is crucial. A fate map of the 6 hpf embryo can be used as a reference (Woo *et al.*, 1995).

4. After transplantation, transfer the agarose dish carefully to the 28.5°C incubator. During gastrulation, donor cells will spread out and form a mosaic patch of fluorescently labeled cells; choose those in which this patch includes cells in the eye. Once embryos have developed to bud stage, it is safe to remove them from the transplant dish and put them in 4-well or 24-well dishes. For experiments in which mutant cells are transplanted, donors should be kept together with their respective hosts until genotyped, either by PCR or by mutant phenotype. If necessary, hosts can be genotyped as well.

2. Method 4: Late Topographic Transplants

While blastula transplants are useful for testing functional cell autonomy and can be easily performed, they cannot target RGCs within specific regions of the retina. Testing the roles of genes specifically expressed in the dorsal or ventral retina, for instance, requires transplanting at later stages in a topographic manner. Here, we describe a detailed protocol for transplanting dorsonasal RGCs into the host dorsonasal retina. These transplants are performed between 30 and 33 hpf, when the first RGCs are specified and have acquired their positional identity within the retina. Donor and host embryos are labeled with *isl2b:TagRFP* and *isl2b:EGFP* transgenes, respectively, so that axons of transplanted RGCs and their projections can be easily visualized by live confocal miscroscopy at 4 days post-fertilization (dpf).

a. Solutions Needed

- E2 medium (15 mM NaCl, 0.5 mM KCl, 1 mM $CaCl_2$, 1 mM $MgSO_4$, 0.15 mM KH_2PO_4, 1.7 mM $NaHCO_3$)
- 0.1 mM phenylthiourea (PTU) in E3 embryo medium (5 mM NaCl, 0.17 mM KCl, 0.33 mM $CaCl_2$, 0.33 mM $MgSO_4$)
- tricaine stock (0.4% tricaine, 10 mM HEPES, pH 7.4)
- 1% low-melt agarose in E2/GN/tricaine (10 µg/ml gentamicin in E2 medium, 0.02% tricaine)

b. Protocol

1. The transplant needle is prepared in advance and can be reused several times. The quality of its preparation is the most important parameter for successful transplants. Pull standard wall, non-filament capillaries and polish them using a microforge, so that the tip displays a 20° angle with a 40 µm diameter opening (Fig. 3C).
2. Raise embryos at 28.5°C in E3 medium containing 0.1 mM PTU to inhibit pigment formation, and dechorionate them between 22 and 28 hpf. At 30 hpf, anesthetize embryos by adding tricaine to a final concentration of 0.02%. Mount laterally in a

drop of 1% low-melt agarose in E2/gentamycin/tricaine deposited on the lid of a Petri dish (Fig. 3B). Donors and hosts should be arranged in lines, so that each donor is close to its respective host. Once the drops have solidified, fill the Petri dish with PTU-E3/tricaine and position it under a dissecting scope.

3. Prepare the transplant setup (Fig. 3A): an oil-filled Hamilton syringe with a micrometer drive is connected by a three-way stopcock to a reservoir filled with mineral oil and to a micropipette holder through flexible plastic tubing. It is important to fill the system completely with mineral oil and ensure that air bubbles have been eliminated (air bubbles impair the ability to control suction and pressure). The transplant pipette is mounted in the micropipette holder, itself mounted onto a three-axis micromanipulator positioned next to the dissecting scope.
4. Using the micromanipulator, bring the transplant pipette near the dorsonasal retina, with a 45° angle (Fig. 3C). Make sure that the needle opening is facing upward, so that ventral RGCs cannot be drawn up into the needle. Insert the needle into the dorsonasal retina close to the lens, and slowly and carefully suck up 40–100 cells into the needle. At this stage, the fluorescence of the transgene expressed in RGCs is not yet visible, so the fraction of RGCs among the removed cells can vary. After cells have been taken up, reverse the pressure in the needle to stop the suction, and remove the needle from the donor eye. Insert the needle into the host retina in a similar way, and slowly expel the cells with as little medium as possible. After transplantation, let embryos recover for few minutes, remove them from the agarose, and raise them in E3 + PTU at 28.5°C in 24-well plates. Axons of transplanted RGCs can then be observed after 48 hpf by live imaging.

IV. Future Directions

The approaches developed over the past decade have greatly improved our ability to label and visualize the retinotectal projection *in vivo,* as well as to perform functional assays for understanding the molecular mechanisms that control its development. Nevertheless, novel techniques will be required for observing retinal axons in greater detail and to ask new biological questions.

Three methods already used in other systems are currently being adapted to study new aspects of zebrafish retinotectal system development. The Brainbow approach, initially developed in mice, allows labeling and mapping of neurons with a wide range of colors by randomly varying the levels of red, green, and blue FPs expressed in individual neurons (Livet *et al*., 2007). It has been used to reconstruct the architecture of neuronal circuits in different systems and will be a powerful tool for analyzing sorting of retinal axons in the tract as well as topographic mapping in the tectum. A second approach is to use enhancer trap (ET) screens to isolate lines expressing transgenes in specific subsets of neurons. For instance, new lines with interesting expression patterns in the tectum have recently been produced with a Gal4 ET screen (Scott and Baier, 2009). Such an approach will potentially allow the identification of new lines driving expression in specific regions of the retina (Picker *et al*., 2009) or RGC subtypes. Finally, calcium

imaging has been used *in vitro* to measure growth cone responses to guidance cues (Guan *et al*., 2007; Tojima *et al*., 2010). Adapted to zebrafish, it will give the ability to monitor, *in vivo*, the activity of retinal axons as they elongate. Combined together, these emerging techniques will improve our ability to examine retinal axons as they navigate, shedding new light on axon guidance *in vivo*.

References

Aizawa, H., Bianco, I. H., Hamaoka, T., Miyashita, T., Uemura, O., Concha, M. L., Russell, C., Wilson, S. W., and Okamoto, H. (2005). Laterotopic representation of left-right information onto the dorso-ventral axis of a zebrafish midbrain target nucleus. Curr. Biol. **15**, 238–243.

Baier, H., Klostermann, S., Trowe, T., Karlstrom, R. O., Nusslein-Volhard, C., and Bonhoeffer, F. (1996). Genetic dissection of the retinotectal projection. Development **123**, 415–425.

Ben Fredj, N., Hammond, S., Otsuna, H., Chien, C. B., Burrone, J., and Meyer, M. P. (2010). Synaptic activity and activity-dependent competition regulates axon arbor maturation, growth arrest, and territory in the retinotectal projection. J. Neurosci. **30**, 10939–10951.

Bianco, I. H., Carl, M., Russell, C., Clarke, J. D., and Wilson, S. W. (2008). Brain asymmetry is encoded at the level of axon terminal morphology. Neural Dev. **3**, 9.

Brand, M., Heisenberg, C. P., Jiang, Y. J., Beuchle, D., Lun, K., Furutani-Seiki, M., Granato, M., Haffter, P., Hammerschmidt, M., Kane, D. A., Kelsh, R. N., Mullins, M. C., *et al*., (1996). Mutations in zebrafish genes affecting the formation of the boundary between midbrain and hindbrain. Development **123**, 179–190.

Campbell, D. S., Stringham, S. A., Timm, A., Xiao, T., Law, M. Y., Baier, H., Nonet, M. L., and Chien, C. B. (2007). Slit1a inhibits retinal ganglion cell arborization and synaptogenesis via Robo2-dependent and -independent pathways. Neuron **55**, 231–245.

Chen, W., Burgess, S., and Hopkins, N. (2001). Analysis of the zebrafish smoothened mutant reveals conserved and divergent functions of hedgehog activity. Development **128**, 2385–2396.

Choy, E., Chiu, V. K., Silletti, J., Feoktistov, M., Morimoto, T., Michaelson, D., Ivanov, I. E., and Philips, M. R. (1999). Endomembrane trafficking of ras: The CAAX motif targets proteins to the ER and Golgi. Cell **98**, 69–80.

Clement, A., Wiweger, M., von der Hardt, S., Rusch, M. A., Selleck, S. B., Chien, C. B., and Roehl, H. H. (2008). Regulation of zebrafish skeletogenesis by ext2/dackel and papst1/pinscher. PLoS Genet. **4**, e1000136.

Del Bene, F., Wehman, A. M., Link, B. A., and Baier, H. (2008). Regulation of neurogenesis by interkinetic nuclear migration through an apical-basal notch gradient. Cell **134**, 1055–1065.

Draper, B. W., Morcos, P. A., and Kimmel, C. B. (2001). Inhibition of zebrafish fgf8 pre-mRNA splicing with morpholino oligos: A quantifiable method for gene knockdown. Genesis **30**, 154–156.

D'Souza, J., Hendricks, M., Le Guyader, S., Subburaju, S., Grunewald, B., Scholich, K., and Jesuthasan, S. (2005). Formation of the retinotectal projection requires Esrom, an ortholog of PAM (protein associated with Myc). Development **132**, 247–256.

Eisen, J. S., and Smith, J. C. (2008). Controlling morpholino experiments: Don't stop making antisense. Development **135**, 1735–1743.

Fricke, C., Lee, J. S., Geiger-Rudolph, S., Bonhoeffer, F., and Chien, C. B. (2001). Astray, a zebrafish roundabout homolog required for retinal axon guidance. Science **292**, 507–510.

Gnuegge, L., Schmid, S., and Neuhauss, S. C. (2001). Analysis of the activity-deprived zebrafish mutant macho reveals an essential requirement of neuronal activity for the development of a fine-grained visuotopic map. J. Neurosci. **21**, 3542–3548.

Gosse, N. J., and Baier, H. (2009). An essential role for Radar (Gdf6a) in inducing dorsal fate in the zebrafish retina. Proc. Natl. Acad. Sci. U.S.A. **106**, 2236–2241.

Guan, C. B., Xu, H. T., Jin, M., Yuan, X. B., and Poo, M. M. (2007). Long-range Ca2+ signaling from growth cone to soma mediates reversal of neuronal migration induced by slit-2. Cell **129**, 385–395.

Halloran, M. C., Sato-Maeda, M., Warren, J. T., Su, F., Lele, Z., Krone, P. H., Kuwada, J. Y., and Shoji, W. (2000). Laser-induced gene expression in specific cells of transgenic zebrafish. Development **127**, 1953–1960.

Hardy, M. E., Ross, L. V., and Chien, C. B. (2007). Focal gene misexpression in zebrafish embryos induced by local heat shock using a modified soldering iron. Dev. Dyn. **236**, 3071–3076.

Ho, R. K., and Kane, D. A. (1990). Cell-autonomous action of zebrafish spt-1 mutation in specific mesodermal precursors. Nature **348**, 728–730.

Honig, M. G., and Hume, R. I. (1989). Dil and diO: Versatile fluorescent dyes for neuronal labelling and pathway tracing. Trends Neurosci. **12**, 333–335, 340–341.

Hu, M., and Easter, S. S. (1999). Retinal neurogenesis: The formation of the initial central patch of postmitotic cells. Dev. Biol. **207**, 309–321.

Hutson, L. D., Campbell, D. S., and Chien, C. B. (2004). Analyzing axon guidance in the zebrafish retinotectal system. Methods Cell Biol. **76**, 13–35.

Hutson, L. D., and Chien, C. B. (2002). Pathfinding and error correction by retinal axons: The role of astray/robo2. Neuron **33**, 205–217.

Kaethner, R. J., and Stuermer, C. A. (1992). Dynamics of terminal arbor formation and target approach of retinotectal axons in living zebrafish embryos: A time-lapse study of single axons. J. Neurosci. **12**, 3257–3271.

Kane, D. A., and Kishimoto, Y. (2002). Cell labelling and transplantation techniques. In "Zebrafish, Practical Approach" (C. Nüsslein-Volhard, R. Dahm, eds.) No. 261, pp. 95–120, Oxford University Press, Tubingen, Germany.

Karlstrom, R. O., Talbot, W. S., and Schier, A. F. (1999). Comparative synteny cloning of zebrafish you-too: Mutations in the Hedgehog target gli2 affect ventral forebrain patterning. Genes Dev. **13**, 388–393.

Karlstrom, R. O., Trowe, T., Klostermann, S., Baier, H., Brand, M., Crawford, A. D., Grunewald, B., Haffter, P., Hoffmann, H., Meyer, S. U., Muller, B. K., Richter, S., *et al.* (1996). Zebrafish mutations affecting retinotectal axon pathfinding. Development **123**, 427–438.

Karlstrom, R. O., Tyurina, O. V., Kawakami, A., Nishioka, N., Talbot, W. S., Sasaki, H., and Schier, A. F. (2003). Genetic analysis of zebrafish gli1 and gli2 reveals divergent requirements for gli genes in vertebrate development. Development **130**, 1549–1564.

Kemp, H. A., Carmany-Rampey, A., and Moens, C. (2009). Generating chimeric zebrafish embryos by transplantation. J. Vis. Exp. Jul 17;(29). pii: 1394. doi: 10.3791/1394.

Knaut, H., Werz, C., Geisler, R., and Nusslein-Volhard, C. (2003). A zebrafish homologue of the chemokine receptor Cxcr4 is a germ-cell guidance receptor. Nature **421**, 279–282.

Koster, R. W., and Fraser, S. E. (2001). Tracing transgene expression in living zebrafish embryos. Dev. Biol. **233**, 329–346.

Laessing, U., Giordano, S., Stecher, B., Lottspeich, F., and Stuermer, C. A. (1994). Molecular characterization of fish neurolin: A growth-associated cell surface protein and member of the immunoglobulin superfamily in the fish retinotectal system with similarities to chick protein DM-GRASP/SC-1/BEN. Differentiation **56**, 21–29.

Laessing, U., and Stuermer, C. A. (1996). Spatiotemporal pattern of retinal ganglion cell differentiation revealed by the expression of neurolin in embryonic zebrafish. J. Neurobiol. **29**, 65–74.

Lee, J. S., von der Hardt, S., Rusch, M. A., Stringer, S. E., Stickney, H. L., Talbot, W. S., Geisler, R., Nusslein-Volhard, C., Selleck, S. B., Chien, C. B., and Roehl, H. (2004). Axon sorting in the optic tract requires HSPG synthesis by ext2 (dackel) and extl3 (boxer). Neuron **44**, 947–960.

Lee, J. S., Willer, J. R., Willer, G. B., Smith, K., Gregg, R. G., and Gross, J. M. (2008). Zebrafish blowout provides genetic evidence for Patched1-mediated negative regulation of Hedgehog signaling within the proximal optic vesicle of the vertebrate eye. Dev. Biol. **319**, 10–22.

Lele, Z., Folchert, A., Concha, M., Rauch, G. J., Geisler, R., Rosa, F., Wilson, S. W., Hammerschmidt, M., and Bally-Cuif, L. (2002). Parachute/n-cadherin is required for morphogenesis and maintained integrity of the zebrafish neural tube. Development **129**, 3281–3294.

Li, Q., Shirabe, K., Thisse, C., Thisse, B., Okamoto, H., Masai, I., and Kuwada, J. Y. (2005). Chemokine signaling guides axons within the retina in zebrafish. J. Neurosci. **25**, 1711–1717.

Livet, J., Weissman, T. A., Kang, H., Draft, R. W., Lu, J., Bennis, R. A., Sanes, J. R., and Lichtman, J. W. (2007). Transgenic strategies for combinatorial expression of fluorescent proteins in the nervous system. Nature **450**, 56–62.

Lorent, K., Liu, K. S., Fetcho, J. R., and Granato, M. (2001). The zebrafish space cadet gene controls axonal pathfinding of neurons that modulate fast turning movements. Development **128**, 2131–2142.

Macdonald, R., Scholes, J., Strahle, U., Brennan, C., Holder, N., Brand, M., and Wilson, S. W. (1997). The Pax protein Noi is required for commissural axon pathway formation in the rostral forebrain. Development **124**, 2397–2408.

Maddison, L. A., Lu, J., Victoroff, T., Scott, E., Baier, H., and Chen, W. (2009). A gain-of-function screen in zebrafish identifies a guanylate cyclase with a role in neuronal degeneration. Mol. Genet. Genomics **281**, 551–563.

Mangrum, W. I., Dowling, J. E., and Cohen, E. D. (2002). A morphological classification of ganglion cells in the zebrafish retina. Vis. Neurosci. **19**, 767–779.

Masai, I., Lele, Z., Yamaguchi, M., Komori, A., Nakata, A., Nishiwaki, Y., Wada, H., Tanaka, H., Nojima, Y., Hammerschmidt, M., Wilson, S. W., and Okamoto, H. (2003). N-cadherin mediates retinal lamination, maintenance of forebrain compartments and patterning of retinal neurites. Development **130**, 2479–2494.

Masai, I., Yamaguchi, M., Tonou-Fujimori, N., Komori, A., and Okamoto, H. (2005). The hedgehog-PKA pathway regulates two distinct steps of the differentiation of retinal ganglion cells: The cell-cycle exit of retinoblasts and their neuronal maturation. Development **132**, 1539–1553.

Matsuda, N., and Mishina, M. (2004). Identification of chaperonin CCT gamma subunit as a determinant of retinotectal development by whole-genome subtraction cloning from zebrafish no tectal neuron mutant. Development **131**, 1913–1925.

Meyer, M. P., and Smith, S. J. (2006). Evidence from in vivo imaging that synaptogenesis guides the growth and branching of axonal arbors by two distinct mechanisms. J. Neurosci. **26**, 3604–3614.

Moens, C. B., and Fritz, A. (1999). Techniques in neural development. Methods Cell Biol. **59**, 253–272.

Moriyoshi, K., Richards, L. J., Akazawa, C., O'Leary, D. D., and Nakanishi, S. (1996). Labeling neural cells using adenoviral gene transfer of membrane-targeted GFP. Neuron **16**, 255–260.

Mumm, J. S., Williams, P. R., Godinho, L., Koerber, A., Pittman, A. J., Roeser, T., Chien, C. B., Baier, H., and Wong, R. O. (2006). In vivo imaging reveals dendritic targeting of laminated afferents by zebrafish retinal ganglion cells. Neuron **52**, 609–621.

Muto, A., Orger, M. B., Wehman, A. M., Smear, M. C., Kay, J. N., Page-McCaw, P. S., Gahtan, E., Xiao, T., Nevin, L. M., Gosse, N. J., Staub, W., Finger-Baier, K., *et al*., (2005). Forward genetic analysis of visual behavior in zebrafish. PLoS Genet. **1**, e66.

Nakano, Y., Kim, H. R., Kawakami, A., Roy, S., Schier, A. F., and Ingham, P. W. (2004). Inactivation of dispatched 1 by the chameleon mutation disrupts Hedgehog signalling in the zebrafish embryo. Dev. Biol. **269**, 381–392.

Nasevicius, A., and Ekker, S. C. (2000). Effective targeted gene "knockdown" in zebrafish. Nat. Genet. **26**, 216–220.

Neumann, C. J., and Nuesslein-Volhard, C. (2000). Patterning of the zebrafish retina by a wave of sonic hedgehog activity. Science **289**, 2137–2139.

Nevin, L. M., Taylor, M. R., and Baier, H. (2008). Hardwiring of fine synaptic layers in the zebrafish visual pathway. Neural Dev. **3**, 36.

O'Brien, G. S., Rieger, S., Martin, S. M., Cavanaugh, A. M., Portera-Cailliau, C., and Sagasti, A. (2009). Two-photon axotomy and time-lapse confocal imaging in live zebrafish embryos. J. Vis. Exp. Feb 16;(24). pii: 1129. doi: 10.3791/1129.

Parsons, M. J., Pollard, S. M., Saude, L., Feldman, B., Coutinho, P., Hirst, E. M., and Stemple, D. L. (2002). Zebrafish mutants identify an essential role for laminins in notochord formation. Development **129**, 3137–3146.

Paulus, J. D., and Halloran, M. C. (2006). Zebrafish bashful/laminin-alpha 1 mutants exhibit multiple axon guidance defects. Dev. Dyn. **235**, 213–224.

Picker, A., Brennan, C., Reifers, F., Clarke, J. D., Holder, N., and Brand, M. (1999). Requirement for the zebrafish mid-hindbrain boundary in midbrain polarisation, mapping and confinement of the retinotectal projection. Development **126**, 2967–2978.

Picker, A., Cavodeassi, F., Machate, A., Bernauer, S., Hans, S., Abe, G., Kawakami, K., Wilson, S. W., and Brand, M. (2009). Dynamic coupling of pattern formation and morphogenesis in the developing vertebrate retina. PLoS Biol. **7**, e1000214.

Pittman, A. J., Gaynes, J. A., and Chien, C. B. (2010). nev (cyfip2) is required for retinal lamination and axon guidance in the zebrafish retinotectal system. Dev. Biol. **344**, 784–794.

Pittman, A. J., Law, M. Y., and Chien, C. B. (2008). Pathfinding in a large vertebrate axon tract: Isotypic interactions guide retinotectal axons at multiple choice points. Development **135**, 2865–2871.

Placinta, M., Shen, M. C., Achermann, M., and Karlstrom, R. O. (2009). A laser pointer driven microheater for precise local heating and conditional gene regulation in vivo. Microheater driven gene regulation in zebrafish. BMC Dev. Biol. **9**, 73.

Poggi, L., Vitorino, M., Masai, I., and Harris, W. A. (2005). Influences on neural lineage and mode of division in the zebrafish retina in vivo. J. Cell Biol. **171**, 991–999.

Rebagliati, M. R., Toyama, R., Haffter, P., and Dawid, I. B. (1998). cyclops encodes a nodal-related factor involved in midline signaling. Proc. Natl. Acad. Sci. U.S.A. **95**, 9932–9937.

Roeser, T., and Baier, H. (2003). Visuomotor behaviors in larval zebrafish after GFP-guided laser ablation of the optic tectum. J. Neurosci. **23**, 3726–3734.

Sampath, K., Rubinstein, A. L., Cheng, A. M., Liang, J. O., Fekany, K., Solnica-Krezel, L., Korzh, V., Halpern, M. E., and Wright, C. V. (1998). Induction of the zebrafish ventral brain and floorplate requires cyclops/nodal signalling. Nature **395**, 185–189.

Sato, T., Hamaoka, T., Aizawa, H., Hosoya, T., and Okamoto, H. (2007). Genetic single-cell mosaic analysis implicates ephrinB2 reverse signaling in projections from the posterior tectum to the hindbrain in zebrafish. J. Neurosci. **27**, 5271–5279.

Schauerte, H. E., van Eeden, F. J., Fricke, C., Odenthal, J., Strahle, U., and Haffter, P. (1998). Sonic hedgehog is not required for the induction of medial floor plate cells in the zebrafish. Development **125**, 2983–2993.

Schmidt, J. T., Buzzard, M., Borress, R., and Dhillon, S. (2000). MK801 increases retinotectal arbor size in developing zebrafish without affecting kinetics of branch elimination and addition. J. Neurobiol. **42**, 303–314.

Scott, E. K., and Baier, H. (2009). The cellular architecture of the larval zebrafish tectum, as revealed by gal4 enhancer trap lines. Front Neural Circuits **3**, 13.

Sekimizu, K., Nishioka, N., Sasaki, H., Takeda, H., Karlstrom, R. O., and Kawakami, A. (2004). The zebrafish iguana locus encodes Dzip1, a novel zinc-finger protein required for proper regulation of Hedgehog signaling. Development **131**, 2521–2532.

Seth, A., Culverwell, J., Walkowicz, M., Toro, S., Rick, J. M., Neuhauss, S. C., Varga, Z. M., and Karlstrom, R. O. (2006). belladonna/(Ihx2) is required for neural patterning and midline axon guidance in the zebrafish forebrain. Development **133**, 725–735.

Shanmugalingam, S., Houart, C., Picker, A., Reifers, F., Macdonald, R., Barth, A., Griffin, K., Brand, M., and Wilson, S. W. (2000). Ace/Fgf8 is required for forebrain commissure formation and patterning of the telencephalon. Development **127**, 2549–2561.

Smear, M. C., Tao, H. W., Staub, W., Orger, M. B., Gosse, N. J., Liu, Y., Takahashi, K., Poo, M. M., and Baier, H. (2007). Vesicular glutamate transport at a central synapse limits the acuity of visual perception in zebrafish. Neuron **53**, 65–77.

Thummel, R., Burket, C. T., Brewer, J. L., Sarras, M. P., Jr., Li, L., Perry, M., McDermott, J. P., Sauer, B., Hyde, D. R., and Godwin, A. R. (2005). Cre-mediated site-specific recombination in zebrafish embryos. Dev. Dyn. **233**, 1366–1377.

Tojima, T., Itofusa, R., and Kamiguchi, H. (2010) Asymmetric clathrin-mediated endocytosis drives repulsive growth cone guidance. Neuron **66**, 370–377.

Tokuoka, H., Yoshida, T., Matsuda, N., and Mishina, M. (2002). Regulation by glycogen synthase kinase-3beta of the arborization field and maturation of retinotectal projection in zebrafish. J. Neurosci. **22**, 10324–10332.

"Analyse von Mutationen mit Einfluss aud die topographische Ordnung von Axonen im retinotektalen System des Zebrabärblings, Danio rerio. PhD Thesis, Eberhard-Karls-Universität Tübingen, Tübingen, Germany.

Trowe, T., Klostermann, S., Baier, H., Granato, M., Crawford, A. D., Grunewald, B., Hoffmann, H., Karlstrom, R. O., Meyer, S. U., Muller, B., Richter, S., Nusslein-Volhard, C., *et al*., (1996). Mutations disrupting the ordering and topographic mapping of axons in the retinotectal projection of the zebrafish, Danio rerio. Development **123**, 439–450.

Varga, Z. M., Amores, A., Lewis, K. E., Yan, Y. L., Postlethwait, J. H., Eisen, J. S., and Westerfield, M. (2001). Zebrafish smoothened functions in ventral neural tube specification and axon tract formation. Development **128**, 3497–3509.

Vitorino, M., Jusuf, P. R., Maurus, D., Kimura, Y., Higashijima, S., and Harris, W. A. (2009). Vsx2 in the zebrafish retina: Restricted lineages through derepression. Neural Dev. **4**, 14.

Wagle, M., Grunewald, B., Subburaju, S., Barzaghi, C., Le Guyader, S., Chan, J., and Jesuthasan, S. (2004). EphrinB2a in the zebrafish retinotectal system. J. Neurobiol. **59**, 57–65.

Wolff, C., Roy, S., Lewis, K. E., Schauerte, H., Joerg-Rauch, G., Kirn, A., Weiler, C., Geisler, R., Haffter, P., and Ingham, P. W. (2004). iguana encodes a novel zinc-finger protein with coiled-coil domains essential for Hedgehog signal transduction in the zebrafish embryo. Genes Dev. **18**, 1565–1576.

Woo, K., Shih, J., and Fraser, S. E. (1995). Fate maps of the zebrafish embryo. Curr. Opin. Genet. Dev. **5**, 439–443.

Xiao, T., and Baier, H. (2007). Lamina-specific axonal projections in the zebrafish tectum require the type IV collagen Dragnet. Nat. Neurosci. **10**, 1529–1537.

Xiao, T., Roeser, T., Staub, W., and Baier, H. (2005). A GFP-based genetic screen reveals mutations that disrupt the architecture of the zebrafish retinotectal projection. Development **132**, 2955–2967.

Yoshida, T., and Mishina, M. (2003). Neuron-specific gene manipulations to transparent zebrafish embryos. Methods Cell Sci. **25**, 15–23.

Zolessi, F. R., Poggi, L., Wilkinson, C. J., Chien, C. B., and Harris, W. A. (2006). Polarization and orientation of retinal ganglion cells in vivo. Neural Dev. **1**, 2.

APPENDIX B

CLONING THE HERMES PROMOTER

The RNA-binding protein Hermes/RBPMS is required for formation of RGC axon arbors on the optic tectum in both zebrafish and *Xenopus laevis* (Hornberg et al. 2013). *In situ* hybridization showed that Hermes is expressed with high specificity in RGCs in zebrafish embryos (Thisse and Thisse 2004). Chi-Bin wanted to clone the promoter for Hermes from genomic DNA. While the isl2b promoter drives expression specifically in RGCs within the retina, it also drives strong expression in the trigeminal axons. This presents a technical hurdle when imaging RCG axons since the trigeminal axons obstruct the view of the retinotectal projection.

I performed PCR on zebrafish genomic DNA to amplify an 8 kilobase region directly upstream (5') of the start for the hermes gene using: f-primer-5'GGGGAC-AACTTTGTATAGAAAAGTTGCTGGCCGGCCAGATCTCGAACCATGCAAGC-3', r-primer 5'-GGGGACTGCTTTTTTGCACAAACTTGTGGCGCGCCGGTGCCACCT-CACATTTACC-3'. I used a BP recombination with pDONRp4-p1R and gel-purified pcr product to make p5E-Hermes and then performed and LR recombination to make Hermes-EGFP-pA and injected it into 1-cell wild-type embryos to generate transient transgenics with strong expression of EGFP in RGCs without expression in other cells in the brain or head (Kwan et al. 2007) (Figure B.1). I have also raised potential founders and will soon have a stable transgenic line with Hermes-EGFP-pA. Cloning of the Hermes promoter contributed a new promoter to the zebrafish community for driving more specific expression in RGCs.

Figure B.1: The Hermes promoter drives RGC-specific expression. 3dpf Hermes-EGPF-pA (green) transient transgenic embryos were imaged live with a confocal microscope (20x lens) with the lens removed from the right eye (B, white arrow), with a dorsal (B) and a ventral (A) view.

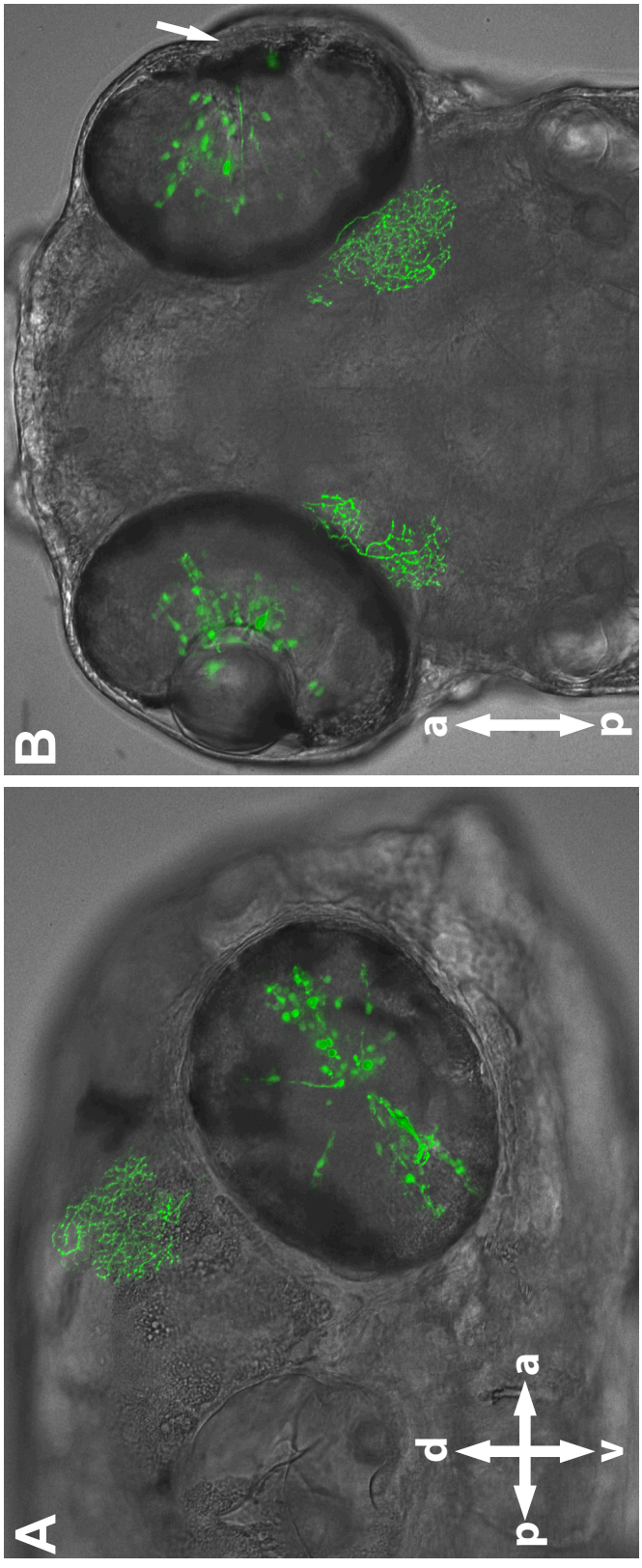
B
a
p
A
a
d
v
p

References

Hörnberg, H., Wollerton-van Horck, F., Maurus, D., Zwart, M., Svoboda, H., Harris, W. A., Holt, C. E. (2013). RNA-binding protein Hermes/RBPMS inversely affects synapse density and axon arbor formation in retinal ganglion cells *in vivo*. The Journal of Neuroscience, 33(25), 10384–10395.

Kwan, K. M., Fujimoto, E., Grabher, C., Mangum, B. D., Hardy, M. E., Campbell, D. S., Chien, C.-B. (2007). The Tol2kit: a multisite gateway-based construction kit for Tol2 transposon transgenesis constructs. Developmental Dynamics, 236(11), 3088–3099.

Thisse, B., Thisse, C. (2004) Fast release clones: a high throughput expression analysis. ZFIN direct data submission (http://zfin.org).